

Modelling Climate Change Impacts on Soybean Yields on the Swiss Plateau

Master Thesis
Faculty of Science, University of Bern
Agroscope Reckenholz

handed in by

Sarah Willi

2023

Supervisor

PD Dr. Annelie Holzkämper

Co-Supervisor

Prof. Dr. Bettina Schaepli

Abstract

Climate change significantly affects agricultural production throughout the world, inter alia with shifts of the suitable areas for certain crops. This includes soybeans, which could become increasingly suitable for cultivation in the northern latitudes of Europe. Soybeans are already grown on the Swiss Plateau on a small scale, but an increase in soybean cultivation is currently witnessed. The objective of this thesis is to assess the impacts of climate change on soybean yields on the Swiss Plateau with a modelling approach. The crop growth model WOFOST was evaluated at two study sites (Reckenholz and Changins) and then applied with climate projection data under RCP4.5 and 8.5. The model was evaluated with yield reference data and measurement data of the leaf area index and soil moisture from Reckenholz 2022. The evaluation showed a satisfactory performance regarding yield simulation, but LAI and soil moisture were not simulated accurately. Based on their simulation performance, the crop parameter files 'SOY0906.CAB' and 'SOYBEAN.W41' were chosen as inputs for the model application. The outputs of the model application focusing on climate impacts differed mainly regarding the two crop parameter files. With crop file w41, a general increase in soybean yield was simulated under climate change scenarios, while with 906, a decline was projected. The main difference between the study sites was, that a higher amount of dry stress days was simulated for Changins, which lead to the conclusion that additional irrigation might become necessary at this site in the near future. In all scenarios and at both locations, a shift towards earlier projected flowering and maturity dates was observed. Due to limitations and uncertainties of the model simulations and climate change projections, further research is recommended. This concerns, inter alia, the parameterization of the model with additional data, and a consideration of CO₂ fertilization effects.

Acknowledgements

I would like to express my gratitude to my supervisor Annelie Holzkämper, who guided and supported me with her expertise during the research and writing process of this master thesis. Also, I would like to thank Bharath Arun and Sabina Kurmann for their motivation and helpful advice.

Table of Contents

List of Tables.....	v
List of Figures.....	vi
Abbreviations	viii
1 Introduction	1
1.1 Objectives	2
1.2 Climate Change in Switzerland	2
1.3 Study Sites.....	3
1.4 Impacts on Soybean Yield.....	5
2 Data	7
2.1 Historical Weather Data by Site.....	7
2.2 Soybean Data by Site.....	7
2.2.1 Yield.....	7
2.2.2 Irrigation.....	8
2.2.3 Sowing and Harvest Dates.....	8
2.3 Soil Data	9
2.4 Climate Projections	10
3 Methodology.....	12
3.1 Field Measurements.....	12
3.2 WOFOST Model Description	14
3.2.1 Soybean Crop Files.....	15
3.3 Model Evaluation.....	15
3.4 Model Application.....	17
4 Results	18
4.1 Leaf Area Index Measurements	18
4.2 Soil Moisture Measurements	19
4.3 Model Evaluation.....	21
4.3.1 Yield.....	21
4.3.2 Leaf Area Index and Flowering.....	26
4.3.3 Soil Water Content	28
4.4 Model Application.....	29
4.4.1 Absolute and Relative Change of Median Yield.....	29
4.4.2 Time Series: Crop File 906.....	30
4.4.3 Time Series: Crop File w41	33
5 Discussion.....	37
5.1 Leaf Area Index Simulation	37
5.2 Soil Moisture Simulation.....	38

5.3	Yield Simulation	40
5.4	Impacts of Climate Change	42
5.4.1	Yield and Drought Stress	42
5.4.2	Flowering and maturity	44
5.5	Limitations	45
5.6	Future Research Ideas	45
6	Conclusion.....	47
7	References.....	48
8	Appendix.....	56
8.1	Results	56
8.1.1	Measurements - Soil Moisture	56
8.1.2	Model evaluation - Yield	57
8.1.3	Model evaluation – Soil water content	63
8.1.4	Model application – raw data	64
8.1.5	Model application – moving average	68
8.1.6	Model application – tables	72
8.2	Discussion – LAI	74

List of Tables

Table 1: Information on study sites Changins and Reckenholz.	4
Table 2: Weather data parameters from IDAweb with unit and abbreviation	7
Table 3: Sowing and harvest dates of the Changins and Reckenholz Agroscope variety tests	9
Table 4: Soil profile information for plot 106N of the 2022 Reckenholz soybean variety trials.	9
Table 5: Soil hydraulic parameters computed with pedotransfer functions euptfv2.....	10
Table 6: Meteorological variables from CH2018 datasets.	10
Table 7: CH2018 model chains used for WOFOST simulations.	10
Table 8: WOFOST default soybean crop files, their corresponding region and a selection of their parameters	15
Table 9: Goodness of fit functions from the R package 'hydrogof'.	16
Table 10: Statistical goodness of fit measures for simulated and observed yield in Changins from 2006 to 2022.	22
Table 11: Statistical goodness of fit measures for simulated and observed yield in Reckenholz from 2014 to 2022.	22
Table 12: Statistical goodness of fit measures for simulated and observed LAI in Reckenholz, 2022.	27
Table 13: Statistical goodness of fit measures for simulated and observed soil water content in Reckenholz, 2022.....	29
Table 14: Median simulated yield [kg/ha] over four time periods: 1981-2010, 2020-2049, 2045-2074, 2070-2099.	29
Table 15: Statistical goodness of fit measures for simulated and observed yield in Changins and Reckenholz.....	57
Table 16: Statistical goodness of fit measures for simulated and observed soil water content in Reckenholz from June 10 to July 27, 2022.	63
Table 17: Median, mean, minimum, maximum, and standard deviation of simulated variable (yield, dry stress days, flowering, maturity) during four time periods (1981-2010, 2020-2049, 2045-2074, 2070-2099). Simulation with crop file 906, in Changins.....	72
Table 18: Median, mean, minimum, maximum, and standard deviation of simulated variable (yield, dry stress days, flowering, maturity) during four time periods (1981-2010, 2020-2049, 2045-2074, 2070-2099). Simulation with crop file 906, in Reckenholz.	72
Table 19: Median, mean, minimum, maximum, and standard deviation of simulated variable (yield, dry stress days, flowering, maturity) during four time periods (1981-2010, 2020-2049, 2045-2074, 2070-2099). Simulation with crop file w41, in Changins.....	73
Table 20: Median, mean, minimum, maximum, and standard deviation of simulated variable (yield, dry stress days, flowering, maturity) during four time periods (1981-2010, 2020-2049, 2045-2074, 2070-2099). Simulation with crop file w41, in Reckenholz.	73

List of Figures

Figure 1: Total soybean dry yield [t], total soybean dry yield per area [kg/ha] and area [ha] covered by soybean cultivation in Switzerland from 1988 to 2021.	1
Figure 2: Temperature (yearly mean) deviation from REF on the Swiss Plateau	3
Figure 3: Projected monthly mean temperatures at the study sites by the end of the century (2085), under RCP4.5 and RCP8.5.	4
Figure 4: Projected monthly mean precipitation at the study sites by the end of the century (2085), under RCP4.5 and RCP8.5.	5
Figure 5: Soybean dry yield from variety tests in Reckenholz and Changins	7
Figure 6: Soybean dry yield variation of the varieties Merlin and M. Arrow in Changins and Reckenholz	8
Figure 7: Plot 106N in REH, plan of parcels.	12
Figure 8: PR2 Profile probe with data logger.	13
Figure 9: Plot 48 affected by lodging	13
Figure 10: Leaf Area Index (LAI) measurements during the growing season of soybeans in Reckenholz 2022.....	18
Figure 11: Soil moisture logger data, parcel 8, Reckenholz 2022.	19
Figure 12: Soil moisture measurements by soil depth.....	20
Figure 13: WOFOST yield simulations with all soybean crop files for CGI and REH.....	21
Figure 14: WOFOST simulated soybean yield with crop file 906 and observed (reference) yield values.....	23
Figure 15: WOFOST simulated soybean yield with crop file w41 and observed (reference) yield values.	24
Figure 16: Simulated dry stress days and yield with crop files 906 and w41 for the locations Changins and Reckenholz.....	25
Figure 17: Leaf-Area-Index measurements of Merlin and M. Arrow in REH, 2022, and WOFOST-simulated LAI.....	26
Figure 18: Observed and simulated soil water content and daily precipitation sum in REH, 2022.	28
Figure 19: Simulation of yield, dry stress days, day of flowering and day of maturity in Changins (906), 1981-2099 with climate data of different model chains from CH2018.	31
Figure 20: Simulation of yield, dry stress days, day of flowering and day of maturity in Reckenholz (906), 1981-2099 with climate data of different model chains from CH2018.....	32
Figure 21: Simulation of yield, dry stress days, day of flowering and day of maturity in Changins (w41), 1981-2099 with climate data of different model chains from CH2018.....	34
Figure 22: Simulation of yield, dry stress days, day of flowering and day of maturity in Reckenholz (w41), 1981-2099 with climate data of different model chains from CH2018.	35
Figure 23: Soil water content [% vol.] on parcel 8, REH, 2022.....	56
Figure 24: Simulated yield and observed yield, crop file 901.	58
Figure 25: Simulated yield and observed yield, crop file 902.	59

Figure 26: Simulated yield and observed yield, crop file 903.	60
Figure 27: Simulated yield and observed yield, crop file 904.	61
Figure 28: Simulated yield and observed yield, crop file 905.	62
Figure 29: Simulation of yield, dry stress days, day of flowering and day of maturity in Changins (906), 1981-2099 with climate data of different model chains from CH2018.	64
Figure 30: Simulation of yield, dry stress days, day of flowering and day of maturity in Changins (w41), 1981-2099 with climate data of different model chains from CH2018.	65
Figure 31: Simulation of yield, dry stress days, day of flowering and day of maturity in Reckenholz (906), 1981-2099 with climate data of different model chains from CH2018.	66
Figure 32: Simulation of yield, dry stress days, day of flowering and day of maturity in Reckenholz (w41), 1981-2099 with climate data of different model chains from CH2018.	67
Figure 33: Simulation of yield, dry stress days, day of flowering and day of maturity in Changins (906), 1981-2099 with climate data of different model chains from CH2018 (moving average).	68
Figure 34: Simulation of yield, dry stress days, day of flowering and day of maturity in Changins (w41), 1981-2099 with climate data of different model chains from CH2018 (moving average).	69
Figure 35: Simulation of yield, dry stress days, day of flowering and day of maturity in Reckenholz (906), 1981-2099, with climate data of different model chains from CH2018 (moving average).	70
Figure 36: Simulation of yield, dry stress days, day of flowering and day of maturity in Reckenholz (w41), 1981-2099, with climate data of different model chains from CH2018 (moving average)	71
Figure 37: Simulated LAI and flowering with crop file w41 for Reckenholz, 2017, 2018, 2020, 2021.	74

Abbreviations

WOFOST	World Food Studies (crop simulation model)
CGI	Changins (study site)
REH	Reckenholz (study site)
M. Arrow	Maple Arrow (soybean variety)
LAI	leaf area index [$\text{m}^2 \cdot \text{m}^{-2}$]
DVS	development stage (WOFOST variable)
MG	maturity group
DOY	day of the year (day number)
TSUM	temperature sum
IPCC	Intergovernmental Panel on Climate Change
RCP	Representative Concentration Pathway
GCM	Global Climate Model
RCM	Regional Climate Model
REF	reference period (1981-2010)
GHG	greenhouse gas

1 Introduction

Soybeans (*Glycine Max*) have been cultivated for 4000 to 5000 years and are currently the most widely grown legume in the world (Kothari et al., 2022; Tanwar & Goyal, 2021). Containing high amounts of protein and oil, soybeans provide nutrition to millions of people and are of utmost importance as an ingredient for animal feed on an international scale (Tanwar & Goyal, 2021). In Switzerland, soybean breeding was introduced in 1981, and cultivation started in 1988 (Roth et al., 2022). Since 1988, the total soybean cropland area and the total amount of soybean yield are listed in the statistics of the Swiss farmer's association. Both varied over time, however in recent years, a growing cropland area is observed (Agristat, 2022), which is depicted in Figure 1.

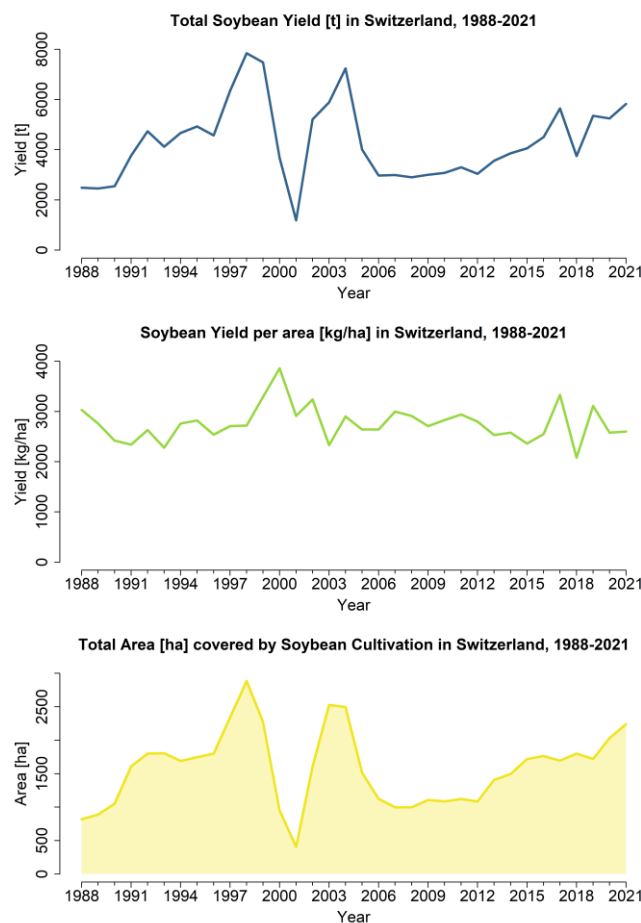


Figure 1: Total soybean dry yield [t], total soybean dry yield per area [kg/ha] and area [ha] covered by soybean cultivation in Switzerland from 1988 to 2021 according to Agristat (2022).

Klaiss et al. (2020) states, that “organic soybean cultivation experiences an upscale at the moment in Switzerland”, and that soybean cultivation is projected to further increase, inter alia due to warmer summers in the future. In addition to their nutritional values, soybeans prove to be interesting from an ecological perspective, as they do not require supplementary treatments of nitrogen. Specifically in Switzerland, the demand for domestically produced animal feed is expected to increase, since starting in 2022, the law requires organic farmers to use feed for ruminants exclusively from Switzerland (Klaiss, 2019). Accordingly, Klaiss (2019) presumes that, due to their high protein content, soybeans and lupines will be used more frequently as animal feed. Therefore, soybeans have a lot of potential for increased cultivation in Switzerland, above all in the context of climate change (Klaiss et al., 2020).

The major purpose of this study is thus to examine the future perspectives for soybean cultivation in Switzerland under changing climatic conditions. Multiple studies have assessed the possible impacts of climate change on soybean production on a global scale; Feng et al. (2021), Fodor et al. (2017) and Soares et al. (2021) worked with species distribution models to simulate future suitability for soybean cultivation. They all mention a shift of the areas considered suitable for soybean cultivation to higher latitudes in the northern hemisphere. According to Feng et al. (2021), large areas from western to eastern Europe are expected to become more suitable to grow soybeans. Soares et al. (2021) also mention a high likelihood of increasing suitability in this region with decreasing cold stress under climate change scenarios. According to Müller-Ferch et al. (2019), besides the ubiquitous general temperature increase, expected climatic changes in Switzerland include more hot days, drier summers, winters with less snow and heavier precipitation events. A sufficient number of warm days is required for soybeans to reach maturity. In addition, soil temperatures lower than 8°C during germination are associated with decreasing soybean yield and plant density (Karges et al., 2022). Therefore, soybeans could potentially benefit from the projected warmer spring and summer temperatures in central Europe (Klaiss et al., 2020).

To investigate possible impacts of climate change on soybean productivity on the Swiss Plateau, the crop growth model WOFOST (de Wit et al., 2014) is applied. WOFOST has been used as an operational crop growth model for yield forecasting for 30 years, notably as part of the European crop yield forecasting system MARS. It exists in different implementations and has been updated and extended several times (de Wit et al., 2019). To the best of our knowledge, no prior study has assessed the future potential for soybean cultivation in Switzerland using a modelling approach with WOFOST. In addition, research regarding soybean yield simulations with any crop model in Switzerland seems to be lacking. In this master thesis, WOFOST will be evaluated for soybean yield simulations on the Swiss Plateau, using the locations Changins and Reckenholz as study sites. The evaluation approach will be enhanced by incorporating leaf area index and soil moisture data obtained from field measurements during the soybean growing season of 2022 in Reckenholz.

1.1 Objectives

This thesis aims at assessing the impacts of climate change on soybean yield production on the Swiss Plateau considering uncertainties from climate projections as well as from WOFOST model simulations. Therefore, the first objective is to evaluate the performance of the WOFOST model regarding the simulation of soybean yield with seven different default crop parameter files, which are already included in WOFOST. As part of the first objective, it will additionally be evaluated how well WOFOST simulates the soybean leaf area index and soil moisture. It is then the goal to select, based on the performance in the model evaluation, two crop parameter sets, with which to conduct a model application with climate scenario data. The second aim of this master thesis is to estimate how climate change could affect the yield of soybeans cultivated on the Swiss Plateau.

1.2 Climate Change in Switzerland

Switzerland is situated in the temperate climate zone (Roth et al., 2022) and is influenced by the westerlies. Its diverse topography results in considerable spatial and altitudinal gradients of climatic conditions (CH2018, 2018b). In Figure 2, the projected increase in yearly mean temperatures on the Swiss plateau is shown. Since 1864, the near-surface air temperature in Switzerland has increased by roughly 2°C, which is more than the global average of 0.9°C. As a consequence, strong impacts are already evident in the bio- and cryosphere; the vegetation

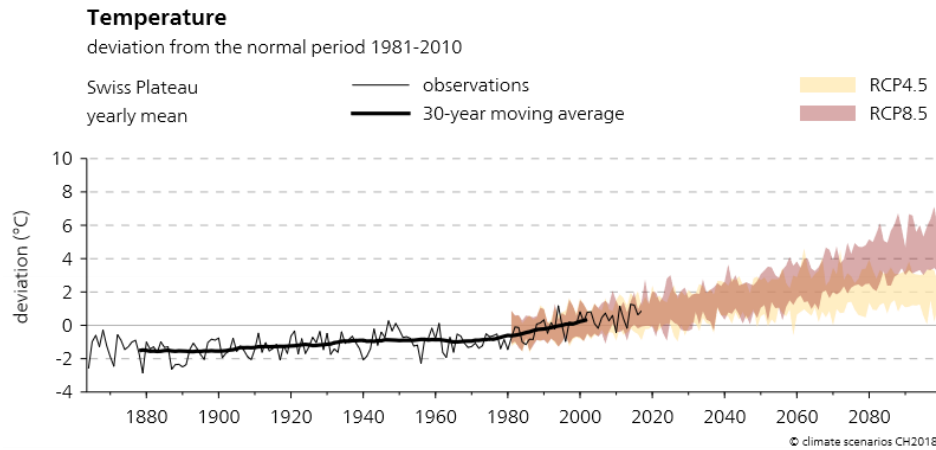


Figure 2: Temperature (yearly mean) deviation from REF on the Swiss Plateau (NCCS, 2018).

period has lengthened and glacial volumes in the Alps have decreased. Throughout the 21st century, temperatures are projected to continue to increase. This applies to all seasons and all regions of Switzerland. The warming will affect summer temperatures more than winter temperatures, but the extent of warming at the end of the century is highly dependent on the Representative Concentration Pathway (RCP). The RCPs are emission scenarios used in the IPCC reports. They are defined by the level of radiative forcing [Wm^{-2}] occurring at the end of the century. In RCP2.6, the increase in global mean temperatures is stabilized below 2°C , which requires a strong reduction of GHG emissions at the beginning of the 21st century. Under RCP4.5, emissions decrease after 2050 and the global mean temperature will rise by approximately 2.5°C . RCP8.5 is the unabated emission scenario, where radiative forcing continues to increase to 8.5 Wm^{-2} , and global mean temperatures will increase between 4 and 5°C . Trends regarding precipitation are less clear, as they vary regarding the considered region, season, and RCP. In the long term due to the increasing temperatures, it is likely that precipitation will increase in the colder months and decline in the warmer season. Nevertheless, these trends might be masked or enhanced by a generally large natural variability (CH2018, 2018b).

With climate change, the characteristics and frequencies of extreme events are affected. Particularly in the context of rising summer temperatures, extreme events such as heatwaves and very hot days are projected to occur more frequently. These events are also estimated to become more long-lasting and intense. Heavy precipitation events are also projected to become more intense throughout the year, with peak events intensifying more than the mean precipitation. Due to the strong warming in summers, longer dry spells and fewer wet days are expected by the end of the century under RCP8.5. Although there is more uncertainty regarding the extent of a drying tendency compared to trends in temperature and precipitation extremes, a strong warming under RCP8.5 could lead to drier soils and therefore an intensification of agricultural droughts (CH2018, 2018b).

1.3 Study Sites

In this study, simulations with WOFOST will be performed for two sites on the Swiss Plateau. Since daily weather data needs to be available for the simulations, the chosen study sites have weather stations. The study sites used in this master thesis are Changins and Reckenholz, which are both Agroscope research stations. The weather stations are part of the SwissMet-Net, which is an automatic weather and climate monitoring network managed by MeteoSwiss (n.d.). Reckenholz and Changins lie on the outskirts of Zurich and Nyon, respectively. Both

locations are surrounded by agricultural areas. In Table 1, some general informations on the study sites are displayed.

Table 1: Information on study sites Changins and Reckenholz, according to MeteoSwiss (2023).

Station	Changins	Zürich Affoltern / Reckenholz
Abbreviation	CGI	REH
Latitude / Longitude	46.401053 / 6.227722	47.427694 / 8.517953
Weather Station Height	458 m. a. sea level	444 m. a. sea level
Exposition	hill (30-100m above valley)	plain

Under climate change scenarios (NCCS, 2018), the temperatures are projected to rise at both study sites and in all their seasons, which is shown in Figure 3. It can also be seen in this figure, that the temperatures in Changins are generally slightly higher than in Reckenholz. By the end of the century, the mean monthly temperature in July is projected to rise by 2 to 3°C under RCP4.5, while under RCP8.5, the increase is more pronounced with approximately +5°C at both study sites (NCCS, 2018).

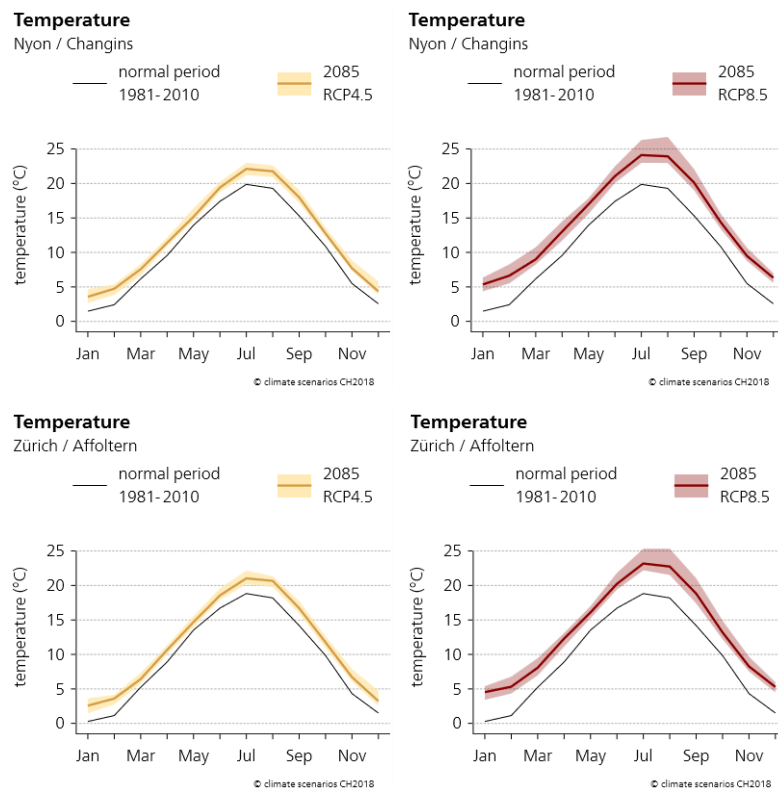


Figure 3: Projected monthly mean temperatures at the study sites by the end of the century (2085), under RCP4.5 and RCP8.5 (NCCS, 2018).

In Changins and Reckenholz, changes in monthly precipitation amounts are projected with climate change, but they differ according to the season. In Figure 4, one can see that Reckenholz generally has more summer precipitation than Changins, which applies to the reference period and the end-of-century projection. While in the spring months, precipitation is projected to increase by 2085 at both locations and under both RCPs, summer precipitation shows a decreasing trend. The decline of precipitation in the months of July to September is particularly pronounced in Changins under RCP8.5. However, as mentioned in chapter 1.2, trends regarding precipitation are more uncertain than trends regarding the temperature

development in the future. The whiskers in Figure 4 depict the 5-95% model range; when considering the whiskers, one can see that some model chains predict a less strong reduction in summer precipitation or even a slight increase (CH2018, 2018b; NCCS, 2018).

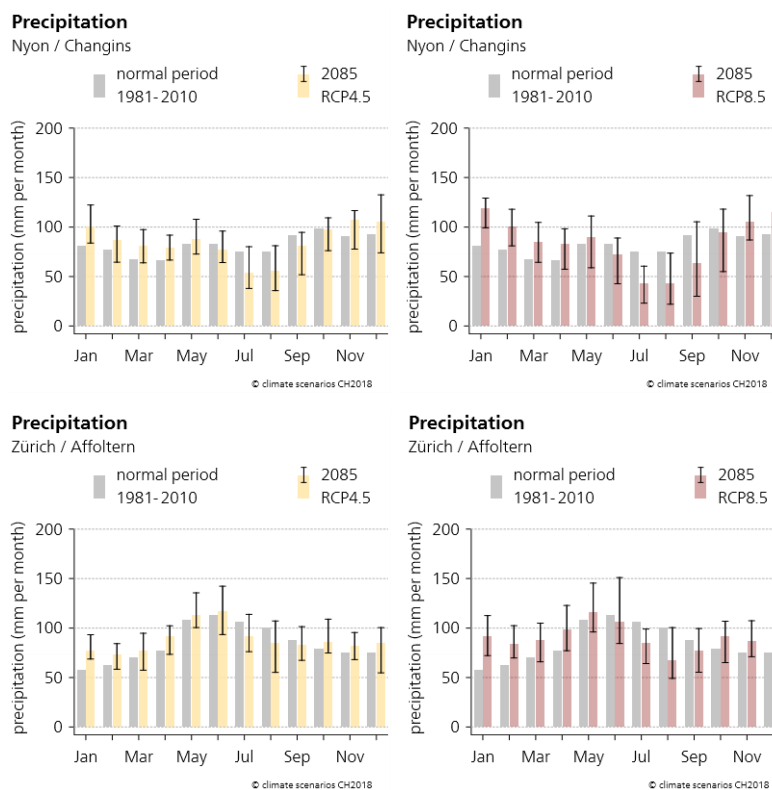


Figure 4: Projected monthly mean precipitation at the study sites by the end of the century (2085), under RCP4.5 and RCP8.5 (NCCS, 2018). The bars represent the median values of the model ensemble, while the whiskers show the 5-95% model range (CH2018, 2018b; NCCS, 2018).

1.4 Impacts on Soybean Yield

Soybeans are thermophilic plants. According to Nendel et al. (2023), although sensitivity to cold temperatures varies from cultivar to cultivar, it is generally agreed upon in literature, that temperatures below 10°C can significantly impair plant growth. Heat stress studies identified a range between 25 and 35°C as optimal for photosynthesis, while a short exposure to temperatures above 45°C can lead to irreversible damage to the plant's ability to perform photosynthesis (Board & Kahlon, 2011). Accordingly, as the maximum temperatures in Switzerland seldomly pose a risk to plant development, current efforts regarding soybean cultivation in this region mostly focus on a sufficient cold tolerance during the early growth stages (Roth et al., 2022). This might change in the future due to climate change impacts, as rising temperatures and atmospheric CO₂ concentrations will contribute the reduction of cold stress and an increase in crop productivity (Nendel et al., 2023). These positive effects can however be hampered by increasing drought stress, which is why breeding efforts in Switzerland currently include a better drought tolerance (Klaiss et al., 2020). Drought stress occurring after flowering, between the pod and seed initiation is considered to have the highest negative impact on yield formation (Board & Kahlon, 2011).

Soybean crops are sensitive to photoperiod and display a short-day plant behaviour, which affects yield potentials in northern latitudes. The duration of phenological stages as well as the onset of flowering are strongly impacted by the photoperiod. As soybeans are short-day plants, varieties had to be adapted to the typically long photoperiods in Europe and northern areas,

which led to the emergence of early-maturing cultivars. The classification of soybean varieties to maturity groups depends on their response to photoperiod and temperatures. Current classifications include thirteen maturity groups, ranging from the very early MG “000” to “X”, the very late maturing cultivars (Elmerich et al., 2023; Schoving et al., 2020). The very early maturing cultivars are known to produce lower yields than late ones, which shows that the length of the growing season is still an important constraining factor on the cultivation of soybeans in Europe (Nendel et al., 2023). However, as the length of the vegetation period will increase with rising temperatures in Switzerland (Calanca & Holzkämper, 2010), later maturing soybean varieties might be cultivated in the region, as noted by Nendel et al. (2023).

2 Data

2.1 Historical Weather Data by Site

For simulations conducted with WOFOST for Reckenholz and Changins, past weather data from the local weather station must be available. WOFOST requires daily weather data, which was obtained from the IDAweb data portal (MeteoSwiss, 2022d). The parameters which were used as inputs are presented in Table 2.

Table 2: Weather data parameters from IDAweb with unit and abbreviation (MeteoSwiss, 2022d).

Parameter	Unit	IDAweb abbreviation
Global radiation (daily mean)	[W·m ⁻²]	gre000d0
Daily minimum temperature at 2m above ground	[°C]	tre200dn
Daily maximum temperature at 2m above ground	[°C]	tre200dx
Vapour pressure at 2m above ground (daily mean)	[hPa]	pva200d0
Wind speed (daily mean)	[m·s ⁻¹]	flk010d0
Precipitation (daily sum)	[mm]	rka150d0

The weather data input for WOFOST must be in a CABO-format file, whose syntax is specified in Boogaard et al. (2021). The conversion of the weather data from IDAweb to the CABO-format was conducted with R.

2.2 Soybean Data by Site

The data introduced in the following subchapters (2.2.1 to 2.2.3) was obtained exclusively from Agroscope soybean variety tests (Agroscope 2006a - 2022a). In Changins, soybean data was available from 2006 to 2022, and in Reckenholz from 2014 to 2022.

2.2.1 Yield

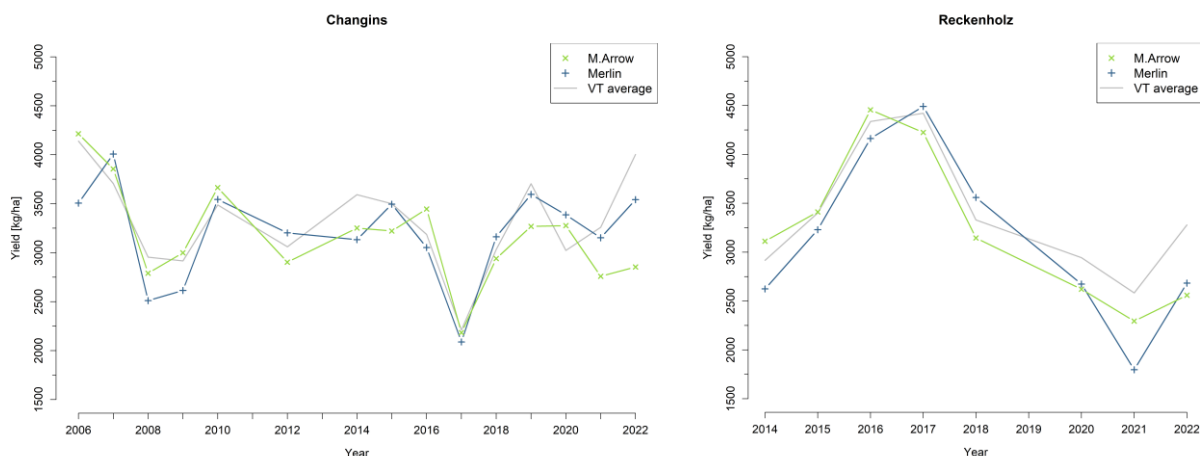


Figure 5: Soybean dry yield from variety tests in Reckenholz and Changins (Agroscope 2006a - 2022a).

At the chosen study locations, soybean yield data must be available to serve as a reference for the simulated WOFOST output. Moreover, in addition to the yield data, the corresponding sowing and harvest dates are also required for an accurate model output. All of the aforementioned data can be obtained from variety tests conducted by Agroscope from 2006 to 2022 in Changins, and from 2014 to 2022 in Reckenholz. The type and number of the tested soybean varieties differed each year, however, the varieties Merlin and M. Arrow were always included. Figure 5 shows the yearly mean dry yield from Merlin, M. Arrow and a yearly average over the yields of all tested varieties in Changins and Reckenholz. The mean yield of one variety

consists of all yields generated on the different parcels on which a variety was grown. Typically, a variety was tested on three to four parcels, each with an area between approximately ten and twelve square metres. In Figure 7 (chapter 3.1), a map from the plot of the 2022 soybean variety trials is displayed. As seen in the figure, there is no yield data for the years 2011 and 2013 in Changins, as well as for the year 2019 in Reckenholz. In those years, crop failures occurred due to different reasons. In 2011, dry weather conditions in spring as well as weeds inhibited the development of the soybean plants. The crops were destroyed by a hailstorm in 2013. In 2019, phytotoxicity occurred when herbicides were applied to the soybean plot in Reckenholz (Agroscope 2006a - 2022a).

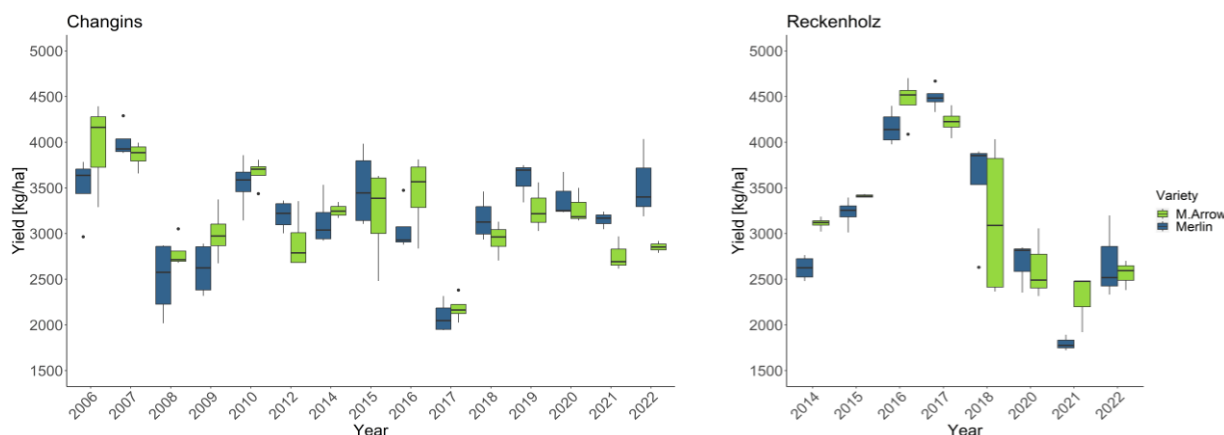


Figure 6: Soybean dry yield variation of the varieties Merlin and M. Arrow in Changins and Reckenholz (Agroscope 2006a - 2022a).

As seen in Figure 6, the yields from Merlin and M. Arrow differ from each other to various degrees each year. The varieties belong to different maturity groups. According to Agroscope (2006a - 2022a), Merlin belongs to group “000”, while M. Arrow is in maturity group “00”, meaning that Merlin matures earlier than M. Arrow (Mourtzinis & Conley, 2017). According to Zimmer et al. (2016), the Merlin variety produces stable yields even under cool growing conditions, which is why it is widely used for cultivation in Central Europe. Serafin-Andrzejewska et al. (2021) state that in Germany and Poland, Merlin is considered the most productive soybean variety. Maple Arrow is a soybean cultivar originating from Canada. Between 1971 and 2000, when the Ontario Province experienced a drastic increase in soybean production, Maple Arrow was often used as a parent cultivar for breeding (Cober & Voldeng, 2012).

2.2.2 Irrigation

The plots where the variety tests of Reckenholz took place were not irrigated, since there is no irrigation infrastructure available at this location. In contrast, the variety testing plots in Changins were irrigated if the soybean plants required water. The irrigation data was acquired from the Agroscope (2006b - 2022b) research station in Changins and subsequently added to the daily precipitation sum in the CABO-files, as there is no other option to add irrigation events to the WOFOST model input (Boogaard et al., 2021).

2.2.3 Sowing and Harvest Dates

In Table 3, the sowing and harvest dates of the Agroscope variety tests in Changins and Reckenholz from 2006 to 2022 are displayed. Both sowing and harvest dates were used as input for the soybean yield simulation during this period. The dates shown in this table apply to all tested cultivars. During the variety tests, no phenology data was collected. Therefore, for

example the dates of crop emergence, flowering and the exact date of maturity are unknown for the cultivars grown during the Agroscope variety tests.

Table 3: Sowing and harvest dates of the Changins and Reckenholz Agroscope variety tests (Agroscope 2006a - 2022a).

Year	CGI Sowing	REH Sowing	CGI Harvest	REH Harvest
2006	03/05/2006	-	28/09/2006	-
2007	01/05/2007	-	08/10/2007	-
2008	09/05/2008	-	02/10/2008	-
2009	09/05/2009	-	02/10/2009	-
2010	25/05/2010	-	06/10/2010	-
2012	14/05/2012	-	02/10/2012	-
2014	05/05/2014	21/05/2014	25/09/2014	20/10/2014
2015	11/05/2015	13/05/2015	22/09/2015	25/09/2015
2016	04/05/2016	05/05/2016	14/09/2016	30/09/2016
2017	18/05/2017	13/05/2017	05/09/2017	09/10/2017
2018	04/05/2018	19/04/2018	04/09/2018	29/08/2018
2019	01/05/2019	-	20/09/2019	-
2020	08/05/2020	08/05/2020	15/09/2020	19/10/2020
2021	28/05/2021	14/05/2021	24/09/2021	12/10/2021
2022	03/05/2022	12/05/2022	08/09/2022	22/09/2022

2.3 Soil Data

Soil data was available for the plot 106N in Reckenholz, where soybeans were cultivated for the 2022 variety tests. The soil of plot 106N is of the type Cambisol (Hanic & Petrsek, 1991). In Table 4, the specific soil profile information assembled by Hanic et al. (2020), is shown. The soil profile information of Table 4 was used to calculate hydraulic parameters required as inputs for the WOFOST soil file.

Table 4: Soil profile information for plot 106N of the 2022 Reckenholz soybean variety trials, according to Hanic et al. (2020). The clay, silt and humus content, as well as the pH-value, were derived via laboratory analysis. The gravel and stone fractions are estimations.

Soil Horizon	Soil depth [cm]	Clay content, weighted %	Silt content, weighted %	Humus content, weighted %	Organic carbon content %	Gravel fraction, vol.%	Stone fraction, vol.%	pH (H ₂ O)
Ah,p	0-25	22.7	24.9	2.5	1.45	2	0	5.9 L
Bw,cn	25-50	22.2	25.8	0.9	0.52	2	0	6.1 L
Bcn	50-80	21.2	22.0	0	0	0	0	6.2 L
BCg	80-110	11.5	22.1	0	0	0	0	6.6 L

The required hydraulic parameters are shown in Table 5. For the calculation of the parameters, the second version of the European pedotransfer functions (euptfv2), developed by Szabó et al. (2021), was used. The WOFOST soil file with the hydraulic parameters from Table 5 was used for all simulations conducted for both study sites throughout this research. Since the yearly variety tests did not always take place on the same plot, uncertainties in relation to the hydraulic parameters must be taken into consideration.

Table 5: Soil hydraulic parameters computed with pedotransfer functions euptfv2 (Szabó et al., 2021).

SMW	SMFCF	SMO	KO
soil moisture content at wilting point [cm ³ ·cm ⁻³]	soil moisture content at field capacity [cm ³ ·cm ⁻³]	soil moisture content at saturation [cm ³ ·cm ⁻³]	hydraulic conductivity of saturated soil [cm·day ⁻¹]
0.1544942	0.3172108	0.4002358	36.41509

2.4 Climate Projections

For the WOFOST application, climate change projection data was used as model input. Localized projection data from the CH2018 climate scenarios is available for numerous Swiss weather stations, including the stations Zürich Affoltern / Reckenholz and Changins / Nyon (CH2018, 2018a). CH2018 projection data is derived from the EURO-CORDEX ensemble of climate simulations. The EURO-CORDEX ensemble produces simulations with RCM (regional climate models), the centre of the model domain being western Europe. Simulations with CGM (global climate models) determine the boundary conditions of the EURO-CORDEX model domain. To generate the localized projection data used in this thesis, the EURO-CORDEX RCM simulations were statistically downscaled (CH2018, 2018b). The datasets obtained from the CH2018 Project Team (2018) consist of daily time series data for a certain weather station and are available from 1981 to 2099 (CH2018, 2018a). The meteorological variables used to create climate input files for WOFOST are presented in Table 6.

Table 6: Meteorological variables from CH2018 datasets (CH2018, 2018a).

Abbreviation	Variable	Unit
hurs	Daily mean relative humidity	%
pr	Daily precipitation sum	[mm]
rsds	Daily mean global radiation	[W·m ⁻²]
sfcWind	Daily mean near-surface wind speed	[m·s ⁻¹]
tasmax	Daily maximum 2m temperature	[°C]
tasmin	Daily minimum 2m temperature	[°C]

The localized CH2018 datasets include meteorological variables simulated with various model chains. In this research, data from seven different model chains was used (see Table 7). The EURO-Cordex RCM simulations were conducted with a common model grid at two resolutions: EUR11, which corresponds to a grid spacing of approximately 12km, and EUR44, which corresponds to about 50km (CH2018, 2018b).

Table 7: CH2018 model chains used for WOFOST simulations (CH2018, 2018a).

GCM	RCM	Resolution	RCP
DMI-HIRHAM	ECEARTH	EUR11	4.5 8.5
DMI-HIRHAM	ECEARTH	EUR44	4.5 8.5
KNMI-RACMO	ECEARTH	EUR44	4.5 8.5
KNMI-RACMO	HADGEM	EUR44	4.5 8.5
SMI-RCA	CCCMA	EUR44	4.5 8.5
SMI-RCA	ECEARTH	EUR44	4.5 8.5
SMI-RCA	HADGEM	EUR44	4.5 8.5

For the analysis of the CH2018 data, three time periods were defined during which average climatic conditions can be described (MeteoSwiss, 2022c). These time periods were used in the CH2018 technical report and the 'Webatlas', where visualized data from the CH2018 scenarios is provided (CH2018, 2018b; NCCS, 2018). The time periods are grouped around the years 2035 (near future period), 2060 (mid-century period) and 2085 (end of century period). Therefore, '2035' / 'near future' refers to the period between 2020 and 2049, '2060' / 'middle of the century' refers to the period from 2045 to 2074, and '2085' / 'end of the century' refers to the period from 2070 to 2099. These three time periods were also used in this thesis to present and discuss the results of the climate impact analysis.

3 Methodology

3.1 Field Measurements

For the evaluation of the simulation performance of WOFOST, soil moisture content and leaf area index (LAI) were measured in Reckenholz during the summer of 2022. The obtained data was then used as a reference for comparisons with simulated LAI and soil moisture data.

In the growing season of 2022, a multitude of soybean varieties were grown on plot 106N, which is located in a protected site of the Reckenholz research compound. The location of the plot as well as the number and type of cultivars grown can vary from year to year. This applies to the variety tests in Reckenholz and Changins. The area of plot 106N was divided into cultivar-specific parcels of 12.3m² each (see Figure 7). Six of those parcels were chosen for conducting the measurements, three of which grew the variety Merlin and three of which grew the variety Maple Arrow. The major factor influencing the decision on which cultivar should be chosen for the measurements was the recurrence in the past variety tests, as the yield data of these varieties would later be used for the model evaluation. In Reckenholz 2022, the sowing date was on the 12th of May, and the harvest took place on the 22nd of September.

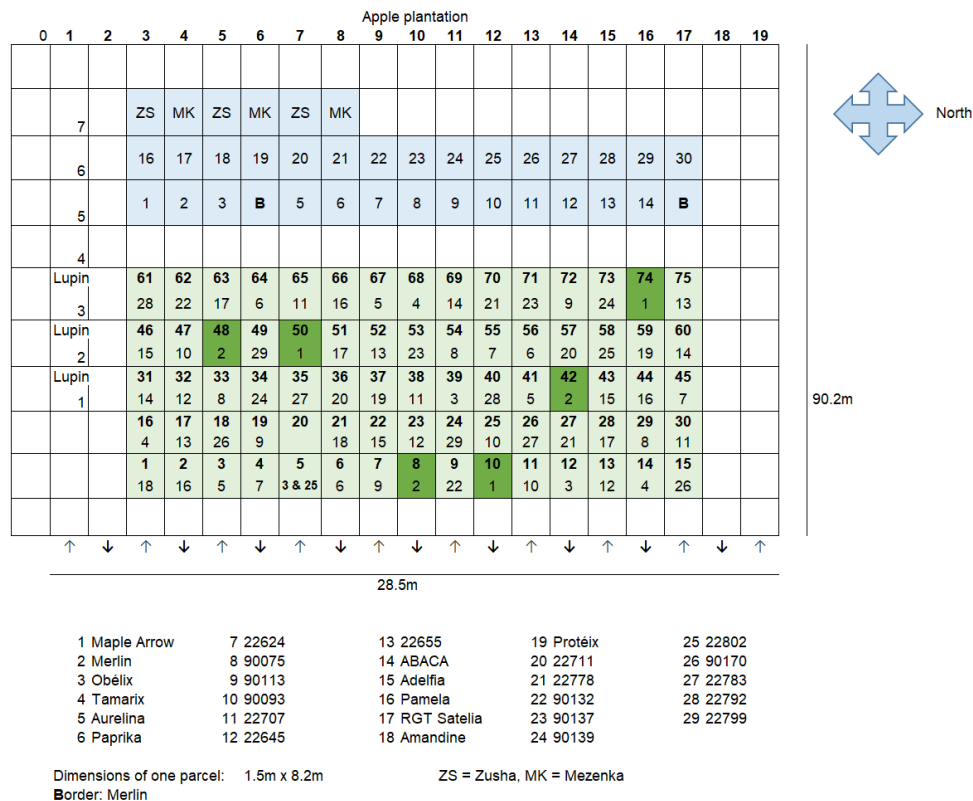


Figure 7: Plot 106N in REH, plan of parcels (Agroscope, 2022c).

The soil water content on parcel 8 (cultivar Merlin) was measured hourly with a PR2 Profile Probe (soil moisture profile sensor) of the brand Delta-T Devices Ltd. The resulting values were recorded by a data logger. With every measurement, the soil water content was determined at six depths: 100mm, 200mm, 300mm, 400mm, 600mm and 1000mm. The set up with a data logger device, as shown in Figure 8, was installed on the 1st of June and removed a few days before the harvest. Due to a battery failure, there is a lack of data from the end of July to the beginning of August. The soil moisture was also measured repeatedly in the other five parcels with the PR2 Profile Probe and a manual readout unit, the HH2 moisture meter, to

capture potential spatial differences in soil moisture between the parcels. In all six parcels, a probe was preinstalled to facilitate measurements. When using the HH2, the soil water content was measured three times on each parcel, meaning that the sensor was rotated by approximately 120° after the first and second measurement. The measurements with the HH2 moisture meter were conducted twice a month. As the PR2 profile probe had to be transferred to the other parcels, a dry canopy was required on the days where the HH2 measurements were conducted. Any moisture from the canopy being transferred onto the sensor could have falsified the following measurements in the other parcels.



Figure 8: PR2 Profile probe with data logger (box on the right) on plot 8, 01/06/23.

The leaf area index is dimensionless but can be seen as [m^2 leaf area / m^2 ground area] (LI-COR Biosciences, 2019). The LAI measurements were conducted on a weekly basis, starting on the 10th of June, after the emergence of the crop. LAI data was retrieved by a plant canopy analyser, the LAI-2200C of the brand LI-COR. On each of the six parcels, the LAI was generally determined at four different positions within the parcel. On a few measurement days however, the LAI was only determined at two or three positions due to impeding conditions, such as a wet canopy and lodging (plants are bent downwards, see Figure 9). The lodging of soybean



Figure 9: Plot 48 affected by lodging on 17/08/2023.

plants on some parcels created difficulties when measuring the LAI, as the lens of the plant canopy analyzer should generally not be too close to the leaves (LI-COR Biosciences, 2019). At each of the positions in the parcel, several readings had to be taken to determine the LAI, depending on the weather of the day. On days with direct sunlight shining on the canopy, a '4A Sequence' consisting of four above-canopy readings, was conducted at each position to reduce scattering errors. On days with uniform cloud overcasts, one above-canopy reading was sufficient (LI-COR Biosciences, 2019). After the above-canopy reading(s), four readings were taken below the canopy. Therefore, the LAI was determined with the above- and below-canopy readings at each of the four positions in a parcel. This resulted in a maximum of 12 LAI values for a cultivar on one measurement day, which were then averaged for comparison with the daily LAI simulated by WOFOST.

3.2 WOFOST Model Description

WOFOST (World Food Studies) is a mechanistic, dynamic crop simulation model developed by the school of De Wit at Wageningen University in the Netherlands. WOFOST simulates crop growth and production with time steps of one day, enabling the user to gain information on total biomass, crop yield, LAI development and water use, inter alia (de Wit & Boogaard, 2021). As inputs, WOFOST requires daily meteorological data, information on the simulation timing, as well as crop, soil and management data. The simulations deliver outputs for potential, water- and nutrient-limited scenarios (Boogaard et al., 2021). In this thesis, version 7.1.7 of WOFOST was used (de Wit et al., 2014). WOFOST simulates crop growth on the basis of eco-physiological processes in the following steps (de Wit & Boogaard, 2021):

CO₂-assimilation and respiration

WOFOST calculates the gross CO₂-assimilation rate of a crop based on the absorbed radiation and the photosynthesis-light response curve of the crop's leaves. The incoming radiation and the leaf area are used to calculate the radiation which is absorbed by the plant. The assimilates produced via photosynthesis are partly used for maintenance respiration. The rest of the carbohydrates can then be transformed to dry matter.

Phenological development

WOFOST utilizes the variable DVS (development stage), which is dimensionless, to describe crop phenological development. DVS is 0 at crop emergence, 1 at flowering, and 2 at maturity. DVS is a function of temperature, differs regarding crop and cultivar type, and can be impacted by the photoperiod. The concept of temperature sum / thermal time is used to explain the impact of temperature on the DVS. The temperature sum (TSUM) is defined as "[...] the integral over time of the daily effective temperature (Te) after crop emergence. Te is the difference between the daily average temperature and a base temperature below which no development occurs" (de Wit & Boogaard, 2021, p. 8). The division of the current TSUM by the TSUM necessary to reach the next development stage results in the current DVS. The DVS is an important variable in the WOFOST model, as it determines, inter alia, the specific leaf area and the partitioning of assimilates over the plant organs (de Wit & Boogaard, 2021).

Partitioning of dry matter

Partitioning describes the process of distributing assimilates produced by photosynthesis to different organs of the plant. Before DVS equals 1, most assimilates are transformed to root, leaf and stem tissue. After flowering, the largest part of assimilates are distributed to the storage organs. The partitioning is described by 'partitioning tables' in WOFOST, in which the fraction of assimilates allocated to the plant organs is defined as a function of DVS.

Transpiration

Transpiration occurs when water vapour diffuses from the open stomata of the crop to the atmosphere. The water loss caused by transpiration is compensated by water uptake from the soil. WOFOST computes the potential transpiration for a reference crop and adjusts it with a specific correction factor to account for differences between crops. The ratio of the actual over the potential transpiration is used as a reduction factor to the gross CO₂-assimilation rate of the crop in WOFOST, and therefore impacts the dry matter production of the plant (de Wit & Boogaard, 2021).

3.2.1 Soybean Crop Files

WOFOST 7.1 includes seven different default soybean ‘crop files’. The crop files contain crop-specific parameters and are used as input for the simulation. The parameters in each of these crop files are adjusted to the characteristics of soybean varieties typically grown in a certain region (Arumugam, 2021). Crop files for European regions were developed by Boons-Prins et al. (1993) in the context of the MARS project (de Wit et al., 2017). In Table 8, the default crop files and their associated regions are displayed. Simulations were conducted with all crop files for both study sites during the model evaluation and two crop files were chosen to conduct the model application focusing on climate impacts based on their respective goodness of fit.

Table 8: WOFOST default soybean crop files, their corresponding region and a selection of their parameters (de Wit et al., 2014).

Crop file name	SOY0901 .CAB	SOY0902 .CAB	SOY0903 .CAB	SOY0904 .CAB	SOY0905 .CAB	SOY0906 .CAB	SOY- BEAN .W41
Region	Northern France	Central France	Northern Spain	Southern France	Italy	Spain, Greece	Tropical regions
TSUM1	350	350	300	500	500	500	699
TSUM2	850	950	900	1100	1100	1300	1050
TSUMEM	70	70	70	70	80	90	70
LAIEM	0.0163	0.0163	0.0163	0.0163	0.0163	0.0163	0.063
CVO	0.480	0.480	0.480	0.480	0.480	0.480	0.720

Crop file	901 - 906		W41	
	DVS	AMAXTB	DVS	AMAXTB
AMAXTB	0	29	0	37
	1.7	29	1.7	37
	2	0	2	0

Crop files 901 to 906 mainly differ regarding the TSUM parameters. TSUMEM is the temperature sum from sowing to emergence. TSUM1 is defined as the temperature sum from crop emergence to anthesis, while TSUM2 is the temperature sum from anthesis to maturity. LAIEM is the LAI at emergence. AMAXTB is the maximum leaf CO₂-assimilation rate as a function of DVS. CVO is the conversion efficiency of assimilates to storage organs. Crop file w41 differs from the others to a larger extent. Besides the TSUM values, w41 also has differing parameters regarding LAI, assimilation, partitioning and conversion efficiency of assimilates into biomass (de Wit et al., 2014).

3.3 Model Evaluation

For the model evaluation, simulations were conducted for Changins and Reckenholz with the input data described in chapters 2.1 to 2.3. All default soybean crop files included in WOFOST were used to generate outputs for the years in which yield data from variety tests was available. The simulation output inter alia consists of the dry seed yield, which is described by the variable

TWSO (total weight of storage organs), the leaf area index and soil moisture. The simulated data was then compared to the measured LAI and soil moisture values from Reckenholz 2022 as well as the observed dry seed yields from all available years at both study sites. The comparison consisted of a visual and statistical evaluation. For the statistical evaluation, several goodness of fit functions, presented in Table 9, were considered.

Table 9: Goodness of fit functions from the R package 'hydroGOF' created by Zambrano-Bigiarini (2020). The function for the Pearson correlation coefficient (r) was obtained from Hartung, J. et al. (2002). N stands for the number of observations, while S refers to the simulated and O to the observed data points.

Abbreviation	Formula	Description
RMSE	$rmse = \sqrt{\frac{1}{N} \sum_{i=1}^N (S_i - O_i)^2}$	Root Mean Square Error
PBIAS%	$PBIAS = 100 * \frac{\sum_{i=1}^N (S_i - O_i)}{\sum_{i=1}^N O_i}$	Percent Bias
d	$d = 1 - \frac{\sum_{i=1}^N (O_i - S_i)^2}{\sum_{i=1}^N (S_i - \bar{O} + O_i - \bar{O})^2}$	Index of Agreement
md	$md = 1 - \frac{\sum_{i=1}^N O_i - S_i ^j}{\sum_{i=1}^N (S_i - \bar{O} + O_i - \bar{O})^j}$	Modified Index of Agreement
rd	$rd = 1 - \frac{\sum_{i=1}^N \left(\frac{O_i - S_i}{O_i}\right)^2}{\sum_{i=1}^N \left(\frac{ S_i - \bar{O} + O_i - \bar{O} }{\bar{O}}\right)^2}$	Relative Index of Agreement
r	$r = \frac{\sum_{i=1}^N (S_i - \bar{S})(O_i - \bar{O})}{\sqrt{\sum_{i=1}^N (S_i - \bar{S})^2 * \sum_{i=1}^N (O_i - \bar{O})^2}}$	Pearson correlation coefficient

The yield simulated by WOFOST was compared with three reference yield values: an average yield of all varieties tested in the yearly tests, and averages of the parcels with Merlin and M. Arrow soybean varieties. The model performance was then evaluated considering these three reference yields and the differences between them.

The LAI and soil moisture simulations could only be evaluated for 2022 at the site of Reckenholz. For the soil water content, reference data was available from the hourly measurements on parcel 8, which grew the variety Merlin. As WOFOST only provides one daily soil moisture value for the whole soil profile in the simulation output, the measured values of different soil depths had to be averaged. The soil profile used for all simulations has a depth of 110cm and the maximum rooting depth of soybeans can exceed 1m (Ordóñez et al., 2018). Considering this, the measured soil water content values of different depths were averaged without applying weights, as it can be expected that the plants are able to access soil water even in greater depths. As elaborated in chapter 3.1, the soil moisture was also measured on the five other parcels twice a month. The resulting data was then compared with the soil moisture data recorded by a logger on parcel 8, to detect possible differences between the parcels with Merlin and M. Arrow soybeans. The simulation performance of WOFOST regarding LAI could be evaluated with data from the weekly LAI measurements on six parcels. To facilitate a comparison, the LAI measurements of a cultivar had to be averaged per parcel and per day. Therefore, the simulated daily LAI values could be compared with a daily LAI of Merlin as well

as a daily LAI of M. Arrow. After evaluating the performance of WOFOST regarding the simulation of soybean yield, LAI and soil moisture, two crop files were determined to be applied as parameter inputs for the climate impact analysis.

3.4 Model Application

In the model application phase, the models were run with CH2018 projection climate data, so that the impact of climate change on the soybean yield in Reckenholz and Changins could be assessed. Data from seven model chains and two RCPs (4.5 and 8.5) was used for the simulations. Two crop parameter files as well as the soil profile information described in chapter 2.3 were used as model inputs. Besides the projected yields, the simulated yearly sum of dry stress days and days of flowering and maturity were also included in the climate impact analysis. The definition of a 'dry stress day' in WOFOST is a day on which crop growth is inhibited due to water shortage (de Wit & Boogaard, 2021). As inputs for the sowing and harvest during the simulation period, a range was given to the model. Based on an assessment of the sowing and harvest dates from the Agroscope soybean variety trials, the sowing date was set to occur between DOY 100 and 140, and the maximum duration from sowing to the end of the simulation was set to 150 days.

As WOFOST was not calibrated, the selection of two crop files allowed for an additional assessment of uncertainty regarding the yield projections, besides the uncertainty exemplified by the differing outputs of each model chain. The projection data was available from 1981 to 2099. Thus, time series plots were created for both study sites in this period. For each study site, plots of the four variables (yield, dry stress days, day of flowering and maturity) were created with the two selected crop files under RCP4.5 and 8.5. For all time series plots, a ten-year moving average was applied to the model chain data to reduce the complexity on a visual level. The calculation was conducted with the R-package 'roll', created by Foster (2020). After calculating the moving averages, new plots were created with the median and a shaded percentile area, ranging from the 25th to the 75th percentile of the data. The median values displayed in these plots present a "best guess" estimation for the future under a specific RCP, while the shaded percentile area hints at the uncertainty of the projection (CH2018, 2018b).

4 Results

4.1 Leaf Area Index Measurements

The leaf area index was measured at weekly intervals on six parcels in Reckenholz during the growing season of 2022. The measurements started roughly one month after sowing. The resulting data is visualized in Figure 10. Each data point represents one LAI value gathered for the variety Merlin or M. Arrow, which are distinguished by shape and colour in the figure. In addition, Figure 10 includes the daily mean LAI for both varieties.

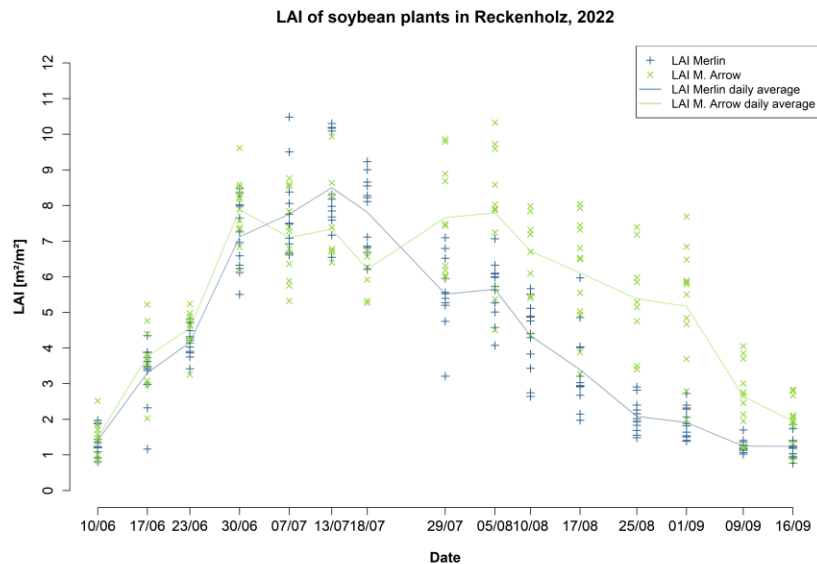


Figure 10: Leaf Area Index (LAI) measurements during the growing season of soybeans in Reckenholz 2022.

The Merlin parcels reach their maximum leaf area index in the middle of July, whereas for M. Arrow, there are two local maxima. The first one is observed on the 30th of June, while the second one is on the 5th of August. However, a LAI curve should comprise of one maximum. An increase of the average value would be expected with each measurement date until the occurrence of a maximum, whereas afterwards, a continuous decline would be presumed. The highest LAI value reached in a single measurement at one position in a parcel is 10.84 for Merlin on the 7th of July, whereas for M. Arrow it is 10.33 on the 5th of August. The highest daily average LAI value is approximately 8.5 for the variety Merlin on the 13th of July; this value was obtained when averaging all LAI measurements on the three parcels growing the Merlin variety.

In the month of June, the leaf area indexes of both soybean varieties are relatively similar. The variety Merlin belongs to a different maturity group than M. Arrow and consequently matures earlier (Agroscope 2006a – 2022a). We can observe this in Figure 10, where the LAI of Merlin starts to decline after the 13th of July, whereas the LAI of M. Arrow decreases only after the 5th of August.

4.2 Soil Moisture Measurements

Figure 11 depicts the variation of soil water content over soil depth and time on parcel 8. At a depth of 1000mm, the soil water content shows the highest values, but the least variation over time; the values always remain within the range of 37 and 39.07 vol%. Nevertheless, a diurnal pattern of increase and decrease in soil moisture can be observed. This applies to the soil water content in all depths, albeit to varying degrees. In general, as shown in Figure 11, the soil moisture increases with depth, while its variation in time decreases with depth. There are very few incidents, where the soil moisture in a greater depth is lower than the value measured above. For instance, this occurred at the beginning of July, where the soil moisture recorded at a 400mm depth was briefly lower than at 300mm. In addition, this event is characterized by a steep increase in soil water content at the depths of 100mm to 400mm. Figure 11 reveals several other incidents where the soil moisture values increased rapidly and reached a local maximum, for example on the 5th of June and the 18th of August.

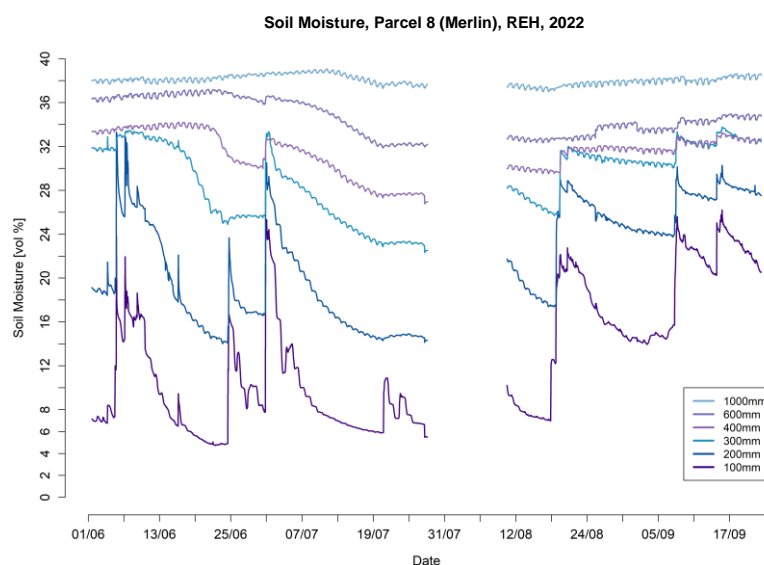


Figure 11: Soil moisture logger data, parcel 8, Reckenholz 2022.

The data recorded by the HH2 moisture meter is visualized in Figure 12, which contains six plots, each depicting the soil moisture at a specific depth in the form of point data. The data from the hourly measurements on plot 8 were included in each plot of Figure 12 with a blue line. The measurements with the HH2 were conducted on a total of ten dates. In each plot of Figure 12, there are 18 soil moisture data points for every measurement date, which depict the variation in soil moisture within and between the varieties Merlin and M. Arrow. Upon taking a closer look at Figure 12, it becomes evident that the logger data from parcel 8 in general shows rather high soil moisture values in comparison to the manually recorded measurements. There seems to be no apparent pattern which distinguishes the soil water contents on the parcels with Merlin and M. Arrow soybeans. However, if only considering the period starting from the 27th of July and the depths of 200mm to 600mm, it is often the case that the highest and lowest values of the day were measured on the parcels with the Merlin variety. At a depth of 1000mm, exactly the opposite is the case. Starting from the end of July, a generally higher variation in soil moisture values on a certain date is also observed, meaning the data points are more widely scattered. This is noticeable across all depths, but less prominent at 600 and 1000mm. In Figure 12, the colours of the data points differentiate between the two soybean varieties

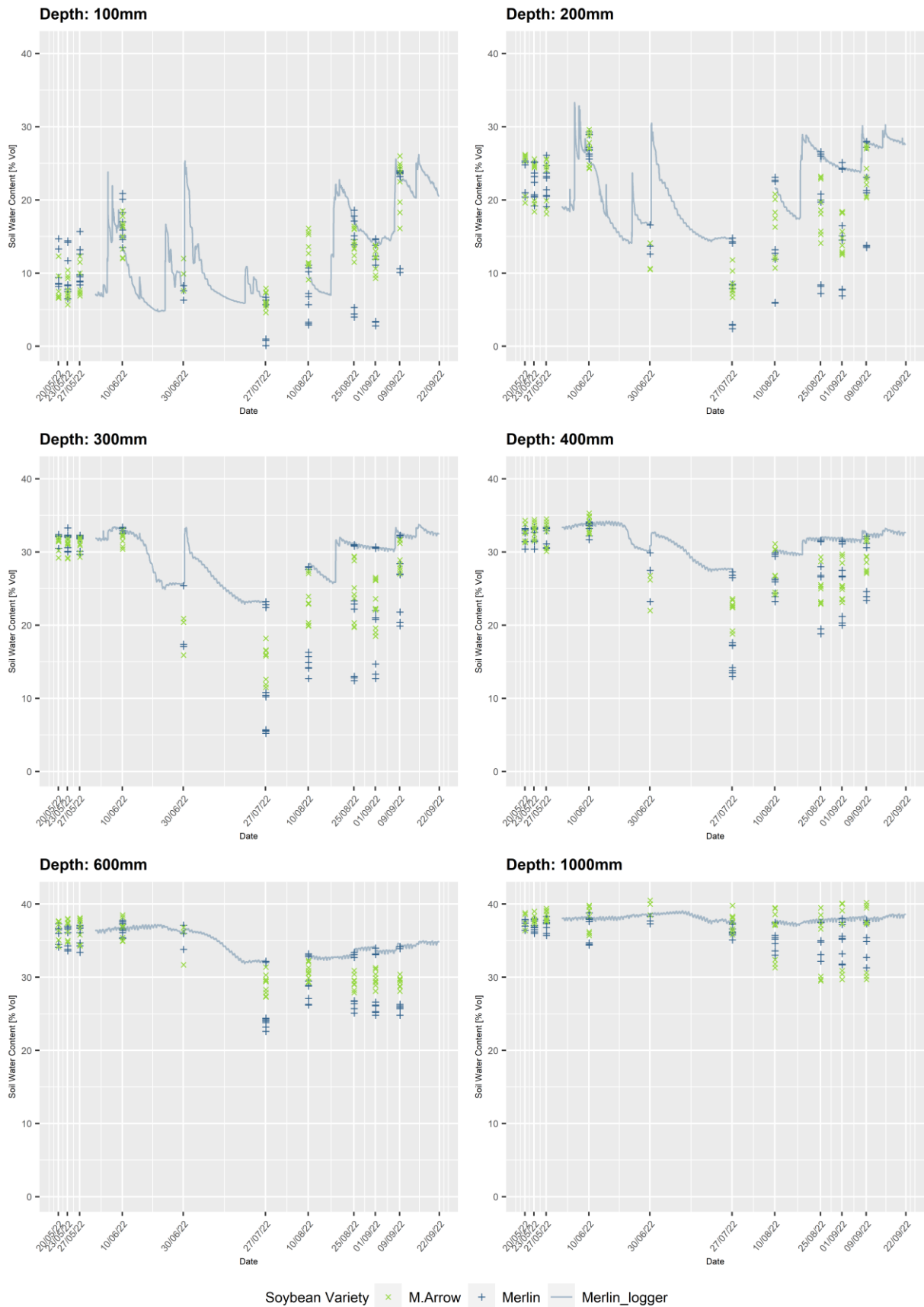


Figure 12: Soil moisture measurements by soil depth. Logger data (lines) and variation in manual measurements (point data).

deviates from the manual measurements on parcel 8. However, the soil water content of only parcel 8, with the data from manual measurements and logger, is depicted in Figure 23 in the appendix. Although there is some variation in the manual measurements, there is no noteworthy deviation from the logger data.

4.3 Model Evaluation

While in chapters 4.1 and 4.2, the results of the conducted field measurements were described, the following subchapters will focus on the results of the model evaluation. Thus, the simulated and observed values of yield, soil moisture and LAI will be examined and compared applying statistical and visual methods.

4.3.1 Yield

WOFOST includes seven different soybean crop files. Simulations were conducted with all crop files for Reckenholz and Changins. The results are shown in Figure 13. This figure indicates that the selection of a certain crop file has an impact on the simulation of the yield, as the different crop files are the only distinction between the simulations. Specifically, crop file w41 stands out with its comparatively large variation in yield values. When averaging the yield over all simulated years, w41 generates the highest and 906 the second highest values for both locations. On average, crop files 901 and 903 simulate the lowest yields, while their yield variation from year to year exhibits a pattern similar to 902, 904 and 905. This is the case for both locations.



Figure 13: WOFOST yield simulations with all soybean crop files for CGI and REH.

As seen in Table 10 and Table 11, when comparing the simulated and the observed yield, crop files 906 and w41 perform the best regarding the goodness of fit. In Changins (see Table 10), the simulated yield with crop file 906 shows a good d-value, as well as the lowest RMSE in Table 10 and Table 11. After 906, w41 has the second highest correlation (r-value). However, the RMSE and PBIAS% values are higher than with other crop files, which indicates, that the WOFOST simulation in this case results in a higher overestimation of the yield. In Reckenholz (see Table 11), the simulated yield with w41 shows good d-, md, rd-, and r-values. However, the RMSE and PBIAS% values are again rather high in comparison to the other crop files. Nonetheless, as the use of crop files 901 to 905 result in a negative correlation with the observed yield, w41 and 906 were chosen as better alternatives to represent the observed yield

in Reckenholz. The observed yield, which was used to calculate the results in Table 10 and Table 11, consists of an average over all soybean varieties tested in the Agroscope variety tests. The goodness of fit was also determined with the observed yield of only the variety Merlin and only the variety M. Arrow. The corresponding results are included in the appendix, chapter 8.1.2.

Table 10: Statistical goodness of fit measures for simulated and observed yield in Changins from 2006 to 2022. The observed yield consists of an average over the yield of all soybean varieties tested in the Agroscope variety test of a certain year.

Location, reference yield	Changins, observed yield: average						
Crop File	901	902	903	904	905	906	w41
RMSE	825.68	582.07	849.64	627.74	617.82	592.59	1417.52
PBIAS%	-19.5	-7.8	-20.3	11.2	11.1	11.3	22
d	0.44	0.45	0.44	0.47	0.48	0.61	0.42
md	0.34	0.39	0.34	0.3	0.32	0.42	0.31
rd	0.55	0.51	0.55	0.3	0.32	0.5	0.37
r	0.05	0.05	0.04	0.24	0.26	0.45	0.35

Table 11: Statistical goodness of fit measures for simulated and observed yield in Reckenholz from 2014 to 2022. The observed yield consists of an average over the yield of all soybean varieties tested in the Agroscope variety test of a certain year.

Location, reference yield	Reckenholz, observed yield: average						
Crop File	901	902	903	904	905	906	w41
RMSE	895.23	734.4	916.53	824.18	801.01	746.21	1018.63
PBIAS%	-16.5	-5.8	-17.2	11.6	11.7	14.5	17.8
d	0.35	0.09	0.36	0.39	0.41	0.58	0.65
md	0.34	0.12	0.36	0.25	0.26	0.4	0.55
rd	0.54	0.19	0.55	0.14	0.18	0.42	0.62
r	-0.32	-0.34	-0.33	-0.21	-0.16	0.43	0.61

In Figure 14, the WOFOST simulations with crop file 906 at Changins and Reckenholz are visualized and compared to three different reference (observed) yields, which include the yield of the variety Merlin and M. Arrow, as well as a yearly average over all varieties tested in the Agroscope variety trials. Figure 15 contains information equivalent to Figure 14, but with crop file w41. Figure 14 shows that, using crop file 906 for the yield simulation, the goodness of fit is generally higher for Changins than for Reckenholz. Regarding r- and d-value, the crop file 906 performs particularly well when comparing it to the yield of M. Arrow in Changins. Considering the RMSE and PBIAS% values, 906 reaches the best fit with a yield averaged over different soybean varieties. Therefore, with 906, WOFOST simulates the least overestimation in said case. In all three plots for Changins in Figure 14, an overestimation of the yield is observed in most years. In addition, there are four years, where the overestimation of the yield is conspicuous: 2008, 2009, 2012 and 2017. Taking a closer look at the three plots of Reckenholz in Figure 14, WOFOST generally overestimates the yield with crop file 906, except in the years of 2016 to 2018. Especially in the years of 2020 and 2021, the overestimation is evident. For Reckenholz, the WOFOST yield simulation reaches the highest goodness of fit with the averaged yield from different varieties. When comparing the simulation to the yields of Merlin and M. Arrow, the RMSE and PBIAS% values are higher, while the correlation is lower than with the averaged yield. However, while the correlation is lower for Merlin and M. Arrow compared to the averaged yield, the differences between the d-values is not as prominent.

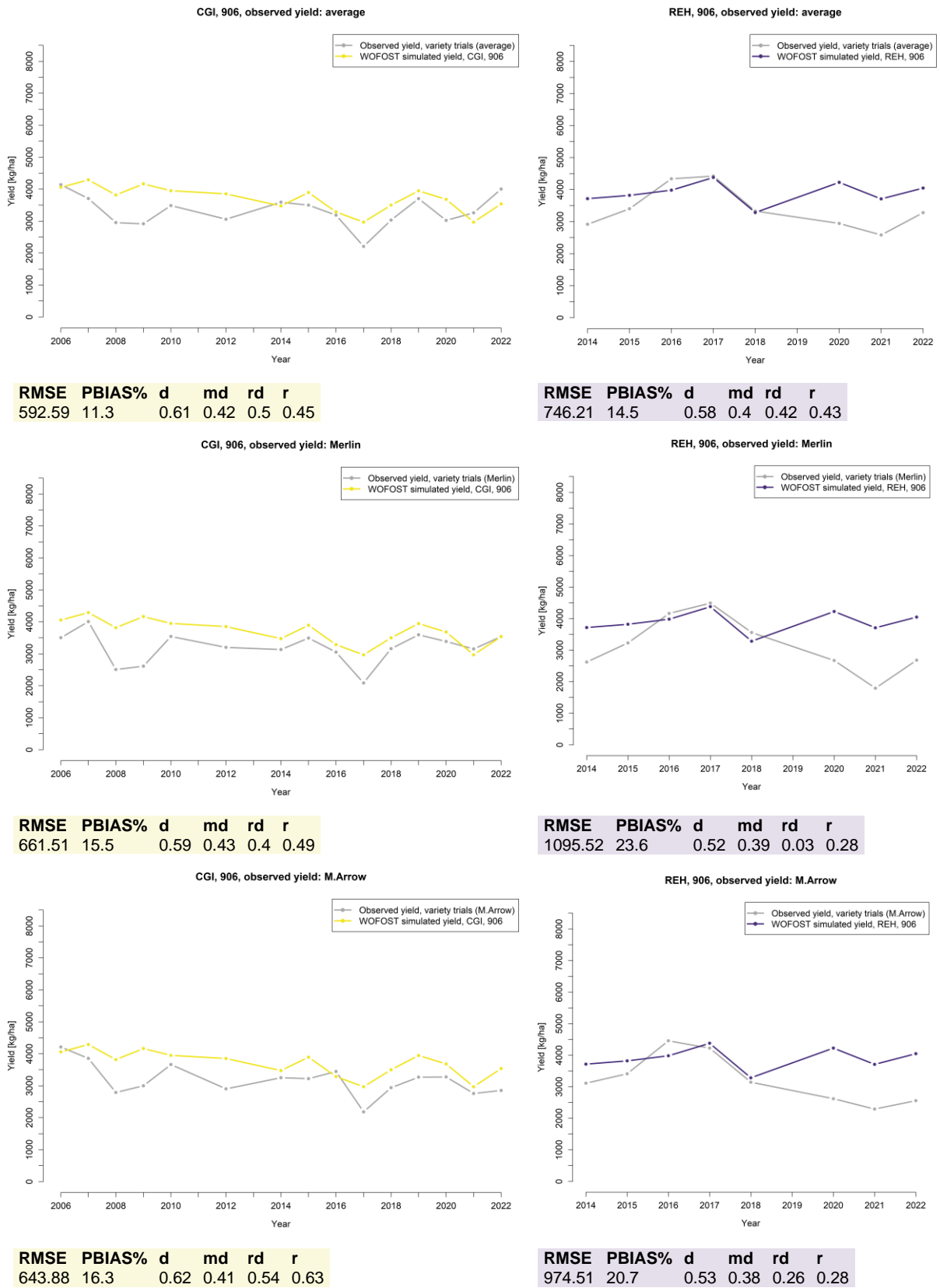


Figure 14: WOFOST simulated soybean yield with crop file 906 and observed (reference) yield values. Reference values: average from CGI / REH variety tests, variety Merlin, variety M. Arrow.

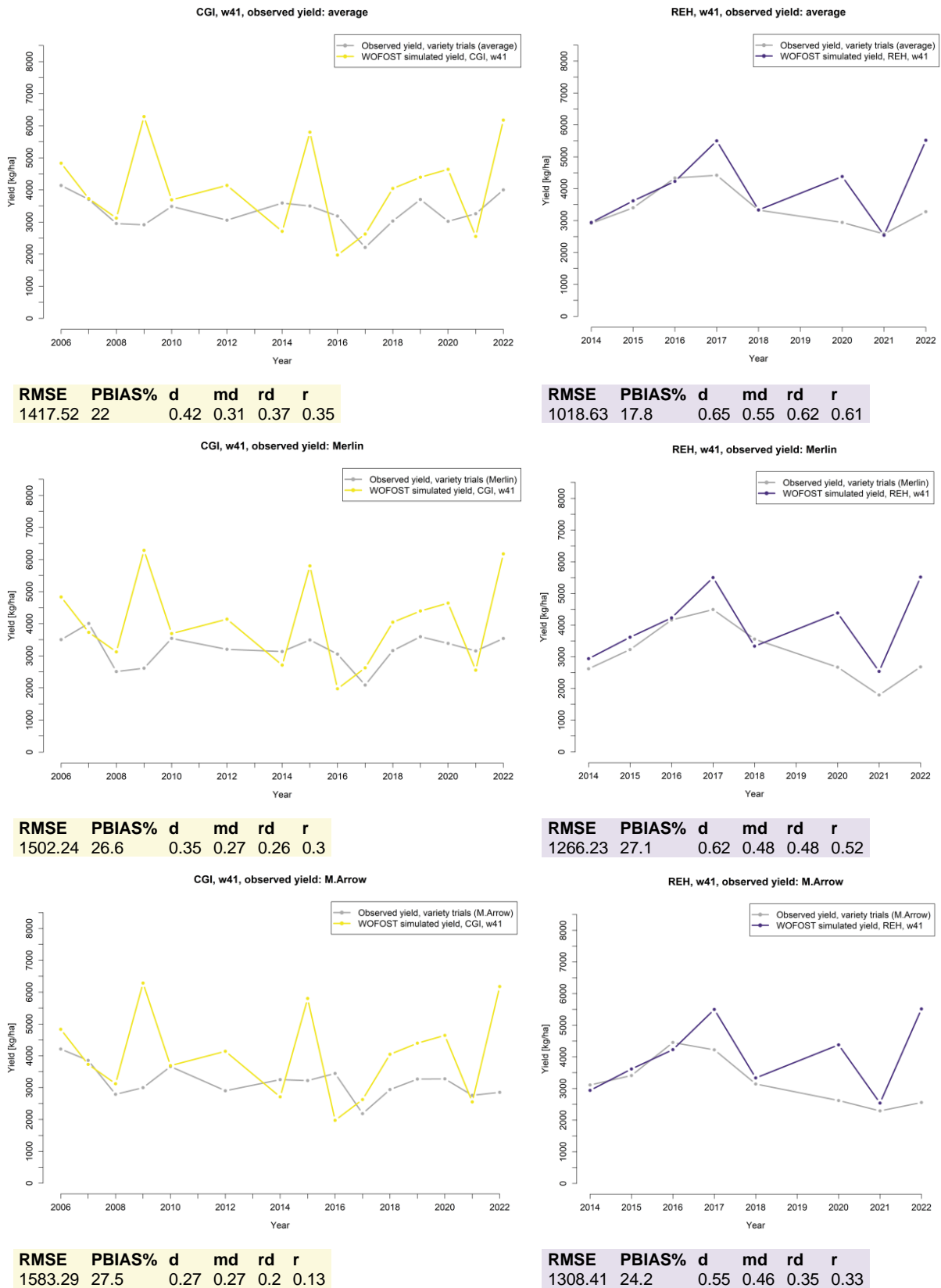


Figure 15: WOFOST simulated soybean yield with crop file w41 and observed (reference) yield values. Reference values: average from CGI / REH variety tests, variety Merlin, variety M. Arrow.

As already seen in Figure 13, the use of crop file w41 for the simulation generates a large variation of the yield from year to year, more so than with other crop files. In Figure 15, the simulated yield with crop file w41 is compared to an averaged yield, as well as the yield of the Merlin and M. Arrow variety. At both locations, the PBIAS% values show a tendency to an overestimation of the yield, with values ranging between 17.8 and 27.5%. In Changins, the overestimation particularly stands out in the years of 2009, 2015 and 2022. The yield of 2022 was also evidently overestimated in Reckenholz, as was the case in the years of 2017 and 2020. In Changins, utilizing an averaged yield as a reference value resulted in the best goodness of fit considering all statistical measures. The option with the yield of Merlin generated lower goodness of fit values, whereas the option with M. Arrow resulted in the lowest goodness of fit for Changins, with a correlation of 0.13. The comparison of the w41-simulated yield with observed values in Reckenholz shows more promising results. The averaged yield exhibits good d-, rd- and r-values. In addition, the RMSE values of Reckenholz are lower than in Changins. Considering the performance of the w41 crop file regarding the varieties Merlin and M. Arrow, one can observe that the correlation of the w41-simulated yield is higher with the yield of Merlin. In general, the goodness of fit is higher with the Merlin reference, except for the PBIAS% value.

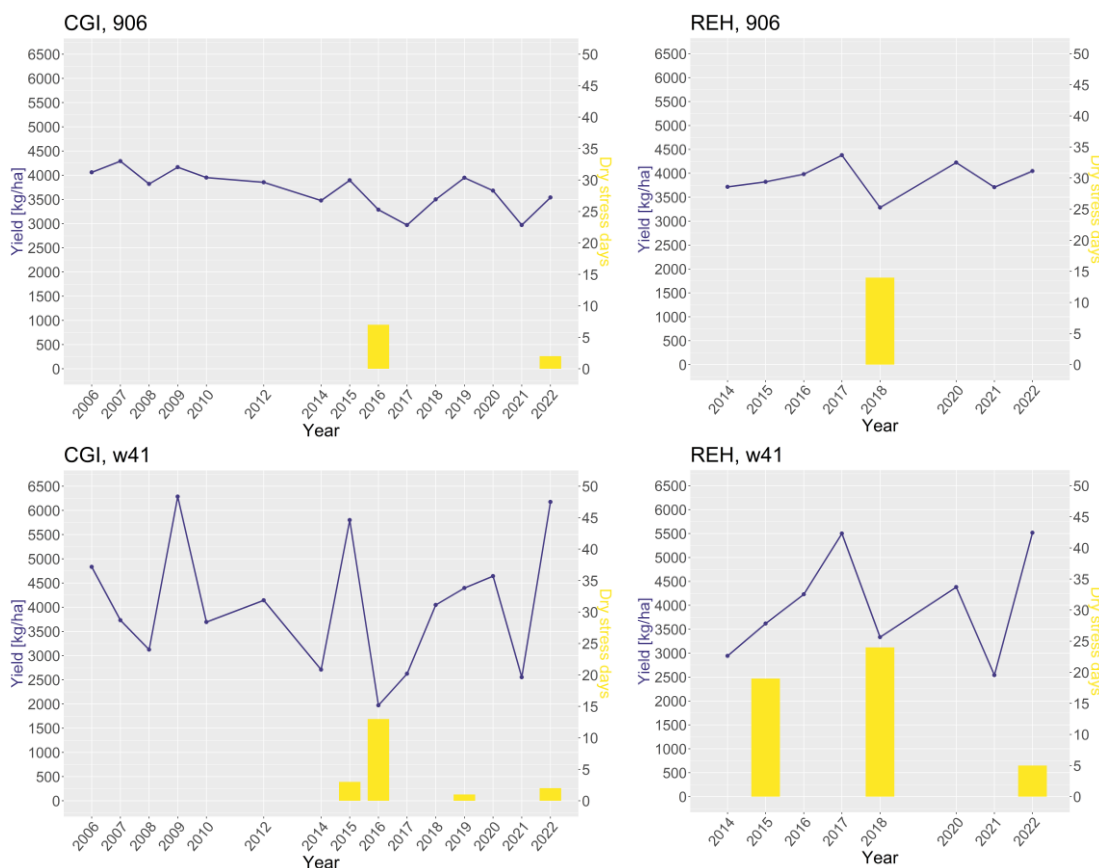


Figure 16: Simulated dry stress days (yellow bars) and yield (purple line) with crop files 906 and w41 for the locations Changins and Reckenholz.

Figure 16 contains information from the WOFOST simulation output only. Included are the simulated yields with crop files 906 and w41, which were already shown in the previous two figures. However, in Figure 16, the yearly sum of simulated dry stress days is added to the yield plots. This could provide useful information for a better understanding of the yield simulation, which will be discussed in chapter 5.3. Simulating with crop file 906, WOFOST identifies

two years with dry stress days in Changins: 2016 with a total of seven and 2022 with a total of two days affected by dry stress. In Reckenholz, 18 dry stress days are simulated in 2018, while the remaining years are not affected by dry stress. At both locations, dry stress is simulated more often with crop file w41. In Changins, four years are impacted: 2015 (three dry stress days), 2016 (13 dry stress days), 2019 (one dry stress day) and 2022 (two dry stress days). In Reckenholz, WOFOST identifies three years affected by dry stress: 2015 (19 dry stress days), 2018 (24 dry stress days), and 2022 (5 dry stress days). As already mentioned in chapter 2.2, on the soybean plots of the variety trials in Changins, an irrigation infrastructure was available, and it was used if the plants required water. This was not the case for Reckenholz, where irrigation was not possible. This must be taken into consideration in a further discussion of these results, as without irrigation, dry stress days in Changins would presumably be simulated to occur more frequently.

4.3.2 Leaf Area Index and Flowering

Figure 17 provides insight into the observed and simulated phenological development of soybeans in Reckenholz, 2022. Depicted are the measured LAI of the variety Merlin and M. Arrow, as well as the WOFOST simulated LAI with the crop files 906 (upper plot) and w41 (lower plot).

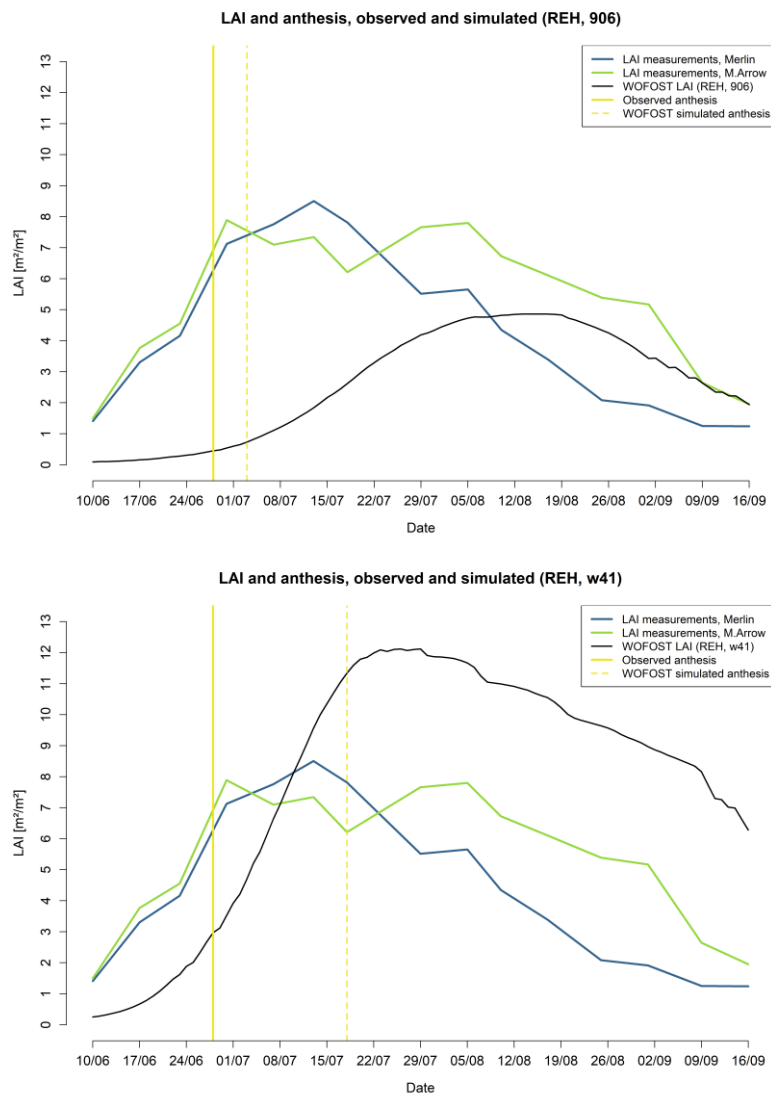


Figure 17: Leaf-Area-Index measurements of Merlin and M. Arrow in REH, 2022, and WOFOST-simulated LAI. Also included: observed and simulated anthesis.

In both plots, the observed and simulated flowering dates are included. The flowering on the field of the Reckenholz variety trials took place on the 28th of June. The anthesis simulated with 906 occurred on the 3rd of July, whereas with w41, the flowering was simulated to take place on the 18th of July.

Regarding the simulated LAI development, crop files 906 and w41 generate differing results. While the LAI with 906 reaches its maximum with a value of 4.86 on the 13th of August, the maximum LAI simulated with w41 is 12.12 on the 26th of July. As evident in Figure 17, the curve of the 906 simulated LAI has a smaller amplitude than the curves of the observed LAI of Merlin and M. Arrow. The opposite is the case for the w41 simulated LAI development, the amplitude of whose curve is larger than that of the observed LAI curve. It is also noteworthy, that while the simulated LAI of both crop files are still increasing at the end of July, the curve of the observed Merlin LAI has already reached its maximum value by Mid-July. Therefore, in this aspect, the development of the simulated leaf area indexes bear more similarity to the M. Arrow variety, whose LAI reaches its maximum after Merlin. At the end of the growing season, there is a short timespan of approximately ten days, where the curves of the 906 simulation and the observed LAI of M. Arrow overlap.

As already noticed via a visual assessment of the LAI development curves, the goodness of fit values in Table 12 show that the LAI of M. Arrow has a higher correlation than the LAI of Merlin with the simulated LAI of both crop files. In addition, the d-, md- and rd-values of Merlin with the two crop files are all lower than the values of M. Arrow. Furthermore, the Merlin LAI has a negative correlation with the 906 simulated LAI. In comparison to the PBIAS% values in chapter 4.3.1, where the yield simulations of WOFOST were evaluated, the PBIAS% values in Table 12 are high, showing an over- or underestimation between 36.9 to 71.1%. Since the simulated and observed LAI values range from 0 to 12.12, the RMSE values in Table 12 are high, showing an error from 3.62 to 5.15. The largest RMSE value with 5.15 was generated when comparing the Merlin LAI with the LAI of crop file w41.

Table 12: Statistical goodness of fit measures for simulated and observed LAI in Reckenholz, 2022.

Location	Reckenholz			
	Merlin		M. Arrow	
Reference LAI (variety)	906	w41	906	w41
Crop File	906	w41	906	w41
RMSE	3.65	5.15	3.62	3.87
PBIAS%	-42.6	71.1	-54	36.9
d	0.4	0.47	0.53	0.6
md	0.31	0.32	0.37	0.38
rd	0.49	-1.17	0.59	0.22
r	-0.08	0.26	0.4	0.56

4.3.3 Soil Water Content

As the WOFOST output contains only one daily value for soil moisture, the measurements depicted in Figure 11 were averaged equally over all depths, so as to facilitate the comparison between the simulated and observed values, depicted in Figure 18. Figure 18 furthermore contains a plot showing the daily precipitation sum.

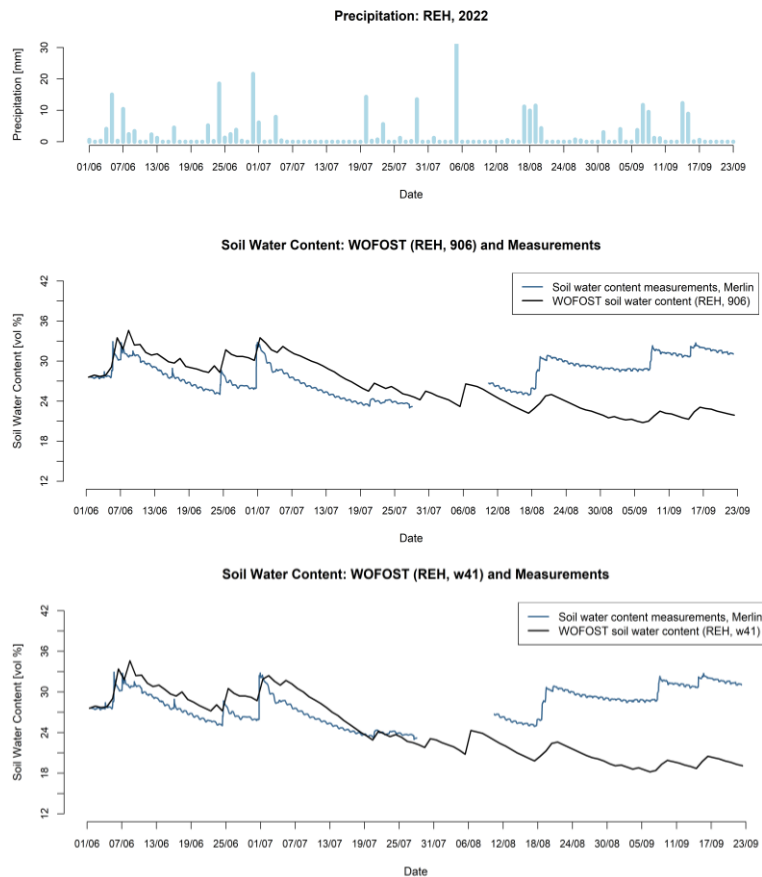


Figure 18: Observed and simulated soil water content and daily precipitation sum in REH, 2022.

Both the simulated and observed soil moisture increased when major precipitation events occurred. A general observation regarding Figure 18 is, that the increase of the measured soil moisture following precipitation events happens in a more rapid manner than the increase of the simulated soil water content. When comparing the simulated soil moisture of the crop files 906 and w41, one can observe the resulting plot lines follow a seemingly identical pattern of increase and decrease. However, the soil water content simulated with w41 is mostly a little lower than the soil moisture simulated with 906, which is visible in Figure 18. From the beginning of the measurement period until the end of July, the soil water content simulated with both crop files, while generally being higher than the observed soil moisture, seems to fit the observed soil moisture quite well. However, after the battery failure and a major precipitation event at the beginning of August, the gap between observed and simulated values widens considerably. From August to September, the simulated soil water content with both crop files is always smaller than the measured value. From June to July, the soil moisture simulated with crop file w41 seems to fit the observed values better, while from August to September, crop file 906 seems to be the better choice to simulate the soil water content. Considering the whole growing season however, both crop files do not perform particularly well simulating the soil water content, as shown in Table 13. While the correlation with the

measured soil moisture is negative for both crop files, the d-, md- and rd-values do not exceed 0.41. The PBIAS% value shows an underestimation of the actual soil water content for the simulations with both crop files, however the underestimation is more pronounced when using crop file w41.

Table 13: Statistical goodness of fit measures for simulated and observed soil water content in Reckenholz, 2022.

Location	Reckenholz	
Variety (measured soil moisture)	Merlin	
Crop File	906	w41
RMSE	5.18	6.47
PBIAS%	-5.1	-11.1
d	0.32	0.32
md	0.25	0.3
rd	0.39	0.41
r	-0.17	-0.14

4.4 Model Application

To assess the possible impact of future climatic changes on the soybean production in Switzerland, four variables were simulated with projected climate data from CH2018 for RCP4.5 and RCP8.5: yield, sum of dry stress days, day of flowering and day of maturity. The resulting time series plots are displayed in Figure 19 to Figure 22.

4.4.1 Absolute and Relative Change of Median Yield

Table 14 contains the simulated median yield for Changins and Reckenholz with crop files 906 and w41 in four different time periods. The yield simulation with crop file 906 exhibits a decreasing trend at both locations over time. In comparison to the reference period 1981-2010, the median simulated yield in Changins decreases by 17.3% under RCP4.5, and by 33% under RCP8.5 by the end of the century. The decline of median yield in Reckenholz amounts to 8.7% under RCP4.5 and to 22.2% under RCP8.5 by the end of the century.

Table 14: Median simulated yield [kg/ha] over four time periods: 1981-2010, 2020-2049, 2045-2074, 2070-2099. The red arrow pointing downwards means a decrease in value in comparison to REF, while the green arrow pointing upwards signifies an increase.

Time Period	RCP	Variable	CGI, 906	REH, 906	CGI, w41	REH, w41
1981-2010 (REF)			2499.0	2426.5	2547.5	1834.5
2020-2049	RCP4.5	median yield [kg/ha]	2247.5 ↓	2366.0 ↓	2967.5 ↑	3391.0 ↑
2045-2074			2099.0 ↓	2274.0 ↓	3046.5 ↑	3857.5 ↑
2070-2099			2065.5 ↓	2214.5 ↓	3190.5 ↑	3962.0 ↑
1981-2010 (REF)			2503.0	2424.5	2503.0	1834.5
2020-2049	RCP8.5	median yield [kg/ha]	2199.5 ↓	2306.0 ↓	3039.5 ↑	3513.0 ↑
2045-2074			1981.0 ↓	2179.5 ↓	2822.0 ↑	4132.5 ↑
2070-2099			1676.5 ↓	1885.5 ↓	1894.5 ↓	4313.5 ↑

In contrast to the results with crop file 906, the median yields simulated with crop file w41 show a general tendency towards increase over time. In Reckenholz, the median yield increases with every time period, until it reaches its maximum at the end of the century. This can be observed under both RCPs and furthermore in Changins under RCP4.5. By 2085, the yield in Reckenholz has risen by 116% under RCP4.5 and by 135.1% under RCP8.5. In Changins

under RCP4.5, there is an increase in median yield of 25.2% by 2085. However, under RCP8.5, a different pattern is observed in Changins. In the near future period, the median yield in Changins is 21.4% higher than in the reference period. After 2035, it decreases again, however, by mid-century, it is still larger than the median yield of the reference period. Nevertheless, by the end of the century, the median yield simulated for Changins with crop file w41 has decreased by 24.3% in comparison to the reference period. Therefore, the yield simulated for Changins with w41 under RCP8.5 marks an exception, where the yield does not increase or decrease consistently over time.

4.4.2 Time Series: Crop File 906

Yield - CGI

As already mentioned in chapter 4.4.1, we can see in Figure 19, that the yield in Changins simulated with crop file 906 is generally decreasing over time. At the end of the century, the yield under RCP8.5 is mostly lower than under RCP4.5. In the earlier time periods, the development of the yield is similar under both RCPs. The green-shaded area, which displays the value range from the 25th to the 75th percentile, increases slightly in size after the near-future period in both RCPs, which indicates a higher uncertainty. The deviation from the median, which is shown as a black line in the plots, does not seem to surpass 300 kg/ha between the 25th and 75th percentile.

Dry Stress Days - CGI

As seen in the third and fourth plots of Figure 19, the yearly sum of dry stress days shows a tendency towards increase in the future. The median sum of dry stress days mostly stays below 10 during the reference period under both RCPs. Nevertheless, under RCP4.5, there is a noticeable increase starting at around 2035. The rise is interrupted by a short descent in the middle of the century. After that, the median increases again. However, at the end of the century, the variation of data between the 25th and 75th percentile is often quite large in comparison to the earlier periods. This also applies to the sum of dry stress days under RCP8.5. But, in this case, a clearer overall tendency towards increase can be observed. While there are hardly any dry stress days in the reference period, by the end of the century, there could be up to 4 per year under RCP4.5, and up to 20.5 per year under RCP8.5. For detailed information on the absolute changes of all variables over different time periods, see the tables of chapter 8.1.6 in the appendix.

Flowering & Maturity - CGI

The four plots in the lower half of Figure 19 show how the day of flowering and maturity could change in the future in Changins. Simulated with crop file 906, the day of flowering and the day of maturity show a tendency to occur earlier in both RCPs. However, under RCP8.5, the shift is more pronounced. The day of flowering could go down from 183 in the reference period to 163 by the end of the century, while maturity could occur 35 days earlier. Considering RCP4.5, soybeans could bloom 12 days earlier by the end of the century, while maturity could also occur 12 days earlier than in the reference period.

Yield - REH

Figure 20 includes the plots of all four variables simulated with 906 in Reckenholz. Under RCP4.5, the yield seems to change very little in the future. No clear trend is recognizable in the plot. Yet, when considering the observations from Table 14, there is a slight decrease of the yield. Similar to Changins (see Figure 19), the decline of the yield by the end of the century

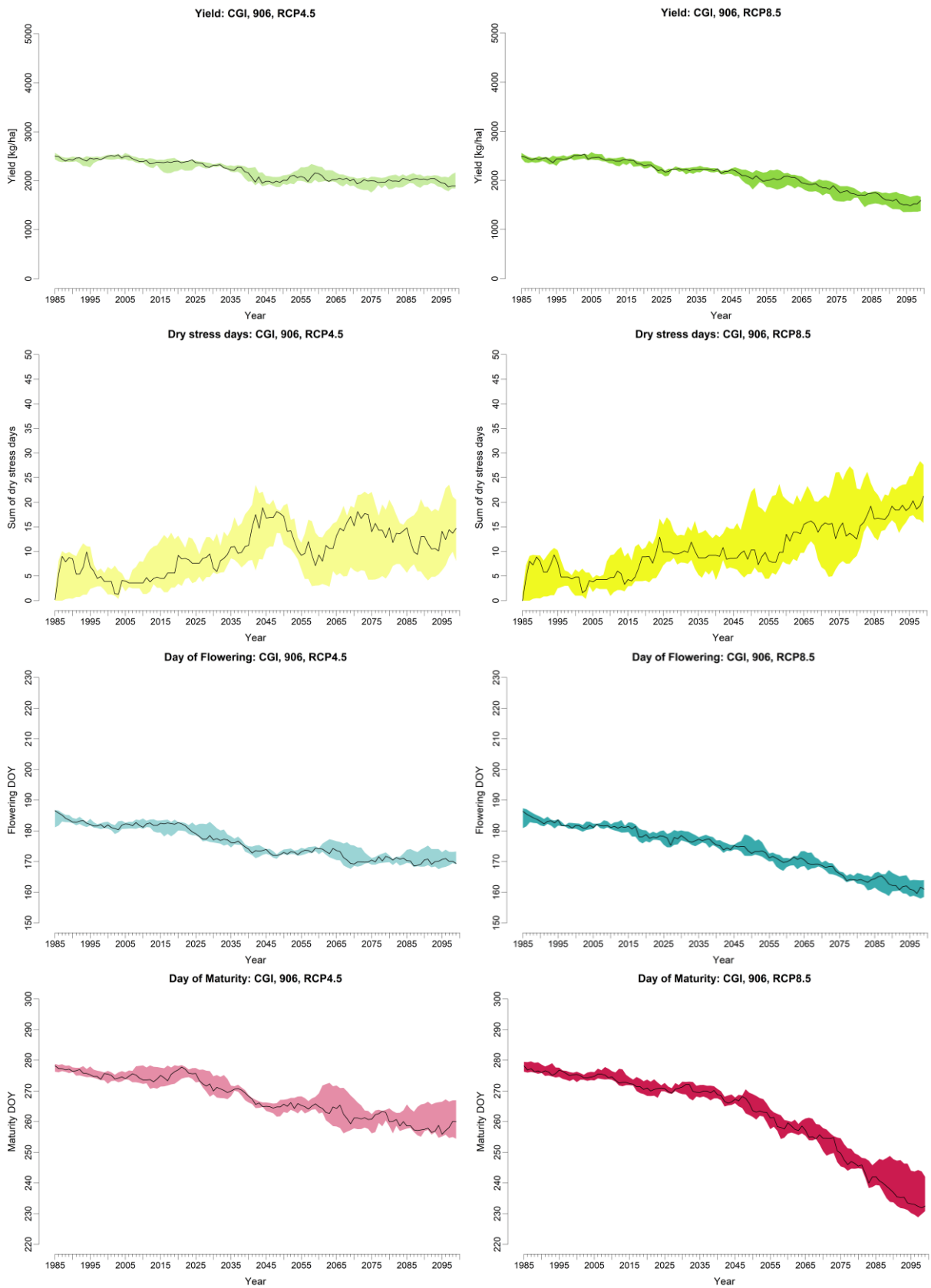


Figure 19: Simulation of yield, dry stress days, day of flowering and day of maturity in Changins (906), 1981-2099 with climate data of different model chains from CH2018. The black line in each plot is the median of the 10-year moving averages of all model chains, while the shaded area represents the range of values from the 25th to the 75th percentile.



Figure 20: Simulation of yield, dry stress days, day of flowering and day of maturity in Reckenholz (906), 1981-2099 with climate data of different model chains from CH2018. The black line in each plot is the median of the 10-year moving averages of all model chains, while the shaded area represents the range of values from the 25th to the 75th percentile.

is also more pronounced under RCP8.5 than 4.5. One aspect which is visibly different from Changins, is the smaller shaded percentile area in both yield plots of Reckenholz. There is also no apparent increase in the percentile area, with exception from the end of the century under RCP8.5.

Dry Stress Days - REH

When simulating with crop file 906, the yearly sum of dry stress days stays low in Reckenholz, particularly under RCP4.5. An increase of the percentile area by the end of the century can be observed, however the values do not surpass 5 days per year in the plot. Under RCP8.5, there is a stronger increase of percentile area and also slightly of the median at around 2090, albeit it is still not as prominent as in Changins. Therefore, regarding the yield and sum of dry stress days, the simulation with 906 in Reckenholz generally has less uncertainty than in Changins.

Flowering & Maturity - REH

In Reckenholz, the day of flowering as well as maturity are projected to occur earlier in future periods compared to 1981-2010. This applies to both RCPs. But, nearing the end of the century, the tendency is for the flowering and maturity to occur even earlier under RCP8.5 than under RCP4.5. Under RCP8.5, soybeans could bloom 18 days and mature 26 days earlier by the end of the century compared to the reference period. Regarding RCP4.5, flowering could occur 10.5 days earlier and maturity could occur 9 days earlier by the end of the century.

4.4.3 Time Series: Crop File w41

Yield - CGI

When simulating the yield with crop file w41, there is a tendency towards increase over time. Taking a look at Figure 21, this is apparent in the first plot, where the yield development in Changins is displayed under RCP4.5. In addition to the increase in yield, there is however also a higher uncertainty nearing the end of the century. Around mid-century, there is a local maximum, after which the median yield decreases until approximately 2070. Under RCP8.5, the yield is generally increasing until mid-century. Starting from around 2055, the yield however starts decreasing. In the mid-century period, the median is very close to the 75th percentile for a while. However, during this interval, the 25th percentile is also quite low in comparison to the median, sometimes being approximately 1000 kg/ha lower. Accordingly, due to this uncertainty, there is also a possibility that the yield starts decreasing by mid-century already. Where we see a decrease in median yield under RCP8.5, the 75th percentile is sometimes much higher, above all at around 2075. This means that the decrease in yield could also be less severe at the end of the century.

Dry Stress Days - CGI

The third and fourth plots in Figure 21 illustrate the yearly number of dry stress days simulated for Changins with w41. Under both RCPs, an increase in dry stress days is projected over time. Under RCP4.5, the increase is interrupted by a local minimum in the mid-century period, at around the same time as the local maximum of the yield under RCP4.5 occurs. As seen in the size of the shaded percentile area, there is often quite some uncertainty in the results, with the upper or lower border sometimes being up to circa ten days higher or lower than the median. In the reference period, there are hardly any dry stress days in Changins. However, by the end of the century, the sum of dry stress days per year could up to 27 under RCP4.5, and up to 36 under RCP8.5.

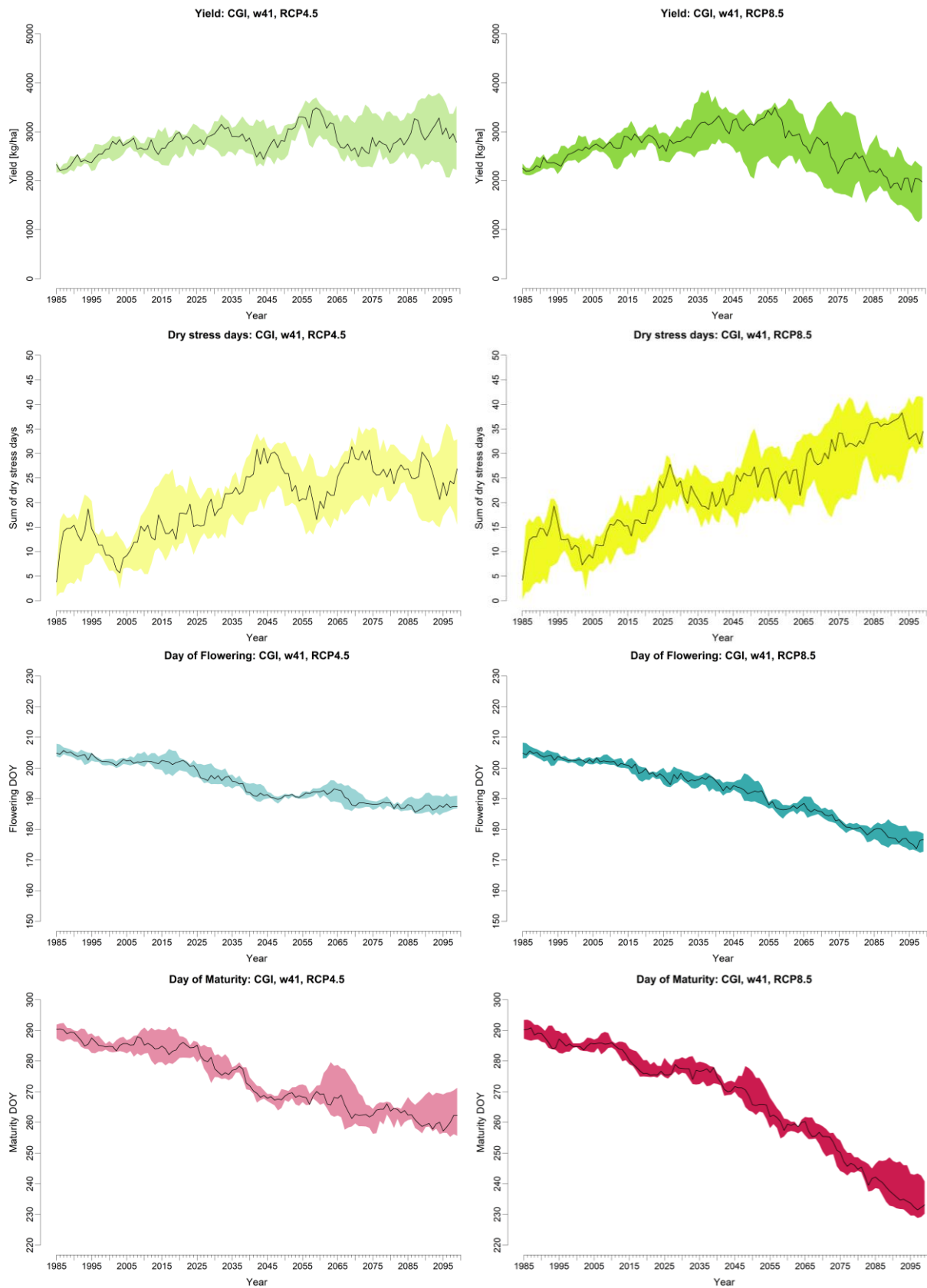


Figure 21: Simulation of yield, dry stress days, day of flowering and day of maturity in Changins (w41), 1981-2099 with climate data of different model chains from CH2018. The black line in each plot is the median of the 10-year moving averages of all model chains, while the shaded area represents the range of values from the 25th to the 75th percentile.

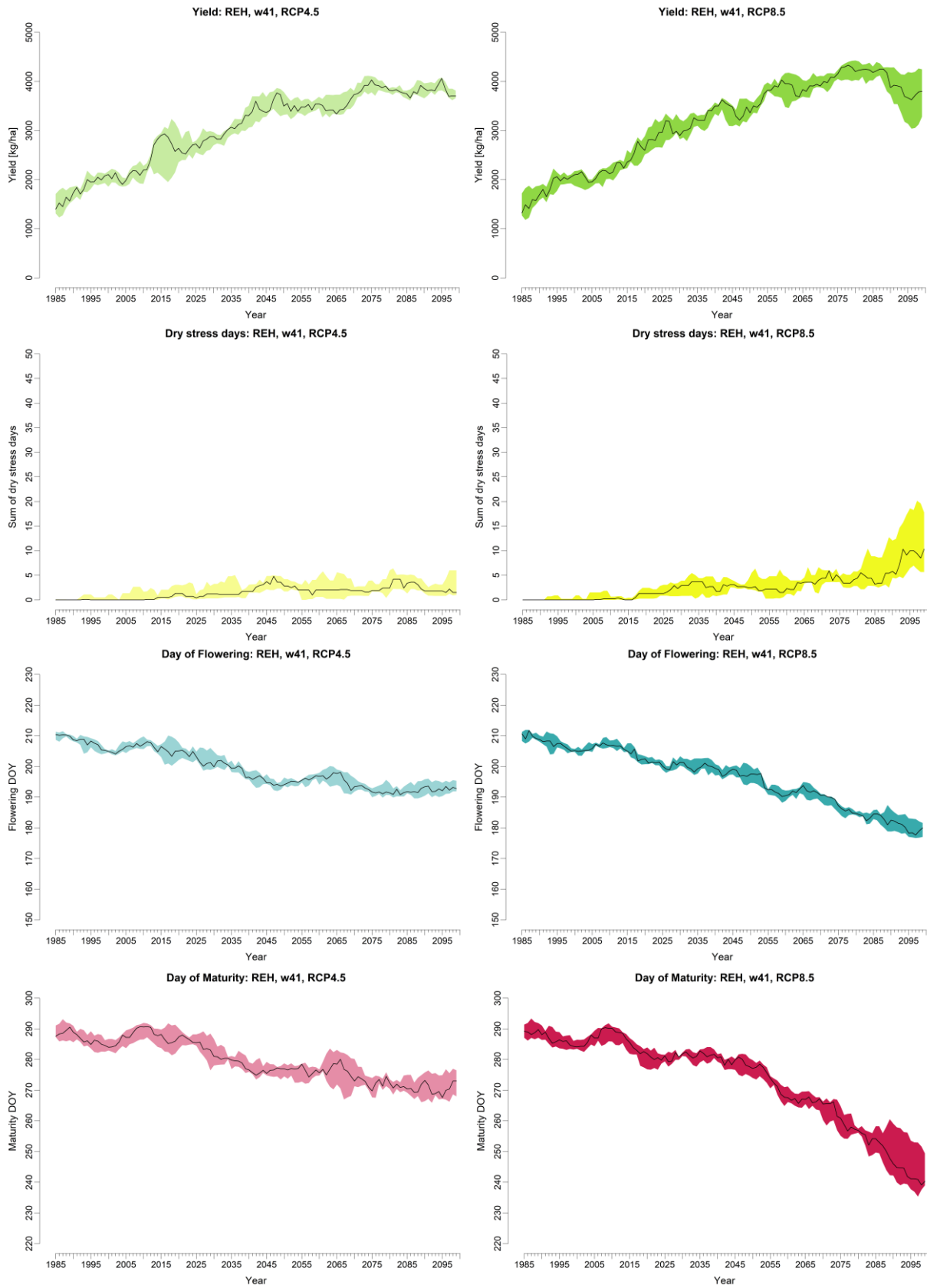


Figure 22: Simulation of yield, dry stress days, day of flowering and day of maturity in Reckenholz (w41), 1981-2099 with climate data of different model chains from CH2018. The black line in each plot is the median of the 10-year moving averages of all model chains, while the shaded area represents the range of values from the 25th to the 75th percentile.

Flowering & Maturity - CGI

The simulated day of flowering and maturity in Figure 21 tend to occur earlier in the future, under both RCPs. While soybeans bloom mostly around day 203.5 in the reference period, by the end of the century, the flowering occurs 14.5 days earlier under RCP4.5, and 24.5 days earlier under RCP8.5. The plots with the day of maturity show a larger uncertainty than the flowering plots. During the reference period, the day of maturity occurs at approximately day 286. However, by the end of the century, it could occur 22 days earlier under RCP4.5. Considering RCP8.5, soybean could mature 47 days earlier by the end of the century.

Yield - REH

Figure 22 contains time series plots of all four variables simulated with crop file w41 in Reckenholz. Comparing the plots of the yield and sum of dry stress days with the results of Changins (see Figure 21), one can observe that the shaded percentile areas, and therefore the uncertainty, are smaller in Reckenholz. Nevertheless, the increase in yield over time also applies to Reckenholz, as seen in the first two plots of Figure 22. Under RCP4.5, there is a local maximum between 2015 and 2025, but there is some uncertainty during this time interval, as seen in the lower border of the percentile area. Under RCP8.5, the yield starts to decrease at around 2090, however the uncertainty there is also quite large compared to the rest of the century.

Dry Stress Days - REH

Under RCP4.5, the sum of dry stress days per year in Reckenholz rarely exceeds 5 days, as seen in the plots. While the median sum of dry stress days is zero in the reference period, it remains zero in the period from 2070 to 2099 under both RCPs. Taking the mean values over the same two periods into consideration, one can see a small increase in the sum of dry stress days over time (see tables in chapter 8.1.6); there is an increase of 2.4 days under RCP4.5, and of 6.2 days under RCP8.5. This increase is visible in the dry stress days plot of RCP8.5.

Flowering & Maturity - REH

Just as in the three previous figures, in Figure 22, an apparent decrease in the number of days it will take for soybeans to flower and mature is observable. Flowering occurs around day 208 in the reference period. By the end of the century, it could happen 14 days earlier under RCP4.5 and 25 days earlier under RCP8.5. Soybeans reach their maturity at approximately day 287 in the reference period. Under RCP4.5, soybeans could mature 14 days earlier by the end of the century. Under RCP8.5, maturity could even be reached 38 days earlier.

5 Discussion

5.1 Leaf Area Index Simulation

As seen in chapter 4.3.2, the magnitudes of the measured versus the simulated LAI differed to quite an extent. Interestingly, the crop files 906 and w41, which were chosen due to their performance regarding yield simulation, produced opposite results when simulating the leaf area index for Reckenholz. In comparison to the measured LAI, the simulation with crop file 906 resulted in an underestimation, whereas with crop file w41, the LAI was overestimated. In addition, the measured LAI of both varieties increased much earlier in the season than the simulated LAI. No study was found where the performance of WOFOST regarding soybean LAI simulation was evaluated with in situ measurements. However, numerous studies exist, where soybean LAI was examined in different cultivars and in relation to yield, as well as management practices such as sowing density and row spacing (Csajbók et al., 2022; Jańczak-Pieniążek et al., 2021; Sobko et al., 2019; Yamamoto et al., 2023). Since in situ LAI measurements were conducted in these studies, they provide information useful for the assessment of the measured LAI values in this thesis.

It was observed in Figure 10 and Figure 17 that the LAI development in Reckenholz differed between the soybean varieties. From the end of July on, the LAI of the variety M. Arrow was consistently higher than the LAI of the earlier maturing variety Merlin. A similar observation was documented by Sobko et al. (2019), who conducted LAI measurements during two growing seasons (2016-2017) in Bavaria, Germany. Sobko et al. (2019) pointed out, that at physical maturity, the LAI of soybeans in maturity group 00 was higher than the LAI of the earlier cultivars in group 000. They measured the LAI two times per growing season: At flowering and the beginning of maturity. Therefore, the maximum LAI of the season was not recorded. In this regard, other studies from different climate zones are available. For instance, Yamamoto et al. (2023) documented weekly LAI measurements on soybean plots near Sendai, Japan from 2017-2020. Throughout these years, the peak LAI ranged between 4 and 6. In Poland, Jańczak-Pieniążek et al. (2021) measured the LAI of the Merlin variety from 2017 to 2019. In each year, they recorded peak LAI values between 5 and 6.

Csajbók et al. (2022) studied agro-biological traits of different soybean cultivars in Hungary, which inter alia included the LAI. The leaf area index was measured from 2017 to 2019, and significant differences between varieties were detected. Peak LAI values ranged between 4 and 9 in 2017, between 6 and 15 in 2018, and between 6 and 10 in 2019. Even within varieties, variation was observed in different growing seasons. For example, the “Boglár” variety from MG 00 had a maximum LAI of 4 in 2017, but in 2019, the peak LAI of this variety was at 8. The peak LAI of the earliest three cultivars (maturity groups 000 and 00) tested by Csajbók et al. (2022) never exceeded a value of 8. Yamamoto et al. (2023) also mentioned the variation in LAI dynamics. Even though their study was limited to the soybean variety Miyagishirome, which belongs to maturity group VII (Asanome & Ikeda, 1998), LAI development differed even among adjacent plots.

In Reckenholz, during the growing season of 2022, the highest daily average LAI range from approximately 7 to 8.5. In comparison to the results presented in the above-mentioned studies, the LAI in REH 2022 was rather high. Reasons could be the particularly favourable meteorological conditions in the growing season of 2022. For instance, the month of May, when the sowing took place, was characterized by warmer temperatures and higher sunshine duration than the mean values from 1991 to 2020 (MeteoSwiss, 2022a). Other explanations for the

differing LAI values might be the type of cultivar or soil / hydrological characteristics. In addition, except from Yamamoto et al. (2023), none of the studies presented above conducted the LAI measurements on a weekly basis. Jańczak-Pieniążek et al. (2021) determined the LAI value three times per growing season, while Csajbók et al. (2022) measured five times per year. Therefore, it might be possible that some years, the peak LAI was not recorded. Even though Yamamoto et al. (2023) measured LAI every week, the plots studied only grew one cultivar, which matures later than Merlin and M. Arrow. In this case, the differences in LAI could be attributed to the different type of cultivar and maturity group. In addition, uncertainties arise regarding the LAI measurements with the LAI-2200C canopy analyzer. Garrigues et al. (2008) mention, that in short canopies such as soybean, measuring below the canopy often results in the lens being too close to the leaves. Subsequently, it may occur that a large leaf fully covers the field-of-view of the device, leading to a transmittance close to zero and therefore an over-estimation of the LAI. With measurements below short canopies, there is also a hazard of interfering with the canopy structure, which further impacts the accuracy of measurements. Consequently, Garrigues et al. (2008) recommend utilizing a downward-looking measurement technique, such as Digital Hemispherical Photographs (DHP).

As already mentioned in the first paragraph, the LAI simulated by WOFOST deviated from the LAI development recorded in Reckenholz, 2022. WOFOST uses static partitioning tables determining the allocation from biomass to leaves depending on the development stage of the plant, and the specific leaf area is also a function of the development stage. As stated by Gaso et al. (2021), if environmental conditions lead to changes in biomass partitioning or specific leaf area, this could lead to uncertainties in the LAI simulation.

Various studies used data derived from remote sensing to estimate soybean LAI, with the objective to generate improved yield predictions through assimilation of the LAI into a crop model: Betbeder et al. (2016), Gaso et al. (2021) and Gaso et al. (2023) all report improved yield simulation results when assimilating satellite-derived LAI data into their models. Therefore, for research concerning the accuracy of yield simulations, it would be advised to assimilate LAI data into the model. Tagliapietra et al. (2018) determined a maximum leaf area index between 6 and 6.5 as ideal for reaching the soybean yield potential. However, this applies to the soybean yield in a subtropical environment, hence the validity in other climatic zones remains unclear. Still, this finding shows that LAI is an important factor in determining soybean yield and their relationship should therefore be studied further.

5.2 Soil Moisture Simulation

In the months of June and July, the observed and simulated soil water content matched regarding magnitude and pattern. WOFOST slightly overestimated the soil moisture. Considering solely these two months, the goodness of fit between the observed and simulated values was high (see Table 16 in the appendix). However, the goodness of fit from the entire measurement period (see Table 13) was considerably lower, due to WOFOST underestimating the soil moisture between August and September. This applies for the simulations with both crop files. The soil moisture simulation with w41 did generally result in slightly lower values than with 906. This could be explained by taking the simulated LAI into consideration. As seen in Figure 17, the LAI simulated by w41 is generally larger than the LAI simulated by 906, which could result in WOFOST assuming a higher crop water use when simulating with w41.

Similar to the literature focusing on LAI discussed in chapter 5.1, the literature where soil moisture in the context of modelling with WOFOST is a topic, often address the assimilation of soil

moisture data into the model so as to improve yield simulation (Pan et al., 2019; Zhuo et al., 2023; Zhuo et al., 2019). In research with objectives focusing primarily on soil hydrology, approaches using model coupling are employed frequently (Eweys et al., 2017; Kroes et al., 2019). One factor limiting an in-depth evaluation of soil moisture simulation with WOFOST, is that processes are only considered in the whole soil profile (Eitzinger et al., 2004). Other models, such as SWAP, simulate soil water content at individual layers. SWAP is a soil hydrological model which integrates WOFOST for the crop growth simulation (Eitzinger et al., 2004; Kroes et al., 2019). Performance evaluations of WOFOST regarding soil moisture simulations were conducted by Amiri et al. (2022) for maize in Nebraska, Dewenam et al. (2021) for winter wheat in Morocco and Eitzinger et al. (2004) for spring barley and winter wheat in Austria.

Eitzinger et al. (2004) evaluated the crop models WOFOST, SWAP and CERES with a lysimeter experiment, where the aforementioned crops were planted on three different soil types. SWAP and CERES both include more intricate soil water routines than WOFOST. Nevertheless, regarding the simulation of soil water content of the whole soil profile, all three models generated similar results. For winter wheat, the other models did not perform significantly better than WOFOST, however for spring barley, the CERES model performed better. In general, a tendency towards underestimating the soil water content was observed. According to Eitzinger et al. (2004), numerous models assume soil moisture depletion to be occurring quicker and from deeper soil layers than observed. This aligns with the observation for the WOFOST soil moisture simulation for Reckenholz 2022, where the model underestimated the soil water content in the months of August and September. Moreover, the deviation between observed and simulated soil moisture values in Eitzinger et al. (2004) was also comparatively small just after sowing, and tended to increase with time.

Dewenam et al. (2021) noticed in their study, that WOFOST was overestimating the measured soil water content during the first few weeks of the simulation. This conforms to the observations of this thesis, albeit the overestimation was more pronounced in the research of Dewenam et al. (2021). Later in the growing season, the deviation between simulated and observed values in Dewenam et al. (2021) declined substantially, contrary to the observations in Reckenholz. Overall, the model performance was described as good, with an R^2 value of 0.76 and an RMSE of 0.05. Hence, the performance in Dewenam et al. (2021) was better than in this research, and important reason probably being that the Dewenam et al. (2021) previously calibrated the model for better fitting simulation results.

Amiri et al. (2022) used field data from maize cultivated in Nebraska over six years to evaluate the performance of WOFOST under four different water regimes. After a calibration, the performance of the model was considered good for many variables, including yield and phenology. However, the ability of WOFOST to simulate soil moisture varied considerably depending on the year and irrigation level, with R^2 values ranging from 0.06 to 0.82. Additionally, it was observed that the performance decreased under water-limited conditions. Particularly under rainfed conditions, the model performance tended to be the poorest. The simulations of soil moisture in Reckenholz 2022 were also conducted under rainfed conditions, as irrigation was not possible at this location. The conclusion of Amiri et al. (2022) might serve as a further explanation of why the simulation of soil moisture with WOFOST was not very accurate for Reckenholz, particularly considering that no calibration was done in this case. Besides that, one possible explanation why the soil water content was underestimated by WOFOST during August and September might be the inaccuracy of the yield simulations in this year. As the yield in 2022 was overestimated with both crop files in Reckenholz, WOFOST may

consequently have overestimated the soil water use during the reproductive phase, leading to an underestimation of soil moisture during this time.

Discussing the performance of soil moisture simulation of soybean plots with WOFOST includes many uncertainties, as the research discussed in the available literature was conducted with different crops and in different climatic regions. Also, there are various uncertainties regarding the model evaluation conducted in this thesis. For instance, uncertainties exist concerning the measurements, the exact soil profile information, and the calculation of soil hydraulic parameters.

5.3 Yield Simulation

In chapter 4.3.1, crop files 906 and w41 were compared regarding the simulation of soybean yield and dry stress days. In general, the simulation with crop file w41 generated a higher variability in the yearly yields, as well as more dry stress days than with 906. This applies to Reckenholz and Changins. Consequently, it seems that the parameters defined in crop file w41 result in a higher sensitivity towards changing weather variables when applied in the simulation. Therefore, it can also be expected that w41 will be more sensitive to climate variability. In contrast to the yield simulation with w41, the LAI simulation does not seem to be sensitive to climate variability. LAI development could only be compared with observed data from 2022 in Reckenholz. However, simulations conducted for the years 2017-2018 and 2020-2021 (see Figure 37 in the appendix) show, that the w41-simulated LAI development in those four years matches the simulation in year 2022 quite well, despite the variability in the yield simulations.

At both locations, the yield was mostly overestimated with crop file w41. The overestimation was particularly pronounced in the years 2009, 2015, 2017, 2020 and 2022. Those years are all characterized by high summer temperatures in Switzerland (MeteoSwiss, 2009, 2015, 2017, 2020, 2022b). During these years, WOFOST might have overestimated the impact of the high temperatures on the soybean yield. The yields of 2020-2022 in Reckenholz were overestimated with crop file 906. During those years, no dry stress is simulated by WOFOST, even though high temperatures and low precipitation values were recorded in 2020 and 2022 (MeteoSwiss, 2020, 2022b). As there is no irrigation infrastructure in Reckenholz, it might be possible that dry stress affected the yield more than estimated by WOFOST. In Changins, where irrigation can be applied, the yield overestimation was much less pronounced than in Reckenholz.

Kroes et al. (2019) used the combined SWAP/WOFOST model to study groundwater recharge, climate and land use changes from soybean to crop rotations and to grassland in different locations of the Pampas region of Argentina. They applied the calibration activities described by de Wit et al. (2017) and added a management factor, which accounts for yield losses due to pests, diseases and weeds. Subsequently, they achieved a good fit of the simulated and observed yield values. The mean error of 856 kg/ha during the period of 1990-2015 was deemed acceptable by the researchers. In this research, RMSE values for crop files 906 and w41 ranged from 592 to 1417 kg/ha, however those values resulted from using only WOFOST without a calibration. The simulated mean yield in Kroes et al. (2019) was 3019 kg/ha, while the observed mean yield was 2255 kg/ha. Thus, the simulations conducted by Kroes et al. (2019) were also characterized by an overestimation of the yield, as was the case in this study. Kroes et al. (2019) attributed the overestimation to the existence of additional stressors not considered in the simulations. The studied locations differed regarding management, drainage, and soil types. This also applies to the research sites of this master thesis. Above all, there are

differences regarding soil types, as the Agroscope variety tests do not take place on the same plots every year.

Besides Kroes et al. (2019), WOFOST was used in two studies simulating soybean yield in Asian countries. Abadi et al. (2018) used WOFOST to simulate the potential soybean yield and analyse the yield gap in East Java, Indonesia. They did not consider simulation data from the water-limited scenario, therefore a comparison to the research conducted for this thesis is not expedient. However, they concluded that WOFOST had a high potential for further application in the region, considering the correlation between the simulated and observed values. Recommended next steps included a calibration and validation of the model for the East Java region. Venugopalan et al. (2010) also conducted a yield gap analysis with WOFOST for different sites in Maharashtra, India. They modified the crop files included in WOFOST with parameters fitting Indian soybean varieties and validated the model. The mean observed yield was 1300 kg/ha, and the mean simulated yield was 1332 kg/ha. The statistical evaluation resulted in an R^2 -value of 0.9, and an RMSE of 11%. The researchers concluded that, after a calibration and validation, WOFOST had good prospects of being applied for soybean yield simulations in the region. The research of Abadi et al. (2018) and Venugopalan et al. (2010) demonstrates the applicability of WOFOST in different climatic regions.

Possible limitations regarding an accurate simulation of the soybean yield with WOFOST in this study are mostly different stress factors which are not included in the model, as mentioned by Kroes et al. (2019). In this master thesis, the yield data from Reckenholz and Changins was not obtained under the same conditions every year. The plot used for cultivation varied from year to year at both locations, and irrigation was only applied in Changins. Therefore, possible stressors limiting the crop growth and yield formation originating in the soil type and structure could not always be accounted for, as only one soil profile was used for the simulations. Consequently, drought stress might not have been accurately simulated by WOFOST for each year and location. Drought stress affects various processes in soybean development, including seed germination, photosynthesis, and nitrogen fixation. Nitrogen is particularly important for soybeans because of their high protein content (Board & Kahlon, 2011). WOFOST does not account for the occurrence of biotic stressors, such as weeds and nematodes, which is an additional limitation (Board & Kahlon, 2011; Boogaard et al., 2021).

A further limitation of the model was described by de Wit et al. (2017) and Groenendijk et al. (2016), who mentioned that WOFOST 7.1 is not able to describe the phenological development of soybeans accurately. In WOFOST, plants follow a sequential development, where no overlapping occurs, whereas the phenological development of soybeans happens in a mostly parallel manner. The sequential development is typical for cereals, who are long-day plants. Soybeans, however, are short-day plants, whose phenological development is stimulated under short-day conditions. In addition, the manner in which WOFOST simulates the impact of temperature on the phenological development does not account for the complexity of the relationship between these two variables that is inherent for soybeans (de Wit et al., 2017; Groenendijk et al., 2016). This finding also corresponds to the comparison of the simulated and observed flowering dates for Reckenholz in 2022; with 906, flowering was simulated five days too late, and with w41, the simulated flowering took place 20 days after the observed flowering. If the phenology is not simulated accurately by a crop model, the performance of the yield simulation could be impacted as well, as the interaction with and sensitivities to weather conditions differ in regards to the current phenological stage of the plant (Board & Kahlon, 2011; Setiyono et al., 2007).

As discussed in chapters 5.1 and 5.2, WOFOST was not able to accurately simulate the soil water content and LAI development of 2022 in Reckenholz. This can also adversely affect the yield simulation and lead to inaccurate results. For instance, the simulation with crop file w41 overestimated the LAI and yield in Reckenholz for 2022. An accurate simulation of the LAI might also have resulted in a lower simulated yield. However, the output with crop file 906 also overestimated the yield in Reckenholz, despite the underestimation of the LAI in this simulation. The evaluation of the soil moisture simulation does also not serve as a clear explanation of why WOFOST simulated higher yields, as WOFOST considerably underestimated soil moisture in August and September of 2022. Drought stress was simulated only with w41, despite the yield overestimation being even more pronounced than with 906. This shows that a further adjustment of the model is necessary to obtain a higher goodness of fit between the simulated and observed values. As the parameters in the WOFOST crop files which describe water use and rooting are equal in w41 and 906, the differences in yield simulations can probably be explained with one or multiple other differing crop parameters. As mentioned in chapter 3.2.1, parameters of TSUM, assimilation, partitioning and conversion efficiency differ in these two crop files. As the parameter CVO (conversion efficiency of assimilates to storage organs, i.e., soybean seeds) is higher for w41 than for 906, this might lead to a higher yield simulation with w41 in years where meteorological conditions are particularly beneficial to photosynthetic activity and an increase of partitioning to the storage organs occurs. However, to fully account for the differences between crop files and their consequences, further research is needed, for instance in the context of a sensitivity analysis, which is discussed in more depth in chapter 5.6.

5.4 Impacts of Climate Change

5.4.1 Yield and Drought Stress

The model application of WOFOST focusing on climate impacts conducted in this thesis shows differing results, depending on the crop file used for the simulation and, albeit to a lesser extent, on the study site. Simulating with 906, the yield is expected to slightly decrease, whereas with w41, an increase in yield is projected. Irrespective of the crop file and RCP, Changins is projected to be more severely impacted by drought stress than Reckenholz.

With crop file w41, the yield in Changins is projected to increase until mid-century, despite a high sum of dry stress days. But, under RCP8.5, after the yearly amount of dry stress days starts to rise above approximately 25 days, the yield starts to decline and continues to do so until the end of the century. Under RCP4.5, the sum of dry stress days does not increase as much as under RCP8.5, and no yield losses are projected in comparison to the reference period. However, by the end of the century, the projected yield in Changins with w41 is slightly less than the yield projected for the mid-century period, therefore the onset of the decline could just be delayed under RCP4.5. With crop file 906, yield losses are projected along with a rising yearly sum of dry stress days for Changins. The decreasing trend of soybean yield is more pronounced under RCP8.5. This emphasizes the significance of irrigation at this location and shows that there is a high possibility it will have to be intensified in the future to prevent yield losses. Another option might be to cultivate more drought-tolerant soybean varieties in this area.

In Reckenholz, drought stress is projected to have a much less frequent occurrence. With crop file 906, dry stress days are almost non-existent under RCP4.5. The yield is still projected to slightly decrease under RCP4.5, and more so under RCP8.5. The decline of the yield in RCP8.5 seems to correspond with a higher occurrence of dry stress projected for the end of

the century. When examining the raw data of the simulations with 906 (see Figure 31 to Figure 34 in the appendix), one can spot spikes where mostly one certain model chain predicts a higher number of dry stress days. This is not visible in the shaded percentiles plot (see Figure 20), as outliers do not impact the median as much. Therefore, depending on which model chain is the most accurate, more dry stress incidents might still occur. This also applies to the simulations with crop file w41, as can be seen in Figure 32 in the appendix. Examining both locations in all scenarios, the strongest increase in yield is projected for Reckenholz with crop file w41. Still, as dry stress days are projected to increase under RCP8.5, a decline in yield also starts at approximately 2090. Therefore, drought stress might also arise in Reckenholz, albeit most probably later in time compared to Changins.

Arumugam (2021) simulated soybean yields under historical (1981-2014) and future (2015-2050) climatic conditions in the Netherlands. The research was conducted with WOFOST and a calibrated crop file. Arumugam (2021) did not disclose which parameters were adjusted in the calibration nor which crop file was used in his research. Until the middle of the century, WOFOST predicted yield losses for soybean cultivation under rainfed (-7.8%) and irrigated (-4.6%) conditions in the Netherlands. These projections were conducted under a high emission scenario (SSP3-RCP7.0). The climate impact analysis for Reckenholz and Changins was conducted under rainfed conditions only. Under RCP8.5, The yield loss projected with 906 for the near future period (2020-2049) ranged from 4.9% (Reckenholz) to 12.1% (Changins) compared to REF. With crop file w41, the yield gains projected for the same period were 21.4% for Changins and 91.5% for Reckenholz. Therefore, the findings of Arumugam (2021) roughly coincide with the results obtained with crop file 906, considering the different emission scenarios used. Arumugam (2021) stated, that soybean cultivation should benefit from the less frequent occurrence of frost days and generally higher temperatures in the Netherlands in the future. As a decrease in precipitation amounts was projected for the Netherlands, he recommended additional irrigation to prevent yield losses. In this study, the projected sum of yearly dry stress days also demonstrates the importance of increased irrigation, above all for Changins.

Wolf (2002) tested the sensitivity of two soybean models (CROPGRO and SOYBEANW) to changes in climate variables, such as increasing temperatures, CO₂ and precipitation. Data from soybean trials in Toulouse, France, were used for the calibration of both models. Wolf (2002) found, that increasing atmospheric CO₂ levels and precipitation led to higher yields in a water-limited scenario, while increasing temperatures had no significant effect on yield, and a higher solar radiation negatively impacted the yield, but only in CROPGRO. However, if irrigation was added, yields increased with higher solar radiation and atmospheric CO₂ levels. Increasing temperatures had a positive effect on yield in CROPGRO. However, Wolf (2002) mentioned that this model has a tendency to overestimate the positive impacts of increasing temperatures, and the yield simulated with SOYBEANW did not change with increasing temperatures. Boulch et al. (2021) also used the CROPGRO model to study impacts on soybean yield in northern France from 1999 to 2018. Even though the study region is generally considered humid, they found that the main limiting factor of yield under rainfed conditions was water. During the grain filling period, a good water supply was found to be particularly important for optimal yield formation. During the vegetative stage, yield was not impacted by drought stress. Mera et al. (2006) also used CROPGRO for a climate impact study on soybean yield in Clayton, North Carolina. They generated insights similar to those of Boulch et al. (2021). Precipitation was identified as the most sensitive factor impacting yield.

The findings of Wolf (2002) and Boulch et al. (2021) are interesting in the context of climate change, as both recommend evaluating irrigation as an option to improve soybean yield. Both studies were conducted in a country neighbouring Switzerland and under historical climatic conditions. Modelling soybean yield and dry stress days with crop file 906 in WOFOST, it also seems that irrigation could improve yield under future climatic conditions. This specifically applies to Changins, but it might also be beneficial in Reckenholz nearing the end of the century. For both locations, precipitation is projected to increase during spring months and decrease during the summer months (see Figure 4). As Boulch et al. (2021) mentioned, the earlier periods of soybean development are not as sensitive to drought stress as the reproductive stage. For the results with 906, this would confirm the decrease in yield due to the reduced precipitation amounts in the summer months, during which soybeans reach their reproductive development stage. As Changins generally has less precipitation during the summer months compared to Reckenholz, the stronger decrease in yield over time also corresponds with this finding.

However, the findings mentioned in the last three paragraphs do not align with the results from modelling yield and dry stress days under climate change with crop file w41. Despite a higher amount of dry stress days compared to the simulations with 906, the yield simulated with w41 increased consistently. Two studies modelling climate change impacts on soybean cultivation in Serbia projected an increase in soybean yield under climate change scenarios (Jancic et al., 2015; Tovjanin et al., 2019). The main reason why their results differ from previously mentioned studies is probably that they both considered the effect of CO₂ fertilization in their simulations. Yet, like the other studies, Jancic et al. (2015) and Tovjanin et al. (2019) also found that the demand for irrigation would significantly increase in the future. These findings do not explain the increase in yield with w41, as CO₂ fertilization effects are not considered in WOFOST 7.1. The reason why the yield simulated with w41 increases stronger compared to 906 therefore lies in the parameter values defined in the crop file. As discussed in chapter 5.3, further research is needed to identify the parameters with the highest impact on yield.

As crop file w41 was originally developed for tropical regions and the crop file parameters are therefore adjusted to varieties grown in the tropics, the results in 906 might show possible future changes in soybean yield more accurately for the Swiss Plateau. This conclusion is also supported by the literature discussed in this chapter. In addition, the uncertainty of the yield simulations with crop file w41 is consistently larger than with crop file 906 at both study sites.

5.4.2 Flowering and maturity

With both crop files, flowering and maturity are projected to occur earlier under climate change scenarios. Under RCP8.5, the shift is more pronounced than under RCP4.5. Crop files 906 and w41 generate similar results, however with w41, flowering and maturity are estimated to occur slightly earlier. As WOFOST simulated the phenological development based on a range of possible sowing and harvest dates (see chapter 3.4), the findings show a shift of the optimum growing period of soybeans in Changins and Reckenholz. This is attributable to the projected higher temperatures under climate change in Switzerland (see Figure 3). Therefore, cultivars with traits similar to the parameters defined in crop files 906 and w41 might benefit from an earlier sowing date in the future. This finding shows that the growing season for soybeans is projected to become longer in the future, which could also point to a shift in suitable cultivars for the region of the Swiss Plateau. Nendel et al. (2023) found that, across Europe, the distribution of areas suitable for certain soybean maturity groups shifted northwards under climate change scenarios. Under present conditions, regions in Switzerland and Germany are mostly mapped as being suitable for early cultivars (MG 000 and 00), but cultivars of the

maturity groups 0 and I are projected become more suitable in the area under RCP4.5, and the effect is even stronger under RCP8.5 (Nendel et al., 2023). This could lead to improvements in the soybean yield potentials in the region, as early maturity groups tend to generate lower grain yields (Bassu et al., 2014; Nendel et al., 2023; Ortel et al., 2020).

5.5 Limitations

The climate impact analysis conducted with WOFOST for soybeans on the Swiss Plateau contains several limitations. There are uncertainties regarding the input data and general performance of the model for the two study sites. This concerns uncertainties regarding the exact soil type and structure mainly for Changins, but also to some extent for Reckenholz when considering uncertainties arising during measurements and data gathering. Specifically for the yield simulations, limitations have already been discussed in chapter 5.3. WOFOST 7.1 does generally not simulate soybean phenology accurately (de Wit et al., 2017; Groenendijk et al., 2016). The simulations of LAI and soil moisture for Reckenholz lacked accuracy, as concluded in this thesis. As LAI and soil moisture data was not gathered for Changins, the performance of WOFOST regarding the simulation of these variables could not be evaluated for this location. Of course, measurement uncertainties also must be considered for the LAI and soil moisture measurements conducted in Reckenholz, 2022.

Soybean yield data for Reckenholz was only collected from 2014 on, whereas in Changins, data is available from 2006 on. WOFOST does not account for the occurrence of biotic stresses (Boogaard et al., 2021). Additionally, the effects of CO₂ fertilization were not considered in WOFOST 7.1 (Bassu et al., 2014; Boogaard et al., 2021). Several studies found that rising CO₂ levels led to an increase in soybean yield (Bassu et al., 2014; Boulch et al., 2021; Fodor et al., 2017; Wolf, 2002). Hence, if CO₂ fertilization effects were included in WOFOST, the projected future yields might generally be higher. An important limitation of this study is also, that the model was not calibrated to the study sites and the specific cultivars grown there, which impacts the yield simulation with observational and projected weather data. Falconnier et al. (2020) concludes the following:

If not calibrated against multiple in-season variables such as soil water content, plant nitrogen content or Leaf Area Index, soil-crop models run the risk of accurately simulating grain yield without accurately simulating growth dynamics. This can undermine their relevance for climate change studies. (p. 11)

Finally, there are uncertainties regarding the simulation with the CH2018 data. Even though the CH2018 datasets are bias-corrected, some biases might still remain according to CH2018 (2018a). The natural variability of the global circulation cannot fully be accounted for, and as with any model predictions, there are various inherent uncertainties. This is particularly true for future extreme events, which can have a considerable impact on crop production. When using a set of CH2018 model chain data for simulating soybean yield in the future, the range of the resulting values hint at the dimension of uncertainty, while the median serves as a “best-guess” estimation. However, these projected ranges are essentially based on a certain RCP, and the RCPs themselves also represent uncertainty regarding political decisions on mitigation and the anthropogenic impact on the future climate (CH2018, 2018b).

5.6 Future Research Ideas

For future modelling studies regarding soybean yield and its development under climate change scenarios in Switzerland, additional data would be beneficial. Several years of soybean yield data was available from the Agroscope variety tests, but phenology data is lacking from these trials. Modelling studies could especially benefit from dates of flowering and maturity for

each variety. The harvest date was recorded for each year, but as not all cultivars reach maturity around the same time, it gives no exact information on when maturity is attained. According to Wolf and de Wit (2010), the first step of the calibration concerns the phenology and growth period length of the crop, which stresses the importance of the respective data. As Falconnier et al. (2020) recommended, LAI and soil moisture data for all study sites could be advantageous for a crop model calibration. It might also be interesting to assimilate LAI and soil moisture derived from remote sensing data into WOFOST, as was conducted successfully by Pan et al. (2019) for winter wheat. To reduce the uncertainties inherent to the structure of WOFOST, meaning the specific formulas used to calculate crop growth processes, ensemble model studies could be performed (Falconnier et al., 2020; Sun et al., 2022).

First efforts at calibrating WOFOST, which were performed for this master thesis, showed that the yield simulation at both study sites might be improved (results not shown). RMSE and PBIAS% values of the simulated yields could be reduced with a reduction of the TSUM1- (temperature sum from emergence to anthesis) and AMAXTB- (maximum leaf CO₂ assimilation rate as a function of the DVS) parameters in the crop files of w41 and 906. These results are not included in this thesis, as a calibration would require many more steps (Wolf & de Wit, 2010). While a calibration can improve the model output for a specific region or research purpose, it can reduce the general applicability of the model (de Wit & Boogaard, 2021). Therefore, a calibration of WOFOST might not be the best option for every research objective.

Prior to calibrating the model, carrying out a sensitivity analysis can help assessing how the modification of certain crop parameters affects soybean yield, LAI or soil moisture. Thus, the most influential parameters on a model output variable can be identified, which may serve as input for the calibration of the model (Dewenam et al., 2021; Lamboni et al., 2009). Multiple studies conducted a sensitivity analysis after calibrating the crop growth model (Eweys et al., 2017; Sun et al., 2022; Wolf, 2002). This approach is used by Sun et al. (2022) as a means of assessing climate change impacts on soybean yields with a model ensemble in the Mississippi Delta, USA. A sensitivity analysis focusing on climate change impacts might likewise provide useful insights for Switzerland. As drought stress might become a limiting factor for soybean yield potentials in the future, it would be interesting to include a scenario with irrigation in a climate impact analysis to assess the potential of irrigation as an adaptation strategy.

6 Conclusion

While on a global scale, an increasing suitability for soybean cultivation in Europe due to climate change is projected, varying conclusions can be drawn when studying cultivation on a regional scale. On the Swiss Plateau, soybean development will benefit from the warmer spring and summer temperatures and the reduction of cold stress in the early growing stages. However, whether the yield will consequently increase, highly depends on the cultivar grown. The simulations with crop file w41 showed an increase in yield throughout most of the 21st century, whereas with 906, yields are projected to decrease in future periods. However, under RCP8.5, the yields simulated with w41 start to decline at the end of the century. As these two crop files were parameterized for different regions and their commonly grown varieties, the results stress the importance of selecting an appropriate soybean cultivar in the context of adaptation to climate change. However, our results also exhibit an increasing demand for irrigation, especially in Changins. In all scenarios, dry stress days are projected to increase. In contrast to Reckenholz, where irrigation might only become necessary by the end of the century, the variety tests in Changins are already being irrigated. Therefore, to prevent future yield losses, adaptation might include more drought tolerant cultivars or additional irrigation, if available. As the yields in most scenarios either decrease throughout the 21st century or start to decline by 2085, additional adaptation measures should be considered. For instance, as the length of the vegetation period is projected to increase, higher yielding varieties from MG 0 and I might be cultivated on the Swiss Plateau in the future. Due to the uncertainty of crop model simulations and climate projections, further research is called for. This concerns the gathering of additional data, for instance of phenology, LAI and soil moisture, which can serve as reference to a model evaluation and calibration, and therefore lead to a higher model accuracy. To study climate impacts on soybean cultivation on the Swiss Plateau in more depth, we would suggest accounting for the effects of CO₂ fertilization, which could not be done in this thesis.

7 References

- Abadi, F. R., Tastra, I. K., & Koentjoro, B. S. (2018). Preliminary Study of WOFOST Crop Simulation in Its Prospect for Soybean (*Glycine max* L.) Optimum Harvest Time and Yield Gap Analysis in East Java. *Agrivita*, 40(3), 544–555.
<https://doi.org/10.17503/agrivita.v40i3.1832>
- Agristat. (2022). *Archiv Statistische Erhebungen und Schätzungen*. <https://www.sbv-usp.ch/de/services/agristat-statistik-der-schweizer-landwirtschaft/statistische-erhebungen-und-schaetzungen-ses/archiv-statistische-erhebungen-und-schaetzungen/>
- Agroscope. (2006a). *Annual Report "Sortenversuch Soja" [Excel file]*. Authors: Charles, R., Deladoey, L., Hebeisen, T. & Hunziker, H. R.
- Agroscope. (2006b). *Carnet des Champs [Word file]*. Nyon/Changins, Switzerland.
- Agroscope. (2007a). *Annual Report "Sortenversuch Soja" [Excel file]*. Authors: Charles, R., Deladoey, L., Hebeisen, T. & Hunziker, H. R.
- Agroscope. (2007b). *Interventions 2007 [Excel file]*. Nyon/Changins, Switzerland.
- Agroscope. (2008a). *Annual Report "Sortenversuch Soja" [Excel file]*. Authors: Charles, R., Streit, C., Bovet, V., Hebeisen, T., Hunziker, H. R., Hiltbrunner, J. & Herzog, C.
- Agroscope. (2008b). *Carnet des Champs 2008 [PDF file]*. Nyon/Changins, Switzerland.
- Agroscope. (2009a). *Annual Report "Sortenversuch Soja" [Excel file]*. Authors: Streit, C., Hiltbrunner, J., Herzog, C. & Bovet, V.
- Agroscope. (2009b). *Carnet des Champs 2009 [PDF file]*. Nyon/Changins, Switzerland.
- Agroscope. (2010a). *Annual Report "Sortenversuch Soja" [Excel file]*. Authors: Streit, C., Hiltbrunner, J., Herzog, C. & Bovet, V.
- Agroscope. (2010b). *Carnet des Champs 2010 [PDF file]*. Nyon/Changins, Switzerland.
- Agroscope. (2011a). *Annual Report "Sortenversuch Soja" [Excel file]*. Authors: Streit, C., Hiltbrunner, J., Herzog, C. & Bovet, V.
- Agroscope. (2011b). *Suivi des Cultures 2011 [PDF file]*. Nyon/Changins, Switzerland.
- Agroscope. (2012a). *Annual Report "Sortenversuch Soja" [Excel file]*. Authors: Charles, R., Hiltbrunner, J., Herzog, C. & Bovet, V.
- Agroscope. (2012b). *Suivi des Cultures 2012 [PDF file]*. Nyon/Changins, Switzerland.
- Agroscope. (2013a). *Annual Report "Sortenversuch Soja" [Excel file]*. Authors: Charles, R., Hiltbrunner, J., Bovet, V., Amrein, U. & Buchmann, U.
- Agroscope. (2013b). *Suivi des Cultures 2013 [PDF file]*. Nyon/Changins, Switzerland.
- Agroscope. (2014a). *Annual Report "Sortenversuch Soja" [Excel file]*. Authors: Schwaerzel, R., Riot, G., Hiltbrunner, J. & Buchmann, U.
- Agroscope. (2014b). *Suivi des Cultures 2014 [PDF file]*. Nyon/Changins, Switzerland.
- Agroscope. (2015a). *Annual Report "Sortenversuch Soja" [Excel file]*. Authors: Schwaerzel, R., Riot, G., Hiltbrunner, J. & Buchmann, U.
- Agroscope. (2015b). *Suivi des Cultures 2015 [PDF file]*. Nyon/Changins, Switzerland.
- Agroscope. (2016a). *Annual Report "Sortenversuch Soja" [Excel file]*. Authors: Schwaerzel, R., Riot, G., Hiltbrunner, J. & Buchmann, U.
- Agroscope. (2016b). *Suivi des Cultures 2016 [PDF file]*. Nyon/Changins, Switzerland.
- Agroscope. (2017a). *Annual Report "Sortenversuch Soja" [Excel file]*. Authors: Schwaerzel, R., Nussbaum, V., Hiltbrunner, J. & Buchmann, U.
- Agroscope. (2017b). *Carnet des Champs 2017 [PDF file]*. Nyon/Changins, Switzerland.
- Agroscope. (2018a). *Annual Report "Sortenversuch Soja" [Excel file]*. Authors: Nussbaum, V., Schwaerzel, R., Hiltbrunner, J. & Buchmann, U.

- Agroscope. (2018b). *Carnet des Champs 2018 [PDF file]*. Nyon/Changins, Switzerland.
- Agroscope. (2019a). *Annual Report "Sortenversuch Soja" [Excel file]*. Authors: Nussbaum, V., Schwaerzel, R., Hiltbrunner, J. & Strahm, S.
- Agroscope. (2019b). *Carnet des Champs 2019 [PDF file]*. Nyon/Changins, Switzerland.
- Agroscope. (2020a). *Annual Report "Sortenversuch Soja" [Excel file]*. Authors: Tallant, M., Vonlanthen, T. & Baux, A.
- Agroscope. (2020b). *Carnet des Champs 2020 [PDF file]*. Nyon/Changins, Switzerland.
- Agroscope. (2021a). *Annual Report "Sortenversuch Soja" [Excel file]*. Authors: Tallant, M., Vonlanthen, T. & Baux, A.
- Agroscope. (2021b). *Carnet des Champs 2021 [PDF file]*. Nyon/Changins, Switzerland.
- Agroscope. (2022a). *Annual Report "Sortenversuch Soja" [Excel file]*. Authors: Vonlanthen, T., Fuchs, Z., Tallant, M. & Baux, A.
- Agroscope. (2022b). *Carnet des Champs 2022 [PDF file]*. Nyon/Changins, Switzerland.
- Amiri, E., Irmak, S., & Yaghouti, H. (2022). Performance of WOFOST Model for Simulating Maize Growth, Leaf Area Index, Biomass, Grain Yield, Yield Gap, and Soil Water under Irrigation and Rainfed Conditions. *Journal of Irrigation and Drainage Engineering*, 148(2), Article 05021005. [https://doi.org/10.1061/\(ASCE\)IR.1943-4774.0001644](https://doi.org/10.1061/(ASCE)IR.1943-4774.0001644)
- Arumugam, P. (2021). *Modeling Crop Yields and Water Balances for the Netherlands with WOFOST*. Wageningen University & Research. <https://edepot.wur.nl/560449>
- Asanome, N., & Ikeda, T. (1998). Effect of Branch Direction's Arrangement on Soybean Yield and Yield Components. *Journal of Agronomy and Crop Science*, 181(2), 95–102. <https://doi.org/10.1111/j.1439-037X.1998.tb00404.x>
- Bassu, S., Brisson, N., Durand, J.-L., Boote, K. J., Lizaso, J., Jones, J. W., Rosenzweig, C., Ruane, A. C., Adam, M., Baron, C., Basso, B., Biernath, C., Boogaard, H. L., Conijn, S., Corbeels, M., Deryng, D., Sanctis, G. de, Gayler, S., Grassini, P., . . . Waha, K. (2014). How do various maize crop models vary in their responses to climate change factors? *Global Change Biology*, 20(7), 2301–2320. <https://doi.org/10.1111/gcb.12520>
- Betbeder, J., Fieuzal, R., & Baup, F. (2016). Assimilation of LAI and Dry Biomass Data From Optical and SAR Images Into an Agro-Meteorological Model to Estimate Soybean Yield. *IEEE Journal of Selected Topics in Applied Earth Observations and Remote Sensing*, 9(6), 2540–2553. <https://doi.org/10.1109/jstars.2016.2541169>
- Board, J. E., & Kahlon, C. S. (2011). Soybean Yield Formation: What Controls It and How It Can Be Improved. In H. El-Shemy (Ed.), *Soybean Physiology and Biochemistry* (pp. 1–36). InTech.
- Boogaard, H. L., de Wit, A. J. W., te Roller, J. A., & van Diepen, C. A. (2021). *WOFOST CONTROL CENTRE 2.1: User's guide for the WOFOST CONTROL CENTRE 2.1 and the crop growth simulation model WOFOST 7.1.7*. Wageningen (Netherlands). Alterra, Wageningen University & Research Centre. <https://www.wur.nl/en/research-results/research-institutes/environmental-research/facilities-tools/software-models-and-databases/wofost/documentation-wofost.htm>
- Boons-Prins, E. R., de Koning, G. H. J., van Diepen, C. A., & Penning de Vries, F. W. T. (1993). *Crop-specific simulation parameters for yield forecasting across the European Community*. Wageningen. CABO-DLO Centre for Agrobiological Research, Dutch Agricultural Research Department. <https://edepot.wur.nl/308997>

- Boulch, G., Elmerich, C., Djemel, A., & Lange, B. (2021). Evaluation of soybean (*Glycine max L.*) adaptation to northern European regions under different agro-climatic scenarios. *IN SILICO PLANTS*, 3(1), 1-13.
<https://doi.org/10.1093/insilicoplants/diab008>
- Calanca, P., & Holzkämper, A. (2010). Agrometeorological conditions on the Swiss Plateau from 1864 to 2050. *Agrarforschung Schweiz*, 1(9), 320–325.
- CH2018. (2018a). *CH2018 - Climate Scenarios for Switzerland: Documentation of localized data, version 1.2*. National Centre for Climate Services.
- CH2018. (2018b). *CH2018 – Climate Scenarios for Switzerland: Technical Report, version 2*. Zurich. National Centre for Climate Services. ISBN: 978-3-9525031-4-0.
- CH2018 Project Team. (2018). *CH2018 - Climate Scenarios for Switzerland*. National Centre for Climate Services. <https://doi.org/10.18751/Climate/Scenarios/CH2018/1.0>
- Cober, E. R., & Voldeng, H. D. (2012). A retrospective look at short-season soybean cultivar development in Ontario. *Canadian Journal of Plant Science*, 92(7), 1239–1243.
<https://doi.org/10.4141/cjps2012-032>
- Csajbók, J., Kutasy, E. T., Melash, A. A., Virág, I. C., & Ábrahám, É. B. (2022). Agro-biological traits of soybean cultivars, their yield quantity and quality under Central European conditions. *Zemdirbyste-Agriculture*, 109(2), 107–114.
<https://doi.org/10.13080/z-a.2022.109.014>
- de Wit, A. J. W., & Boogaard, H. L. (2021). *A gentle introduction to WOFOST*. Wageningen. Wageningen Environmental Research.
- de Wit, A. J. W., d'Abelleyra, D., Veron, S., Kroes, J. G., Supit, I., & Boogaard, H. L. (2017). *Technical description of crop model (WOFOST) calibration and simulation activities for Argentina, pampas region*. SIGMA. <https://edepot.wur.nl/441498>
- de Wit, A. J. W., Franke, J., van Diepen, K., & te Roller, J. A. (2014). *Wofost Control Centre / WOFOST (Version 2.1 / 7.1.7) [Computer software]*. Alterra, Wageningen University & Research Centre. Wageningen, Netherlands. <https://www.wur.nl/en/research-results/research-institutes/environmental-research/facilities-tools/software-models-and-databases/wofost/downloads-wofost.htm>
- Dewenam, L. E. F., Er-Raki, S., Ezzahar, J., & Chehbouni, A. (2021). Performance Evaluation of the WOFOST Model for Estimating Evapotranspiration, Soil Water Content, Grain Yield and Total Above-Ground Biomass of Winter Wheat in Tensift Al Haouz (Morocco): Application to Yield Gap Estimation. *Agronomy*, 11(12), 2480.
<https://doi.org/10.3390/agronomy11122480>
- Eitzinger, J., Trnka, M., Hösch, J., Žalud, Z., & Dubrovský, M. (2004). Comparison of CERES, WOFOST and SWAP models in simulating soil water content during growing season under different soil conditions. *Ecological Modelling*, 171(3), 223–246.
- Elmerich, C., Boulch, G., Faucon, M. P., Lakhal, L., & Lange, B. (2023). Identification of Eco-Climatic Factors Driving Yields and Genotype by Environment Interactions for Yield in Early Maturity Soybean Using Crop Simulation. *Agronomy-Basel*, 13(2), 322.
<https://doi.org/10.3390/agronomy13020322>
- Eweys, O. A., Elwan, A. A., & Borham, T. I. (2017). Integrating WOFOST and Noah LSM for modeling maize production and soil moisture with sensitivity analysis, in the east of The Netherlands. *Field Crops Research*, 210, 147–161.
<https://doi.org/10.1016/j.fcr.2017.06.004>
- Falconnier, G. N., Vermue, A., Journet, E.-P., Christina, M., Bedoussac, L., & Justes, E. (2020). Contrasted response to climate change of winter and spring grain legumes in

- southwestern France. *Field Crops Research*, 259, 107967.
<https://doi.org/10.1016/j.fcr.2020.107967>
- Feng, L., Wang, H. Y., Ma, X. W., Peng, H. B., & Shan, J. R. (2021). Modeling the current land suitability and future dynamics of global soybean cultivation under climate change scenarios. *Field Crops Research*, 263, 108069.
<https://doi.org/10.1016/j.fcr.2021.108069>
- Fodor, N., Challinor, A., Droutsas, I., Ramirez-Villegas, J., Zabel, F., Koehler, A. K., & Foyer, C. H. (2017). Integrating Plant Science and Crop Modeling: Assessment of the Impact of Climate Change on Soybean and Maize Production. *Plant and Cell Physiology*, 58(11), 1833–1847. <https://doi.org/10.1093/pcp/pcx141>
- Foster, J. (2020). *roll: Rolling and Expanding Statistics*. R package, version 1.1.5.
<https://github.com/jjf234/roll>
- Garrigues, S., Shabanov, N. V., Swanson, K., Morissette, J. T., Baret, F., & Myneni, R. B. (2008). Intercomparison and sensitivity analysis of Leaf Area Index retrievals from LAI-2000, AccuPAR, and digital hemispherical photography over croplands. *Agricultural and Forest Meteorology*, 148(8-9), 1193–1209.
<https://doi.org/10.1016/j.agrformet.2008.02.014>
- Gasó, D. V., de Wit, A. J. W., Berger, A. G., & Kooistra, L. (2021). Predicting within-field soybean yield variability by coupling Sentinel-2 leaf area index with a crop growth model. *Agricultural and Forest Meteorology*, 308, 108553.
<https://doi.org/10.1016/j.agrformet.2021.108553>
- Gasó, D. V., de Wit, A. J. W., de Bruin, S., Puntel, L. A., Berger, A. G., & Kooistra, L. (2023). Efficiency of assimilating leaf area index into a soybean model to assess within-field yield variability. *European Journal of Agronomy*, 143, 126718.
<https://doi.org/10.1016/j.eja.2022.126718>
- Groenendijk, P., Boogaard, H. L., Heinen, M., Kroes, J. G., Supit, I., & de Wit, A. J. W. (2016). *Simulation nitrogen-limited crop growth with SWAP/WOFOST : Process descriptions and user manual* (Wageningen Environmental Research No. 2721). Wageningen. Wageningen Environmental Research.
<https://library.wur.nl/webquery/wurpubs/alterra-reports/510610>
- Hanic, R., & Petrasek, M. (1991). *Bodenkarte Versuchsländ (1:2'500): Reckenholz, 2. Ausgabe*. 8046, Zürich-Reckenholz. FAL, Eidgenössische Forschungsanstalt für Agrarökologie und Landbau.
- Hanic, R., Petrasek, M., & Zihlmann, U. (2020). *Bodenkartierung Versuchsländ Reckenholz: Bodenprofile*. Agroscope, Swiss Federal Office for Agriculture.
- Hartung, J., Elpelt, B., & Klösener, K.-H. (2002). *Statistik: Lehr- und Handbuch der angewandten Statistik*. Oldenbourg Wissenschaftsverlag.
<https://doi.org/10.1515/9783486810585>
- Jancic, M., Lalic, B., Mihailovic, D. T., & Jacimovic, G. (2015). Impact of climate change and carbon dioxide fertilization effect on irrigation water demand and yield of soybean in Serbia. *Journal of Agricultural Science*, 153(8), 1365–1379.
<https://doi.org/10.1017/S0021859615000179>
- Jańczak-Pieniążek, M., Buczek, J., Bobrecka-Jamro, D., Szpunar-Krok, E., Tobiasz-Salach, R., & Jarecki, W. (2021). Morphophysiology, Productivity and Quality of Soybean (*Glycine max* (L.) Merr.) cv. Merlin in Response to Row Spacing and Seeding Systems. *Agronomy*, 11(2), 403. <https://doi.org/10.3390/agronomy11020403>
- Karges, K., Bellingrath-Kimura, S. D., Watson, C. A., Stoddard, F. L., Halwani, M., & Reckling, M. (2022). Agro-economic prospects for expanding soybean production

- beyond its current northerly limit in Europe. *European Journal of Agronomy*, 133, 126415. <https://doi.org/10.1016/j.eja.2021.126415>
- Klaiss, M. (2019). Neue Marktchancen für Soja und Lupinen. *Bioaktuell*(5), 14–15.
- Klaiss, M., Schmid, N., Betrix, C. A., Baux, A., Charles, R., & Messmer, M. M. (2020). Organic soybean production in Switzerland. *Ocl-Oilseeds and Fats Crops and Lipids*, 27, Article 64. <https://doi.org/10.1051/ocl/2020059>
- Kothari, K., Battisti, R., Boote, K. J., Archontoulis, S. V., Confalone, A., Constantin, J., Cuadra, S. V., Debaeke, P., Faye, B., Grant, B., Hoogenboom, G., Jing, Q., van der Laan, M., Da Macena Silva, F. A., Marin, F. R., Nehbandani, A., Nendel, C., Purcell, L. C., Qian, B., . . . Salmerón, M. (2022). Are soybean models ready for climate change food impact assessments? *European Journal of Agronomy*, 135, 126482. <https://doi.org/10.1016/j.eja.2022.126482>
- Kroes, J., van Dam, J. C., Supit, I., d'Abelleyra, D., Verón, S., de Wit, A. J. W., Boogaard, H. L., Angelini, M., Damiano, F., Groenendijk, P., Wesseling, J. G., & Veldhuizen, Ab (2019). Agrohydrological analysis of groundwater recharge and land use changes in the Pampas of Argentina. *Agricultural Water Management*, 213, 843–857. <https://doi.org/10.1016/j.agwat.2018.12.008>
- Lamboni, M., Makowski, D., Lehuger, S., Gabrielle, B., & Monod, H. (2009). Multivariate global sensitivity analysis for dynamic crop models. *Field Crops Research*, 113(3), 312–320. <https://doi.org/10.1016/j.fcr.2009.06.007>
- LI-COR Biosciences. (2019). *LAI-2200C Plant Canopy Analyzer: Instruction Manual*. Lincoln, Nebraska. <https://www.licor.com/env/support/MicroContent/Resources/MicroContent/manuals/lai-2200c-instruction-manuals.html>
- Mera, R. J., Niyogi, D., Buol, G. S., Wilkerson, G. G., & Semazzi, F. H. M. (2006). Potential individual versus simultaneous climate change effects on soybean (C-3) and maize (C-4) crops: An agrotechnology model based study. *Global and Planetary Change*, 54(1-2), 163–182. <https://doi.org/10.1016/j.gloplacha.2005.11.003>
- MeteoSwiss. (n.d.). *Automatic Measurement Network*. Retrieved September 8, 2023, from <https://www.meteoswiss.admin.ch/weather/measurement-systems/land-based-stations/automatic-measurement-network.html>
- MeteoSwiss. (2009). *Annalen 2009*. Zurich. MeteoSwiss. <https://www.meteoschweiz.admin.ch/wetter/wetter-und-klima-von-a-bis-z/wetterarchiv-der-schweiz.html>
- MeteoSwiss. (2015). *Klimabulletin Sommer 2015*. Zurich. MeteoSwiss. <https://www.meteoschweiz.admin.ch/service-und-publikationen/publikationen/berichte-und-bulletins/2015/klimabulletin-sommer-2015.html>
- MeteoSwiss. (2017). *Klimabulletin Sommer 2017*. Zurich. MeteoSwiss. <https://www.meteoschweiz.admin.ch/service-und-publikationen/publikationen/berichte-und-bulletins/2017/klimabulletin-sommer-2017.html>
- MeteoSwiss. (2020). *Klimabulletin Sommer 2020*. Zurich. MeteoSwiss. <https://www.meteoschweiz.admin.ch/service-und-publikationen/publikationen/berichte-und-bulletins/2016/2020/klimabulletin-sommer-2020.html>

- MeteoSwiss. (2022a). *Klimabulletin Frühling 2022*. Zurich. MeteoSwiss.
<https://www.meteoswiss.admin.ch/services-and-publications/publications.html#order=date-desc&page=1&pageGroup=publication>
- MeteoSwiss. (2022b). *Klimabulletin Sommer 2022*. Zurich. MeteoSwiss.
<https://www.meteoswiss.admin.ch/service-und-publikationen/publikationen/berichte-und-bulletins/2022/klimabulletin-sommer-2022.html>
- MeteoSwiss. (2022c). *Overview of CH2018 data*. Zurich. Swiss Federal Office of Meteorology and Climatology. <https://www.nccs.admin.ch/nccs/en/home/climate-change-and-impacts/swiss-climate-change-scenarios/ch2018---climate-scenarios-for-switzerland/overview-ch2018-data.html>
- MeteoSwiss. (2022d). *Weather data from stations CGI and REH, 01.01.2000-31.12.2022*. IDAweb Data Portal, Swiss Federal Office of Meteorology and Climatology.
- MeteoSwiss. (2023). *Measurement values: Automatic weather stations*.
<https://www.meteoswiss.admin.ch/services-and-publications/applications/measurement-values-and-measuring-networks.html#param=messnetz-automatisch&lang=en>
- Mourtzinis, S., & Conley, S. P. (2017). Delineating Soybean Maturity Groups across the United States. *Agronomy Journal*, 109(4), 1397–1403.
<https://doi.org/10.2134/agronj2016.10.0581>
- NCCS. (2018). *CH2018 - Webatlas*. National Centre for Climate Services.
<https://www.nccs.admin.ch/nccs/en/home/climate-change-and-impacts/swiss-climate-change-scenarios/ch2018-web-atlas.html>
- Nendel, C., Reckling, M., Debaeke, P., Schulz, S., Berg-Mohnicke, M., Constantin, J., Fronzek, S., Hoffmann, M., Jakšić, S., Kersebaum, K. C., Klimek-Kopyra, A., Raynal, H., Schoving, C., Stella, T., & Battisti, R. (2023). Future area expansion outweighs increasing drought risk for soybean in Europe. *Global Change Biology*, 29(5), 1340–1358. <https://doi.org/10.1111/gcb.16562>
- Ordóñez, R. A., Castellano, M. J., Hatfield, J. L., Helmers, M. J., Licht, M. A., Liebman, M., Dietzel, R., Martinez-Feria, R., Iqbal, J., Puntel, L. A., Córdova, S., Togliatti, K., Wright, E. E., & Archontoulis, S. V. (2018). Maize and soybean root front velocity and maximum depth in Iowa, USA. *Field Crops Research*, 215, 122–131.
<https://doi.org/10.1016/j.fcr.2017.09.003>
- Ortel, C. C., Roberts, T. L., Hoegenauer, K. A., Purcell, L. C., Slaton, N. A., & Gbur, E. E. (2020). Soybean maturity group and planting date influence grain yield and nitrogen dynamics. *Agrosystems, Geosciences & Environment*, 3(1), Article e20077.
<https://doi.org/10.1002/agg2.20077>
- Pan, H., Chen, Z., de Wit, A. J. W., & Ren, J. (2019). Joint Assimilation of Leaf Area Index and Soil Moisture from Sentinel-1 and Sentinel-2 Data into the WOFOST Model for Winter Wheat Yield Estimation. *Sensors*, 19(14), 3161.
<https://doi.org/10.3390/s19143161>
- Roth, L., Barendregt, C., Betrix, C. A., Hund, A., & Walter, A. (2022). High-throughput field phenotyping of soybean: Spotting an ideotype. *Remote Sensing of Environment*, 269.
<https://doi.org/10.1016/j.rse.2021.112797>
- Schoving, C., Stockle, C. O., Colombet, C., Champolivier, L., Debaeke, P., & Maury, P. (2020). Combining Simple Phenotyping and Photothermal Algorithm for the Prediction of Soybean Phenology: Application to a Range of Common Cultivars Grown in Europe. *Frontiers in Plant Science*, 10. <https://doi.org/10.3389/fpls.2019.01755>

- Serafin-Andrzejewska, M., Helios, W., Jama-Rodzeńska, A., Kozak, M., Kotecki, A., & Kuchar, L. (2021). Effect of Sowing Date on Soybean Development in South-Western Poland. *Agriculture*, 11(5), 413. <https://doi.org/10.3390/agriculture11050413>
- Setiyono, T. D., Weiss, A., Specht, J. E., Bastidas, A. M., Cassman, K. G., & Dobermann, A. (2007). Understanding and modeling the effect of temperature and daylength on soybean phenology under high-yield conditions. *Field Crops Research*, 100(2-3), 257–271. <https://doi.org/10.1016/j.fcr.2006.07.011>
- Soares, J. R. S., Ramos, R. S., Da Silva, R. S., Neves, D. V. C., & Picanco, M. C. (2021). Climate change impact assessment on worldwide rain fed soybean based on species distribution models. *Tropical Ecology*, 62(4), 612–625. <https://doi.org/10.1007/s42965-021-00174-1>
- Sobko, O., Hartung, J., Zikeli, S., Claupein, W., & Gruber, S. (2019). Effect of sowing density on grain yield, protein and oil content and plant morphology of soybean (*Glycine max* L. Merrill). *Plant, Soil and Environment*, 65(12), 594–601. <https://doi.org/10.17221/346/2019-PSE>
- Sun, W. G., Fleisher, D., Timlin, D., Li, S. N., Wang, Z. J., Beegum, S., & Reddy, V. (2022). Evaluation of models for simulating soybean growth and climate sensitivity in the US Mississippi Delta. *European Journal of Agronomy*, 140, 126610. <https://doi.org/10.1016/j.eja.2022.126610>
- Szabó, B., Weynants, M., & Weber, T. K. D. (2021). Updated European hydraulic pedotransfer functions with communicated uncertainties in the predicted variables (euptfv2). *Geoscientific Model Development*, 14(1), 151–175. <https://doi.org/10.5194/gmd-14-151-2021>
- Tagliapietra, E. L., Streck, N. A., Da Rocha, T. S. M., Richter, G. L., Da Silva, M. R., Cera, J. C., Guedes, J. V. C., & Zanon, A. J. (2018). Optimum Leaf Area Index to Reach Soybean Yield Potential in Subtropical Environment. *Agronomy Journal*, 110(3), 932–938. <https://doi.org/10.2134/agronj2017.09.0523>
- Tanwar, B., & Goyal, A. (2021). *Oilseeds: Health Attributes and Food Applications*. Springer.
- Tovjanin, M. J., Djurdjevic, V., Pejic, B., Novkovic, N., Mutavdzic, B., Markovic, M., & Mackic, K. (2019). Modeling the impact of climate change on yield, water requirements, and water use efficiency of maize and soybean grown under moderate continental climate in the Pannonian lowland. *Idojaras*, 123(4), 469–486. <https://doi.org/10.28974/idojaras.2019.4.4>
- Venugopalan, M., Tiwary, P., Mandal, D., & Challa, O. (2010). Validation and application of WOFOST model for yield gap analysis in selected soils of Maharashtra. *Agropedology*, 20, 30–37.
- Wolf, J. (2002). Comparison of two soya bean simulation models under climate change. I. Model calibration and sensitivity analyses. *Climate Research*, 20, 55–70. <https://doi.org/10.3354/cr020055>
- Wolf, J., & de Wit, A. J. W. (2010). *Calibration of WOFOST crop growth simulation model for use within CGMS*. Wageningen. Alterra, Wageningen University & Research Centre.
- Yamamoto, S., Hashimoto, N., & Homma, K. (2023). Evaluation of LAI Dynamics by Using Plant Canopy Analyzer and Its Relationship to Yield Variation of Soybean in Farmer Field. *Agriculture*, 13(3), 609. <https://doi.org/10.3390/agriculture13030609>
- Zambrano-Bigiarini, M. (2020). *hydroGOF: Goodness-of-fit functions for comparison of simulated and observed hydrological time series*. R package, version 0.4-0. <https://github.com/hzambran/hydroGOF>, <https://doi.org/10.5281/zenodo.839854>

- Zhuo, W., Huang, H., Gao, X., Li, X., & Huang, J. (2023). An Improved Approach of Winter Wheat Yield Estimation by Jointly Assimilating Remotely Sensed Leaf Area Index and Soil Moisture into the WOFOST Model. *Remote Sensing*, *15*(7), 1825. <https://doi.org/10.3390/rs15071825>
- Zhuo, W., Huang, J., Li, L., Zhang, X., Ma, H., Gao, X., Huang, H., Xu, B., & Xiao, X. (2019). Assimilating Soil Moisture Retrieved from Sentinel-1 and Sentinel-2 Data into WOFOST Model to Improve Winter Wheat Yield Estimation. *Remote Sensing*, *11*(13), 1618. <https://doi.org/10.3390/rs11131618>
- Zimmer, S., Messmer, M., Haase, T., Piepho, H.-P., Mindermann, A., Schulz, H., Habekuss, A., Ordon, F., Wilbois, K. P., & Heß, J. (2016). Effects of soybean variety and Bradyrhizobium strains on yield, protein content and biological nitrogen fixation under cool growing conditions in Germany. *European Journal of Agronomy*, *72*, 38–46. <https://doi.org/10.1016/j.eja.2015.09.008>

8 Appendix

8.1 Results

8.1.1 Measurements - Soil Moisture

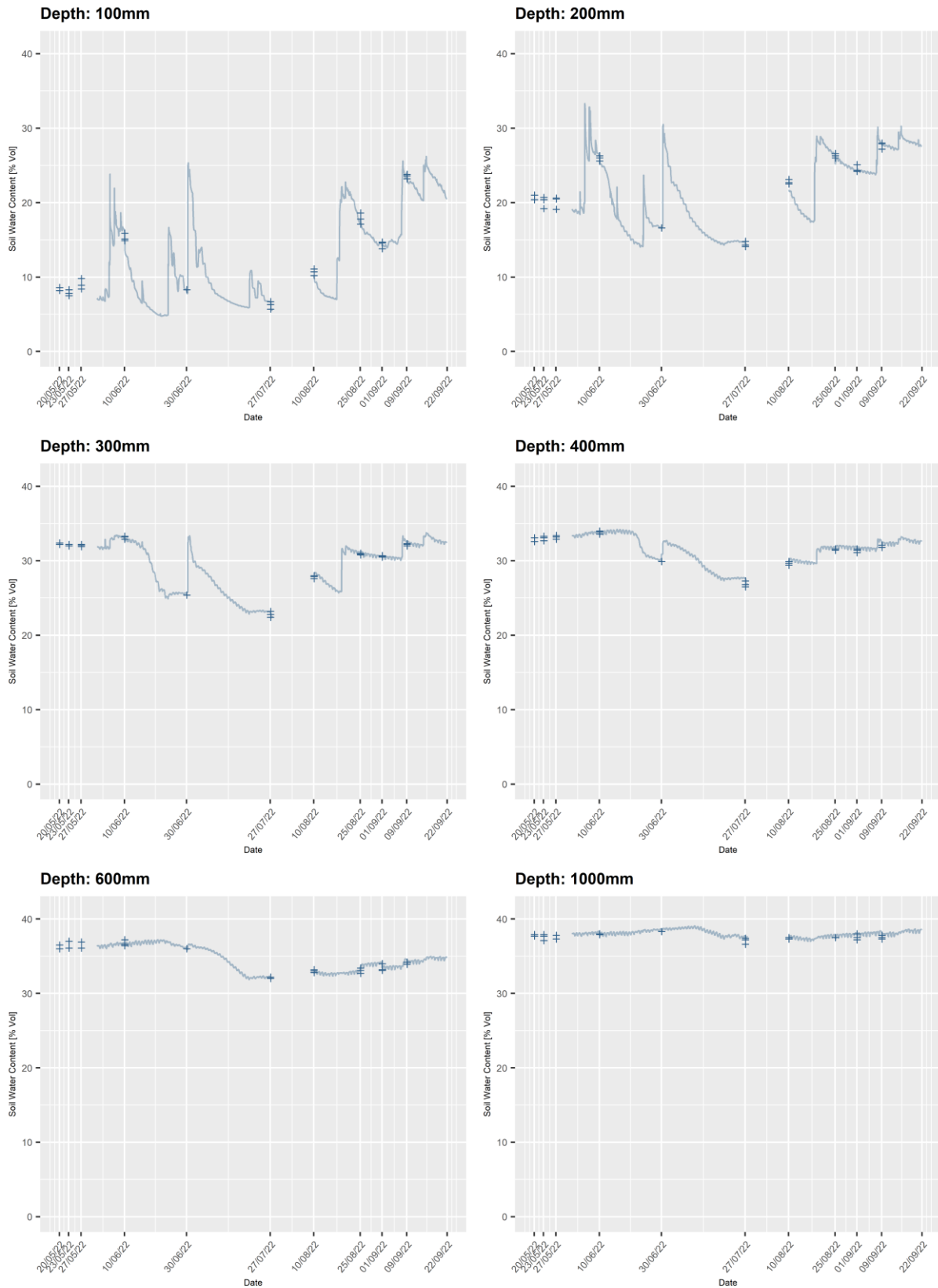


Figure 23: Soil water content [% vol.] on parcel 8, REH, 2022.

8.1.2 Model evaluation - Yield

Table 15: Statistical goodness of fit measures for simulated and observed yield in Changins and Reckenholz.

Location, reference yield	Changins, observed yield: Merlin						
Crop File	901	902	903	904	905	906	w41
RMSE	733.81	543.57	757.68	690.96	680.2	661.51	1502.24
PBIAS%	-16.5	-4.3	-17.3	15.3	15.2	15.5	26.6
d	0.42	0.38	0.42	0.5	0.51	0.59	0.35
md	0.28	0.18	0.28	0.35	0.36	0.43	0.27
rd	0.5	0.27	0.5	0.23	0.24	0.4	0.26
r	0.06	0.03	0.04	0.29	0.33	0.49	0.3
Location, reference yield	Reckenholz, observed yield: Merlin						
Crop File	901	902	903	904	905	906	w41
RMSE	959.54	934.47	969.38	1167.99	1144.71	1095.52	1266.23
PBIAS%	-9.9	1.6	-10.7	20.4	20.5	23.6	27.1
d	0.24	0.05	0.27	0.38	0.4	0.52	0.62
md	0.21	0.03	0.23	0.27	0.29	0.39	0.48
rd	0.18	-0.57	0.26	-0.34	-0.29	0.03	0.48
r	-0.32	-0.43	-0.3	-0.41	-0.36	0.28	0.52
Location, reference yield	Changins, observed yield: M. Arrow						
Crop File	901	902	903	904	905	906	w41
RMSE	684.79	481.7	712.77	651.53	642.96	643.88	1583.29
PBIAS%	-15.8	-3.6	-16.7	16.2	16.1	16.3	27.5
d	0.49	0.49	0.48	0.58	0.59	0.62	0.27
md	0.38	0.33	0.38	0.36	0.37	0.41	0.27
rd	0.6	0.52	0.6	0.45	0.46	0.54	0.2
r	0.3	0.3	0.25	0.56	0.59	0.63	0.13
Location, reference yield	Reckenholz, observed yield: M. Arrow						
Crop File	901	902	903	904	905	906	w41
RMSE	889.83	806.6	905.38	989.09	969.95	974.51	1308.41
PBIAS%	-12	-0.8	-12.8	17.6	17.7	20.7	24.2
d	0.32	0.02	0.34	0.43	0.44	0.53	0.55
md	0.3	0.03	0.31	0.31	0.31	0.38	0.46
rd	0.5	-0.07	0.53	0.08	0.11	0.26	0.35
r	-0.3	-0.29	-0.29	-0.14	-0.08	0.28	0.33

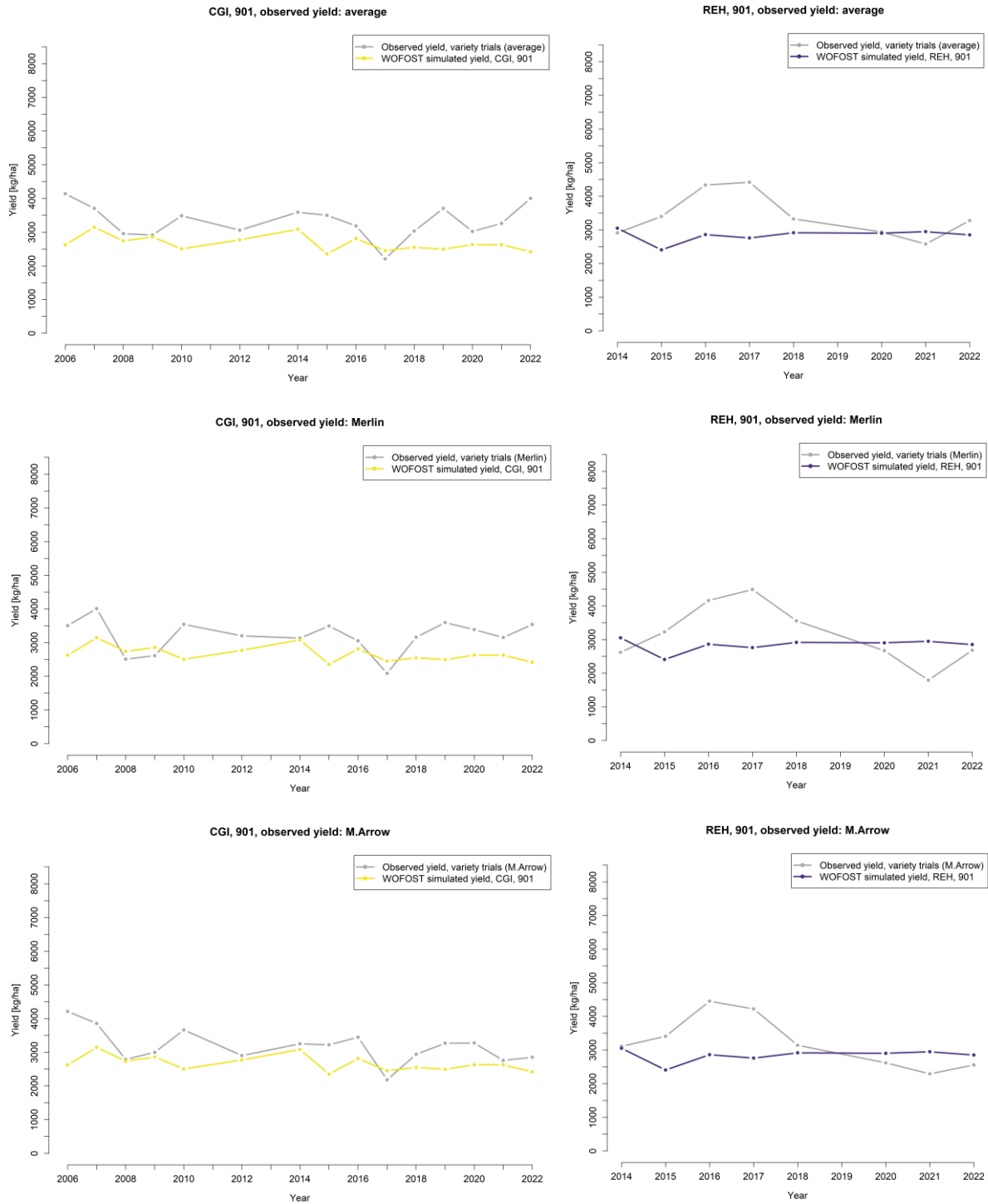


Figure 24: Simulated yield and observed yield, crop file 901.

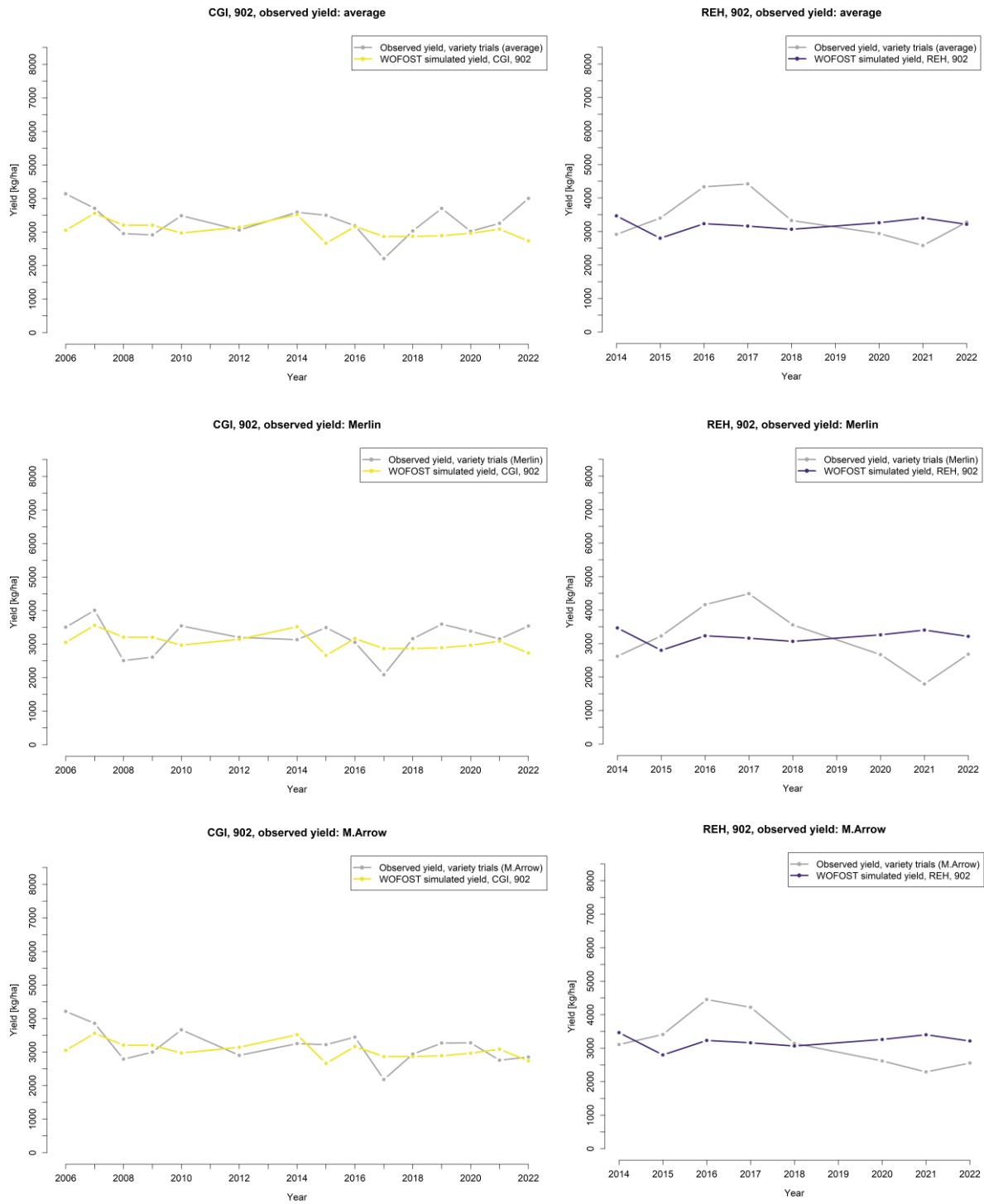


Figure 25: Simulated yield and observed yield, crop file 902.

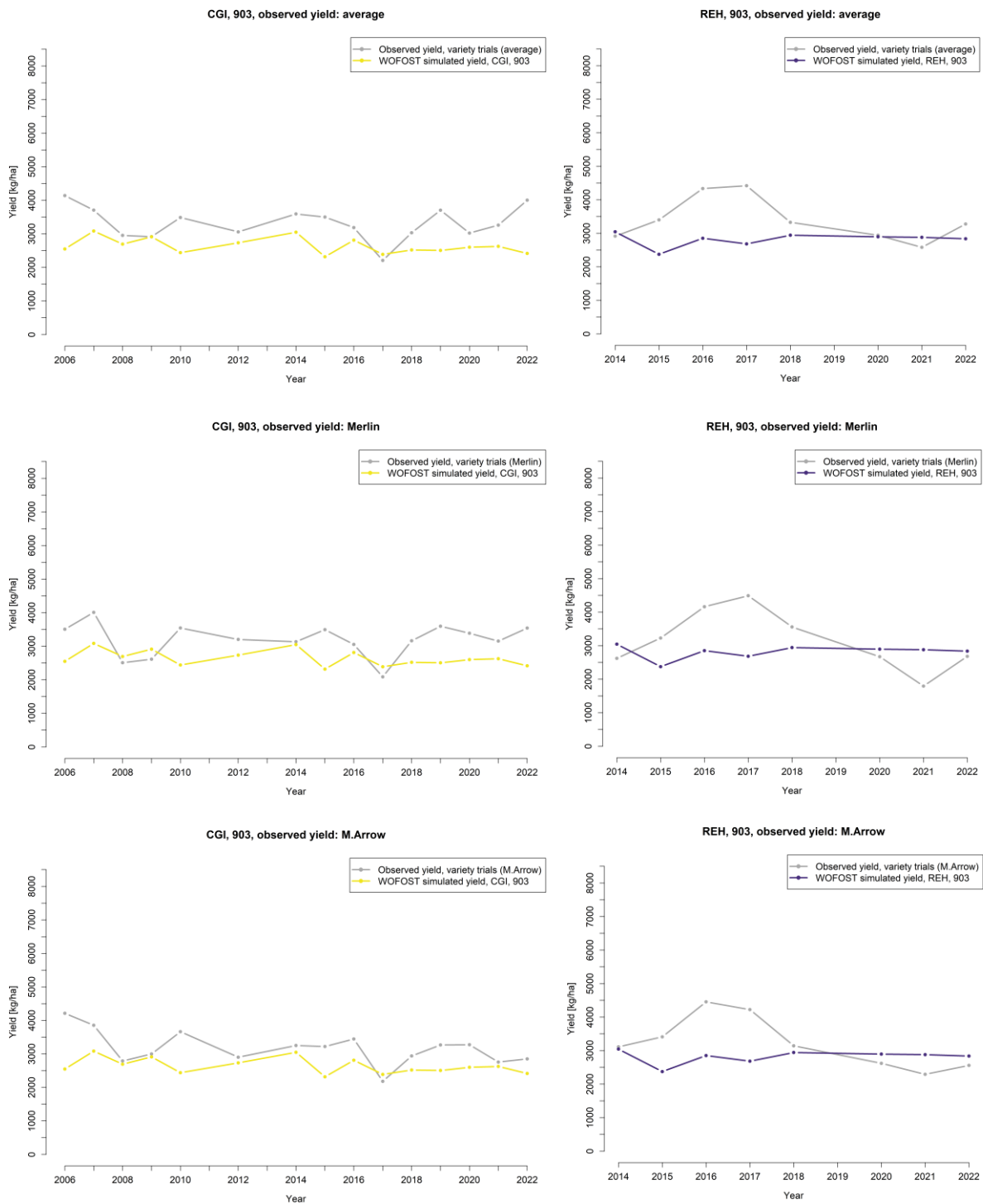


Figure 26: Simulated yield and observed yield, crop file 903.

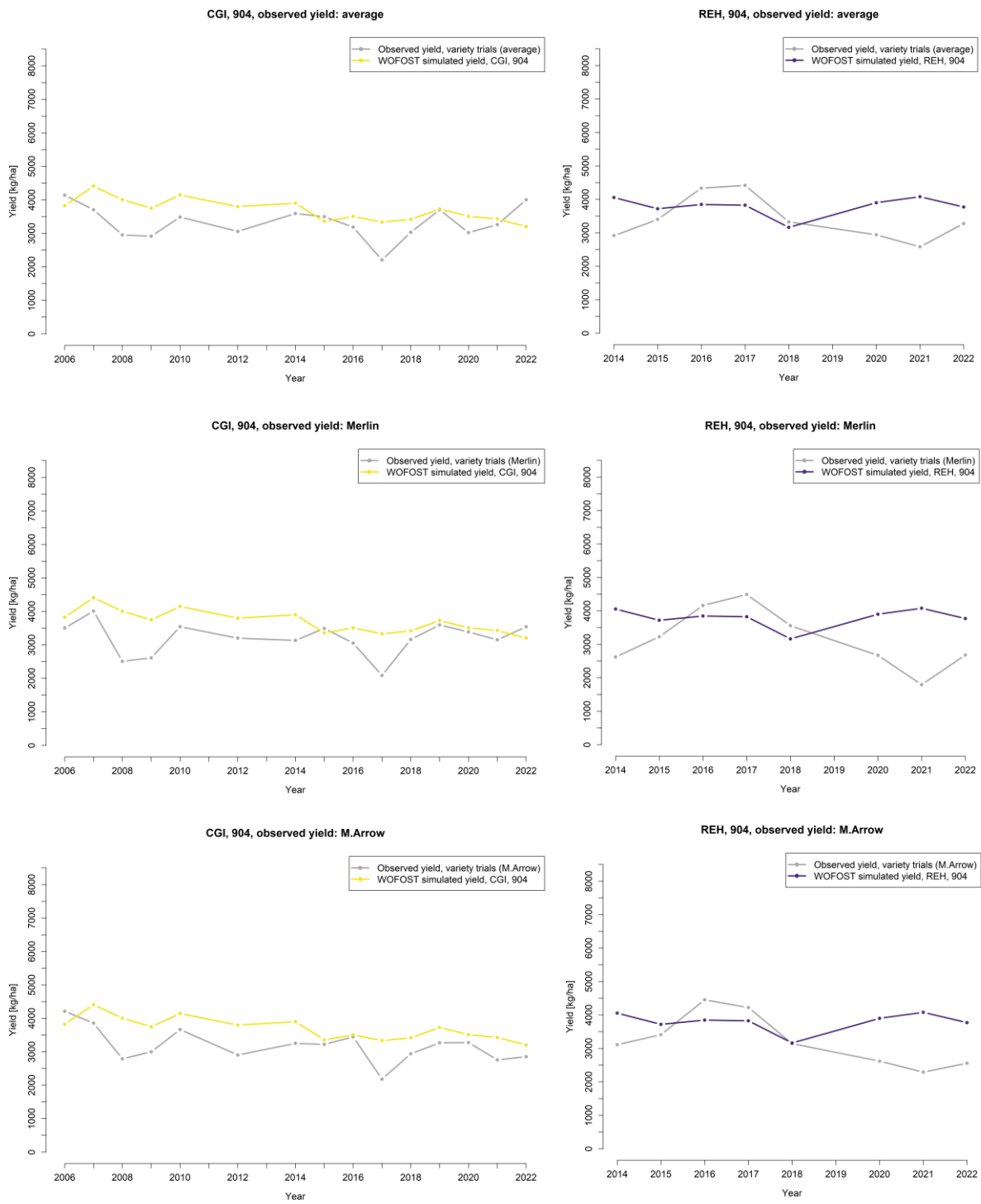


Figure 27: Simulated yield and observed yield, crop file 904.

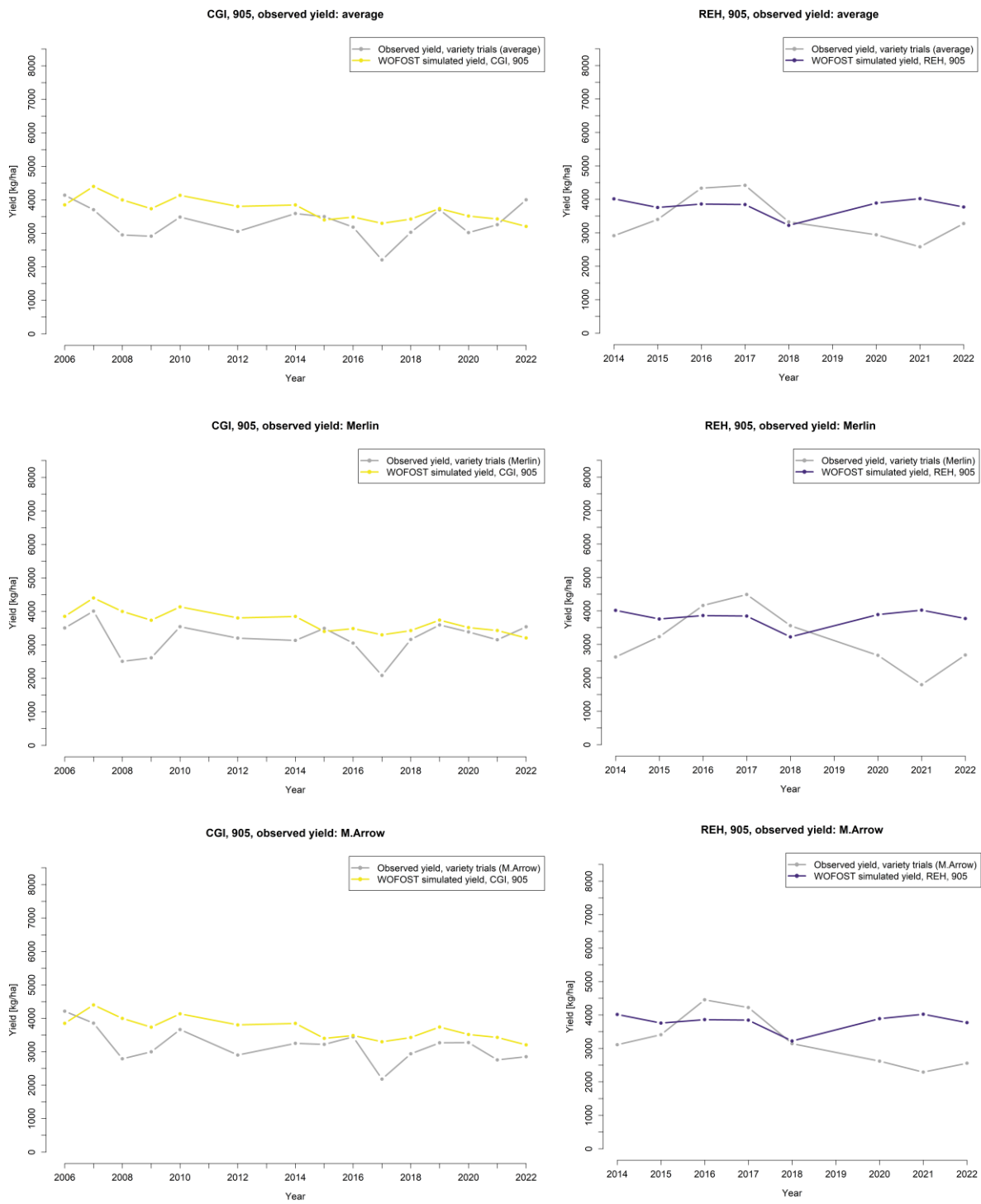


Figure 28: Simulated yield and observed yield, crop file 905.

8.1.3 Model evaluation – Soil water content

Table 16: Statistical goodness of fit measures for simulated and observed soil water content in Reckenholz from June 10 to July 27, 2022.

Location	Reckenholz	
Measured soil moisture (variety)	Merlin	
Crop File	906	w41
RMSE	2.81	1.99
PBIAS%	9.5	5.5
d	0.73	0.87
md	0.47	0.66
rd	0.72	0.88
r	0.87	0.92

8.1.4 Model application – raw data

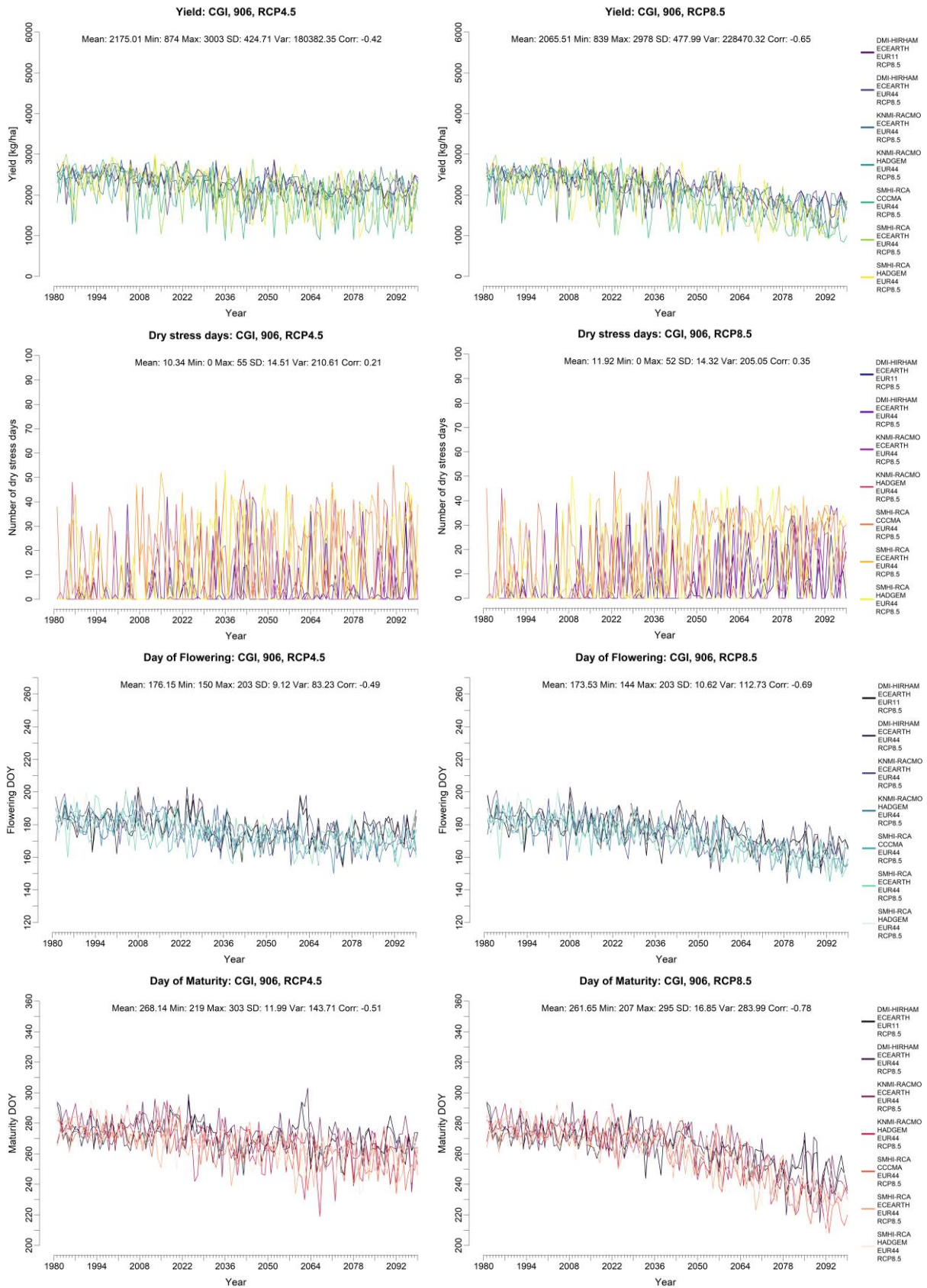


Figure 29: Simulation of yield, dry stress days, day of flowering and day of maturity in Changins (906), 1981-2099 with climate data of different model chains from CH2018.

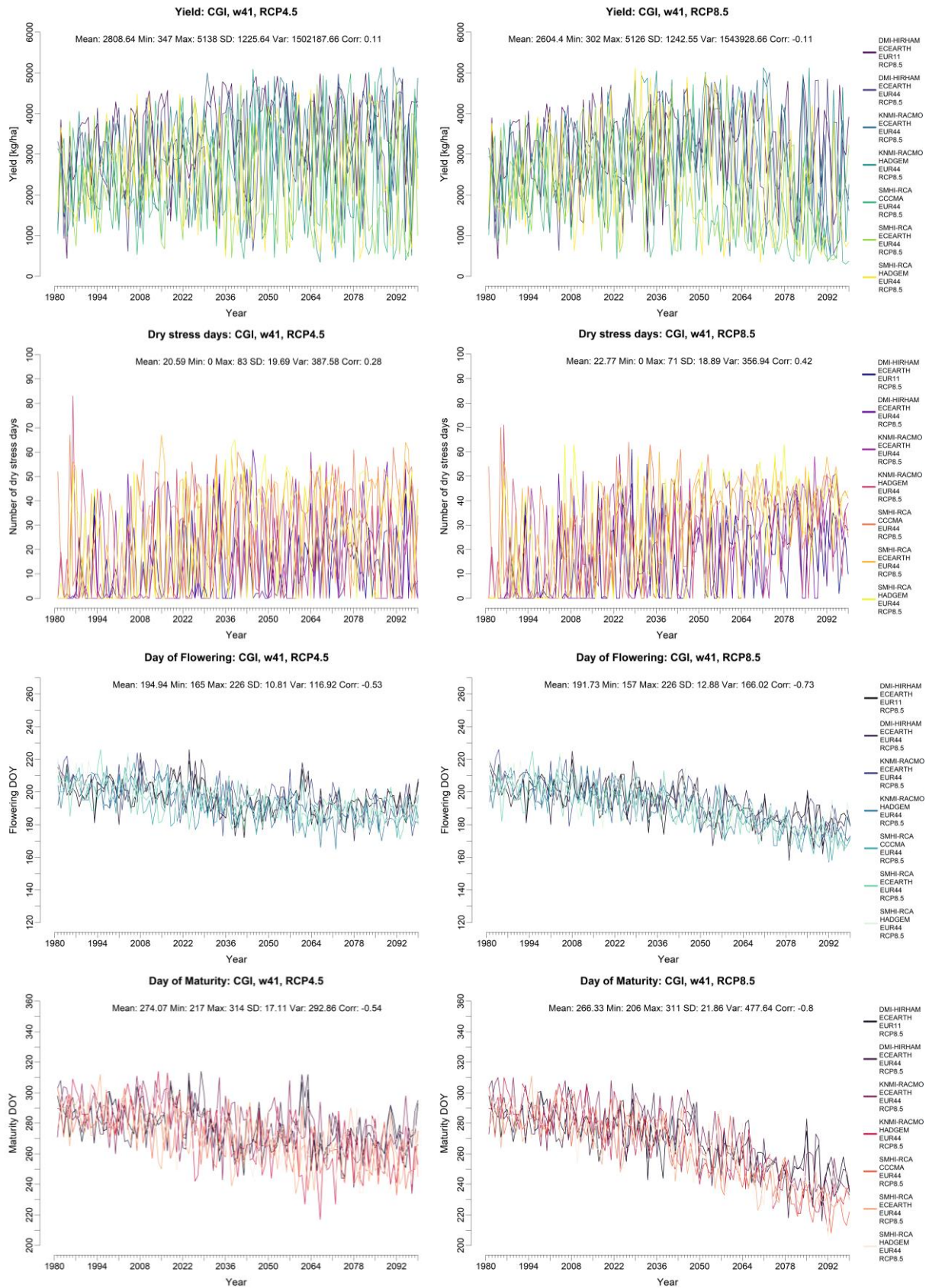


Figure 30: Simulation of yield, dry stress days, day of flowering and day of maturity in Changins (w41), 1981-2099 with climate data of different model chains from CH2018.

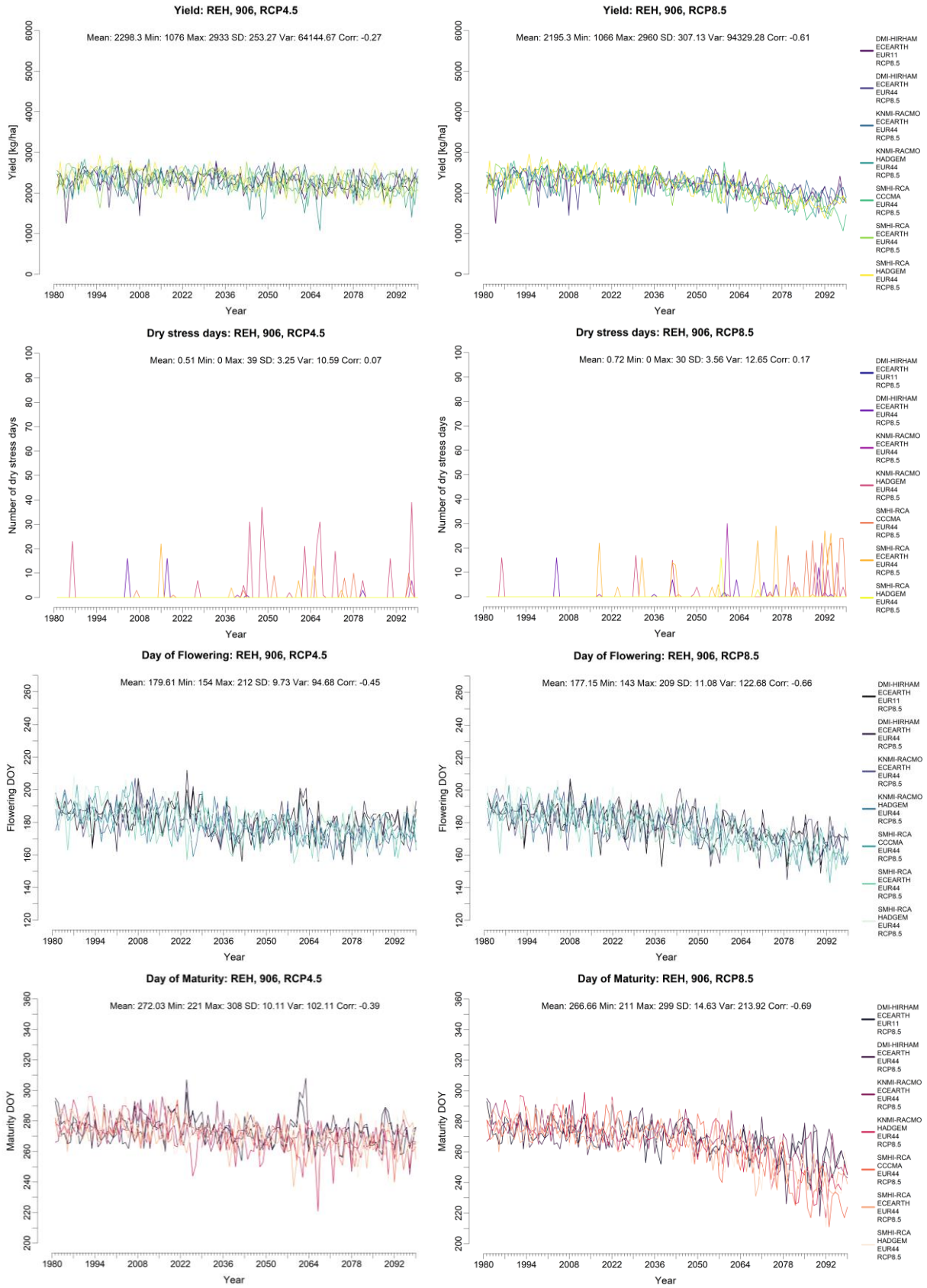


Figure 31: Simulation of yield, dry stress days, day of flowering and day of maturity in Reckenholz (906), 1981-2099 with climate data of different model chains from CH2018.

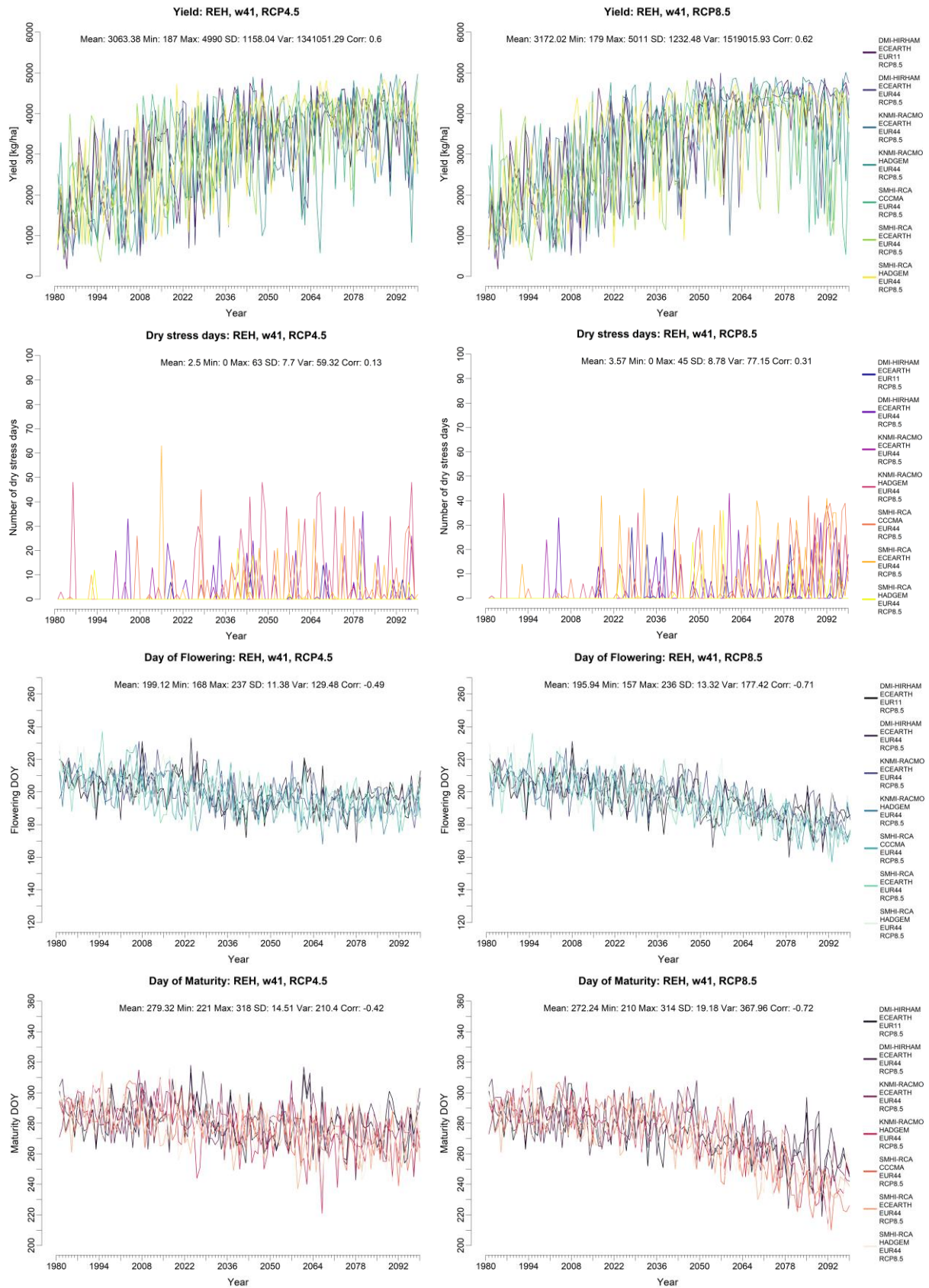


Figure 32: Simulation of yield, dry stress days, day of flowering and day of maturity in Reckenholz (w41), 1981-2099 with climate data of different model chains from CH2018.

8.1.5 Model application – moving average



Figure 33: Simulation of yield, dry stress days, day of flowering and day of maturity in Changins (906), 1981-2099 with climate data of different model chains from CH2018. The data of each plot was transformed using a 10-year moving average for more visual clarity.

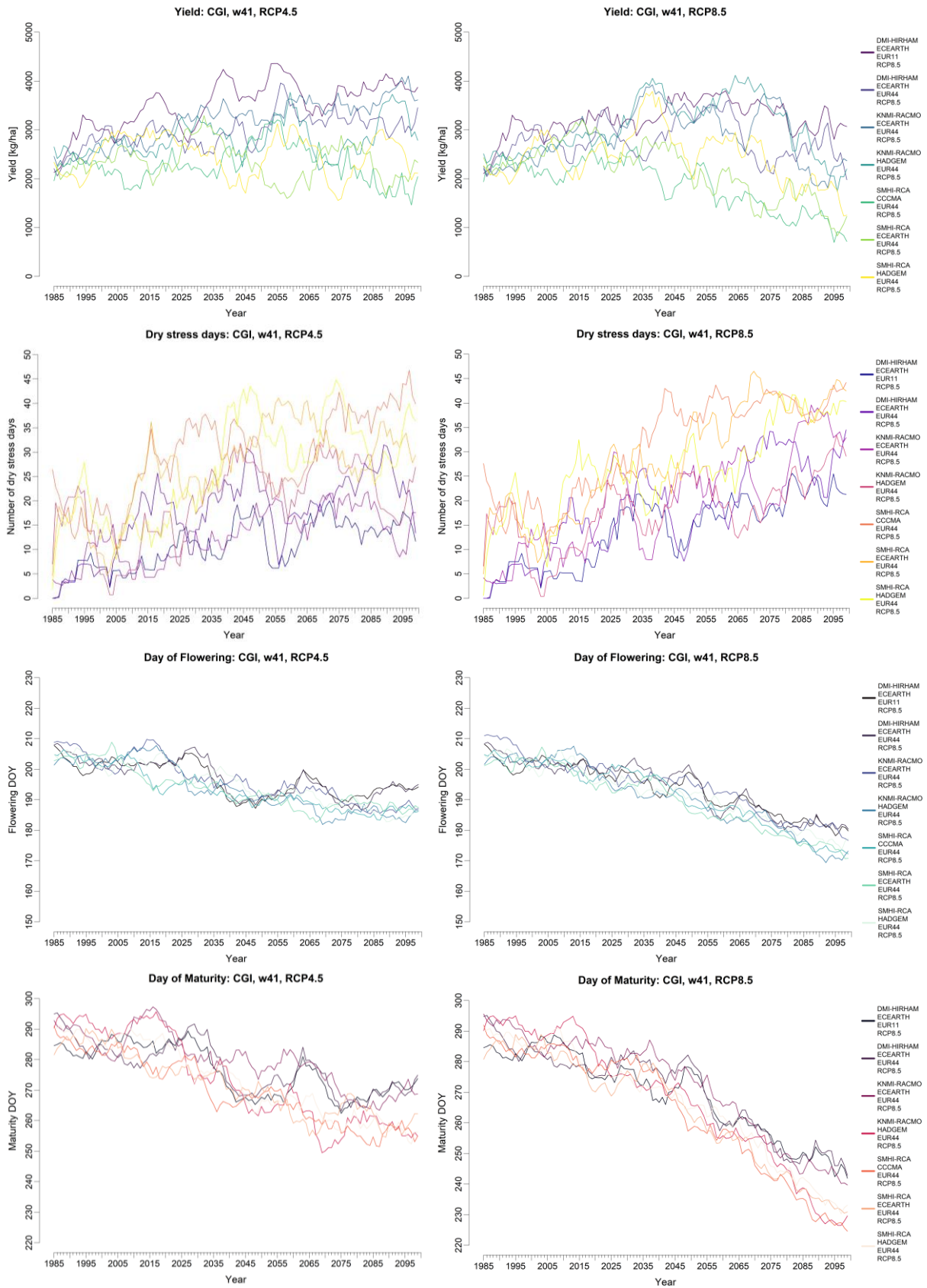


Figure 34: Simulation of yield, dry stress days, day of flowering and day of maturity in Changins (w41), 1981-2099 with climate data of different model chains from CH2018. The data of each plot was transformed using a 10-year moving average for more visual clarity.

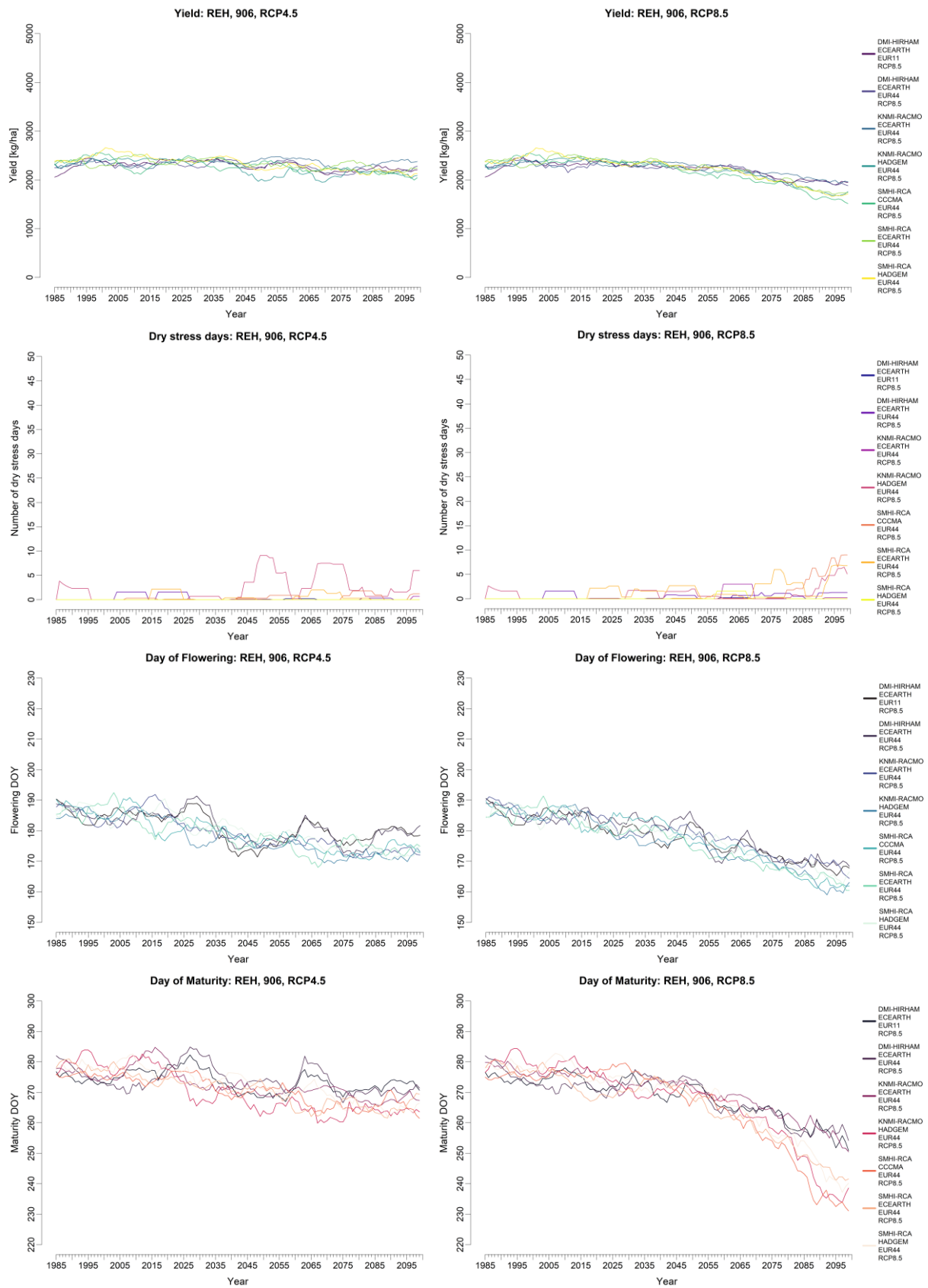


Figure 35: Simulation of yield, dry stress days, day of flowering and day of maturity in Reckenholz (906), 1981-2099, with climate data of different model chains from CH2018. The data of each plot was transformed using a 10-year moving average for more visual clarity.

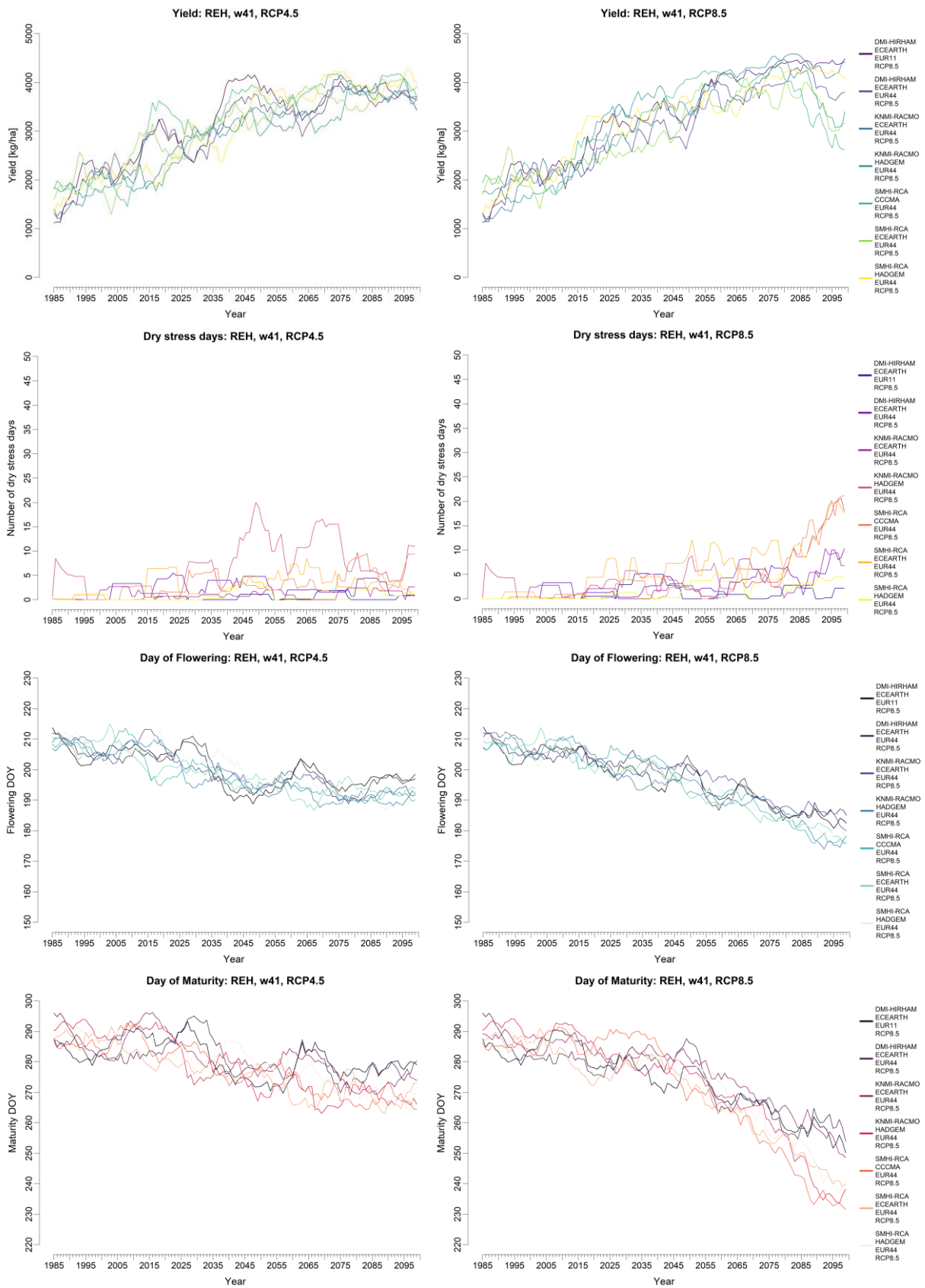


Figure 36: Simulation of yield, dry stress days, day of flowering and day of maturity in Reckenholz (w41), 1981-2099, with climate data of different model chains from CH2018. The data of each plot was transformed using a 10-year moving average for more visual clarity.

8.1.6 Model application – tables

Table 17: Median, mean, minimum, maximum, and standard deviation of simulated variable (yield, dry stress days, flowering, maturity) during four time periods (1981-2010, 2020-2049, 2045-2074, 2070-2099). Simulation with crop file 906, in Changins.

Time Period	Station	Crop File	RCP	Variable	Median	Mean	Min	Max	SD
1981-2010	CGI	906	RCP4.5	yield	2499.0	2433.6	1041.0	3002.0	314.4
2020-2049	CGI	906	RCP4.5	yield	2247.5	2147.4	874.0	2885.0	420.9
2045-2074	CGI	906	RCP4.5	yield	2099.0	2036.6	902.0	2885.0	400.1
2070-2099	CGI	906	RCP4.5	yield	2065.5	1981.6	903.0	2694.0	411.5
1981-2010	CGI	906	RCP8.5	yield	2503.0	2435.2	1307.0	2978.0	309.3
2020-2049	CGI	906	RCP8.5	yield	2199.5	2156.6	935.0	2911.0	397.4
2045-2074	CGI	906	RCP8.5	yield	1981.0	1933.2	850.0	2813.0	372.7
2070-2099	CGI	906	RCP8.5	yield	1676.5	1613.5	839.0	2384.0	356.6
1981-2010	CGI	906	RCP4.5	dry stress days	0.0	5.1	0.0	48.0	11.0
2020-2049	CGI	906	RCP4.5	dry stress days	3.0	12.6	0.0	53.0	15.6
2045-2074	CGI	906	RCP4.5	dry stress days	3.0	12.2	0.0	48.0	15.0
2070-2099	CGI	906	RCP4.5	dry stress days	4.0	13.2	0.0	55.0	15.7
1981-2010	CGI	906	RCP8.5	dry stress days	0.0	5.2	0.0	50.0	10.9
2020-2049	CGI	906	RCP8.5	dry stress days	2.0	11.2	0.0	52.0	14.6
2045-2074	CGI	906	RCP8.5	dry stress days	8.5	14.0	0.0	46.0	14.6
2070-2099	CGI	906	RCP8.5	dry stress days	20.5	18.7	0.0	46.0	13.7
1981-2010	CGI	906	RCP4.5	Flowering	183.0	182.3	160.0	203.0	7.8
2020-2049	CGI	906	RCP4.5	Flowering	175.0	175.6	156.0	203.0	8.5
2045-2074	CGI	906	RCP4.5	Flowering	172.5	172.4	150.0	198.0	7.8
2070-2099	CGI	906	RCP4.5	Flowering	171.0	171.4	150.0	189.0	7.5
1981-2010	CGI	906	RCP8.5	Flowering	183.0	182.3	158.0	203.0	7.8
2020-2049	CGI	906	RCP8.5	Flowering	177.0	176.5	156.0	195.0	7.7
2045-2074	CGI	906	RCP8.5	Flowering	169.0	169.9	151.0	191.0	8.1
2070-2099	CGI	906	RCP8.5	Flowering	163.0	163.0	144.0	183.0	7.4
1981-2010	CGI	906	RCP4.5	Maturity	275.0	275.6	261.0	295.0	7.6
2020-2049	CGI	906	RCP4.5	Maturity	269.0	268.4	239.0	299.0	10.3
2045-2074	CGI	906	RCP4.5	Maturity	265.0	263.8	219.0	303.0	11.8
2070-2099	CGI	906	RCP4.5	Maturity	263.0	260.8	229.0	285.0	11.4
1981-2010	CGI	906	RCP8.5	Maturity	275.0	275.7	256.0	295.0	7.5
2020-2049	CGI	906	RCP8.5	Maturity	269.0	268.7	244.0	293.0	9.4
2045-2074	CGI	906	RCP8.5	Maturity	258.0	257.4	223.0	284.0	12.2
2070-2099	CGI	906	RCP8.5	Maturity	240.0	241.0	207.0	274.0	12.9

Table 18: Median, mean, minimum, maximum, and standard deviation of simulated variable (yield, dry stress days, flowering, maturity) during four time periods (1981-2010, 2020-2049, 2045-2074, 2070-2099). Simulation with crop file 906, in Reckenholz.

Time Period	Station	Crop File	RCP	Variable	Median	Mean	Min	Max	SD
1981-2010	REH	906	RCP4.5	yield	2426.5	2367.4	1253.0	2933.0	272.6
2020-2049	REH	906	RCP4.5	yield	2366.0	2329.1	1351.0	2790.0	228.8
2045-2074	REH	906	RCP4.5	yield	2274.0	2251.1	1076.0	2767.0	251.9
2070-2099	REH	906	RCP4.5	yield	2214.5	2205.7	1401.0	2744.0	233.3
1981-2010	REH	906	RCP8.5	yield	2424.5	2373.0	1253.0	2960.0	265.4
2020-2049	REH	906	RCP8.5	yield	2306.0	2301.3	1690.0	2728.0	198.5
2045-2074	REH	906	RCP8.5	yield	2179.5	2154.9	1499.0	2767.0	230.2
2070-2099	REH	906	RCP8.5	yield	1885.5	1873.8	1066.0	2460.0	235.9
1981-2010	REH	906	RCP4.5	dry stress days	0.0	0.2	0.0	23.0	1.9
2020-2049	REH	906	RCP4.5	dry stress days	0.0	0.5	0.0	37.0	3.6
2045-2074	REH	906	RCP4.5	dry stress days	0.0	0.9	0.0	37.0	4.4
2070-2099	REH	906	RCP4.5	dry stress days	0.0	0.6	0.0	39.0	3.4
1981-2010	REH	906	RCP8.5	dry stress days	0.0	0.2	0.0	16.0	1.6
2020-2049	REH	906	RCP8.5	dry stress days	0.0	0.4	0.0	17.0	2.4
2045-2074	REH	906	RCP8.5	dry stress days	0.0	0.5	0.0	30.0	3.0
2070-2099	REH	906	RCP8.5	dry stress days	0.0	1.8	0.0	29.0	5.7
1981-2010	REH	906	RCP4.5	Flowering	185.5	185.8	162.0	209.0	8.6
2020-2049	REH	906	RCP4.5	Flowering	178.0	178.9	156.0	212.0	9.4
2045-2074	REH	906	RCP4.5	Flowering	176.0	175.9	155.0	201.0	8.2
2070-2099	REH	906	RCP4.5	Flowering	175.0	174.9	154.0	193.0	7.9

1981-2010	REH	906	RCP8.5	Flowering	185.0	185.8	161.0	209.0	8.6
2020-2049	REH	906	RCP8.5	Flowering	180.0	180.1	153.0	202.0	8.4
2045-2074	REH	906	RCP8.5	Flowering	173.0	173.6	152.0	196.0	8.5
2070-2099	REH	906	RCP8.5	Flowering	167.0	166.7	143.0	188.0	8.0
1981-2010	REH	906	RCP4.5	Maturity	276.0	276.9	260.0	296.0	8.3
2020-2049	REH	906	RCP4.5	Maturity	273.0	272.2	244.0	307.0	8.9
2045-2074	REH	906	RCP4.5	Maturity	269.0	269.0	221.0	308.0	10.2
2070-2099	REH	906	RCP4.5	Maturity	267.0	267.3	239.0	289.0	9.4
1981-2010	REH	906	RCP8.5	Maturity	276.0	276.9	260.0	297.0	8.3
2020-2049	REH	906	RCP8.5	Maturity	272.0	272.5	252.0	296.0	8.0
2045-2074	REH	906	RCP8.5	Maturity	265.0	264.8	231.0	289.0	10.5
2070-2099	REH	906	RCP8.5	Maturity	250.0	250.2	211.0	283.0	14.5

Table 19: Median, mean, minimum, maximum, and standard deviation of simulated variable (yield, dry stress days, flowering, maturity) during four time periods (1981-2010, 2020-2049, 2045-2074, 2070-2099). Simulation with crop file w41, in Changins.

Time Period	Station	Crop File	RCP	Variable	Median	Mean	Min	Max	SD
1981-2010	CGI	w41	RCP4.5	yield	2547.5	2542.8	444.0	4487.0	938.9
2020-2049	CGI	w41	RCP4.5	yield	2967.5	2843.9	432.0	5090.0	1240.7
2045-2074	CGI	w41	RCP4.5	yield	3046.5	2978.2	347.0	5090.0	1353.3
2070-2099	CGI	w41	RCP4.5	yield	3190.5	2915.8	351.0	5138.0	1420.5
1981-2010	CGI	w41	RCP8.5	yield	2503.0	2524.4	433.0	4241.0	923.7
2020-2049	CGI	w41	RCP8.5	yield	3039.5	2941.6	436.0	5110.0	1212.1
2045-2074	CGI	w41	RCP8.5	yield	2822.0	2818.0	347.0	5126.0	1352.3
2070-2099	CGI	w41	RCP8.5	yield	1894.5	2141.7	302.0	5126.0	1386.8
1981-2010	CGI	w41	RCP4.5	dry stress days	0.0	11.3	0.0	83.0	17.3
2020-2049	CGI	w41	RCP4.5	dry stress days	21.5	23.5	0.0	65.0	20.5
2045-2074	CGI	w41	RCP4.5	dry stress days	25.0	24.5	0.0	61.0	18.9
2070-2099	CGI	w41	RCP4.5	dry stress days	27.0	25.7	0.0	64.0	18.3
1981-2010	CGI	w41	RCP8.5	dry stress days	1.0	11.6	0.0	71.0	17.1
2020-2049	CGI	w41	RCP8.5	dry stress days	22.0	22.9	0.0	64.0	19.4
2045-2074	CGI	w41	RCP8.5	dry stress days	30.0	27.0	0.0	59.0	17.2
2070-2099	CGI	w41	RCP8.5	dry stress days	36.0	32.5	0.0	63.0	14.6
1981-2010	CGI	w41	RCP4.5	Flowering	203.5	203.2	180.0	226.0	8.9
2020-2049	CGI	w41	RCP4.5	Flowering	193.0	194.0	172.0	226.0	10.1
2045-2074	CGI	w41	RCP4.5	Flowering	190.0	190.2	165.0	218.0	8.9
2070-2099	CGI	w41	RCP4.5	Flowering	189.0	188.7	165.0	208.0	8.1
1981-2010	CGI	w41	RCP8.5	Flowering	203.5	203.1	179.0	226.0	9.0
2020-2049	CGI	w41	RCP8.5	Flowering	195.5	195.3	174.0	219.0	9.1
2045-2074	CGI	w41	RCP8.5	Flowering	187.0	186.9	167.0	215.0	9.1
2070-2099	CGI	w41	RCP8.5	Flowering	179.0	178.3	157.0	201.0	8.3
1981-2010	CGI	w41	RCP4.5	Maturity	286.0	286.4	260.0	312.0	11.1
2020-2049	CGI	w41	RCP4.5	Maturity	274.0	273.8	239.0	314.0	15.3
2045-2074	CGI	w41	RCP4.5	Maturity	266.0	266.9	217.0	312.0	15.8
2070-2099	CGI	w41	RCP4.5	Maturity	264.0	263.2	227.0	298.0	14.7
1981-2010	CGI	w41	RCP8.5	Maturity	287.0	286.4	254.0	311.0	11.2
2020-2049	CGI	w41	RCP8.5	Maturity	276.5	274.6	241.0	308.0	14.1
2045-2074	CGI	w41	RCP8.5	Maturity	257.0	258.5	223.0	302.0	15.5
2070-2099	CGI	w41	RCP8.5	Maturity	240.0	240.4	206.0	283.0	13.2

Table 20: Median, mean, minimum, maximum, and standard deviation of simulated variable (yield, dry stress days, flowering, maturity) during four time periods (1981-2010, 2020-2049, 2045-2074, 2070-2099). Simulation with crop file w41, in Reckenholz.

Time Period	Station	Crop File	RCP	Variable	Median	Mean	Min	Max	SD
1981-2010	REH	w41	RCP4.5	yield	1834.5	1956.8	187.0	4437.0	969.0
2020-2049	REH	w41	RCP4.5	yield	3391.0	3206.3	694.0	4900.0	1029.3
2045-2074	REH	w41	RCP4.5	yield	3857.5	3621.9	576.0	4900.0	847.3
2070-2099	REH	w41	RCP4.5	yield	3962.0	3804.0	835.0	4990.0	728.5
1981-2010	REH	w41	RCP8.5	yield	1834.5	1957.4	179.0	4389.0	944.1
2020-2049	REH	w41	RCP8.5	yield	3513.0	3261.9	723.0	4831.0	993.3

2045-2074	REH	w41	RCP8.5	yield	4132.5	3891.7	896.0	4993.0	787.5
2070-2099	REH	w41	RCP8.5	yield	4313.5	3952.3	534.0	5011.0	933.7
1981-2010	REH	w41	RCP4.5	dry stress days	0.0	0.8	0.0	48.0	4.7
2020-2049	REH	w41	RCP4.5	dry stress days	0.0	3.1	0.0	48.0	8.1
2045-2074	REH	w41	RCP4.5	dry stress days	0.0	3.3	0.0	48.0	9.0
2070-2099	REH	w41	RCP4.5	dry stress days	0.0	3.2	0.0	48.0	8.4
1981-2010	REH	w41	RCP8.5	dry stress days	0.0	0.6	0.0	43.0	4.2
2020-2049	REH	w41	RCP8.5	dry stress days	0.0	2.7	0.0	45.0	7.8
2045-2074	REH	w41	RCP8.5	dry stress days	0.0	3.6	0.0	43.0	8.4
2070-2099	REH	w41	RCP8.5	dry stress days	0.0	7.8	0.0	42.0	11.6
1981-2010	REH	w41	RCP4.5	Flowering	208.0	207.4	183.0	237.0	9.9
2020-2049	REH	w41	RCP4.5	Flowering	197.0	197.9	172.0	233.0	11.0
2045-2074	REH	w41	RCP4.5	Flowering	194.5	194.4	168.0	221.0	9.3
2070-2099	REH	w41	RCP4.5	Flowering	194.0	193.1	169.0	213.0	8.2
1981-2010	REH	w41	RCP8.5	Flowering	208.0	207.3	183.0	236.0	9.7
2020-2049	REH	w41	RCP8.5	Flowering	199.0	199.4	174.0	222.0	9.7
2045-2074	REH	w41	RCP8.5	Flowering	191.0	191.4	166.0	221.0	9.8
2070-2099	REH	w41	RCP8.5	Flowering	183.0	182.6	157.0	204.0	9.1
1981-2010	REH	w41	RCP4.5	Maturity	287.0	287.2	261.0	315.0	11.2
2020-2049	REH	w41	RCP4.5	Maturity	279.0	279.0	244.0	318.0	12.9
2045-2074	REH	w41	RCP4.5	Maturity	274.0	274.6	221.0	317.0	14.4
2070-2099	REH	w41	RCP4.5	Maturity	273.0	272.1	238.0	303.0	13.5
1981-2010	REH	w41	RCP8.5	Maturity	288.0	287.2	261.0	314.0	10.8
2020-2049	REH	w41	RCP8.5	Maturity	280.0	280.2	250.0	308.0	12.1
2045-2074	REH	w41	RCP8.5	Maturity	268.0	268.0	230.0	308.0	14.5
2070-2099	REH	w41	RCP8.5	Maturity	250.0	250.3	210.0	297.0	15.8

8.2 Discussion – LAI

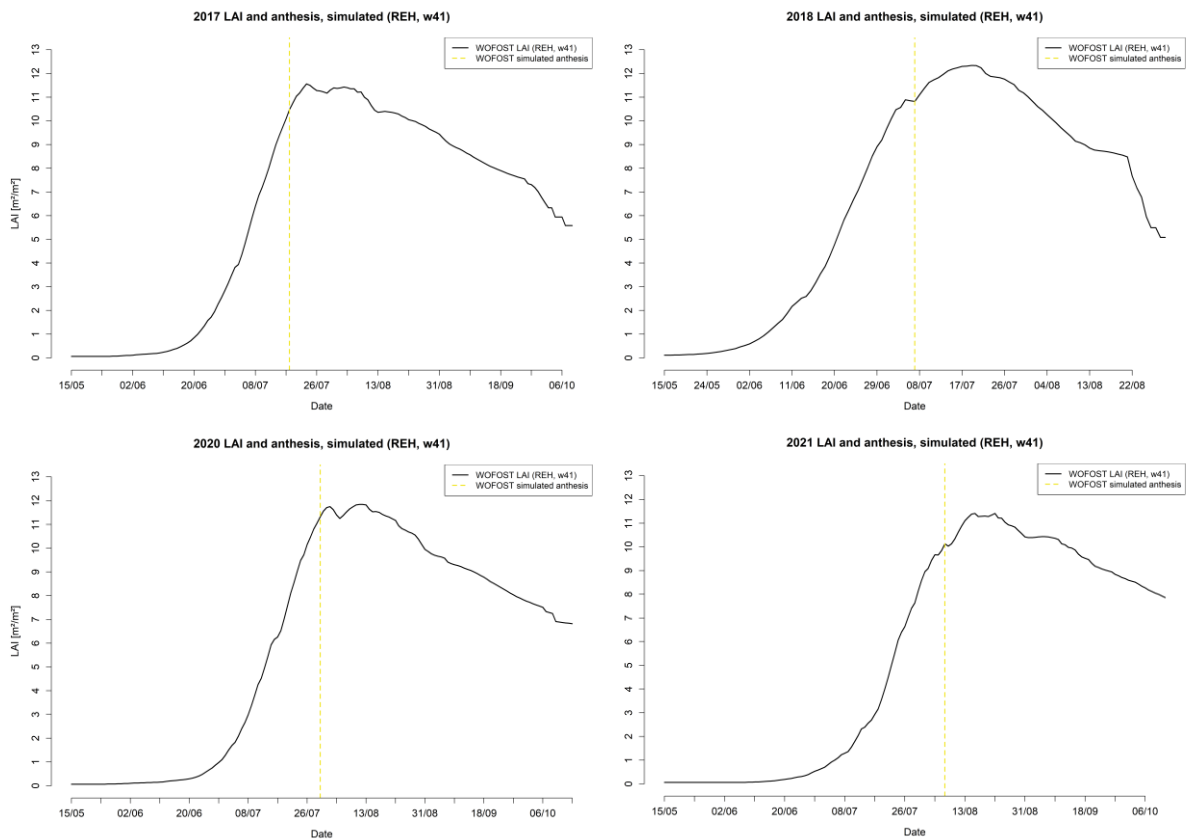


Figure 37: Simulated LAI and flowering with crop file w41 for Reckenholz, 2017, 2018, 2020, 2021.

Declaration of consent

on the basis of Article 30 of the RSL Phil.-nat. 18

Name/First Name: Willi Sarah

Registration Number: 16-700-726

Study program: MSc Climate Sciences

Bachelor

Master

Dissertation

Title of the thesis: Modelling Climate Change Impacts on Soybean Yields on the Swiss Plateau

Supervisor: PD Dr. Annelie Holzkämper
Prof. Dr. Bettina Schaefli

I declare herewith that this thesis is my own work and that I have not used any sources other than those stated. I have indicated the adoption of quotations as well as thoughts taken from other authors as such in the thesis. I am aware that the Senate pursuant to Article 36 paragraph 1 litera r of the University Act of 5 September, 1996 is authorized to revoke the title awarded on the basis of this thesis.

For the purposes of evaluation and verification of compliance with the declaration of originality and the regulations governing plagiarism, I hereby grant the University of Bern the right to process my personal data and to perform the acts of use this requires, in particular, to reproduce the written thesis and to store it permanently in a database, and to use said database, or to make said database available, to enable comparison with future theses submitted by others.

Zurich, 18.09.2023

Place/Date



Signature